

UNIVERSIDADE FEDERAL DO RIO GRANDE DO SUL
INSTITUTO DE CIÊNCIAS BÁSICAS DA SAÚDE
PROGRAMA DE PÓS-GRADUAÇÃO EM CIÊNCIAS BIOLÓGICAS:
FISIOLOGIA

Juliana Girón Bastidas

**DESENVOLVIMENTO DE ESTRATÉGIAS PARA REGENERAÇÃO CUTÂNEA
COM BASE EM UM BIOMATERIAL NANOFIBROSO DE PLGA/FIBRINA E
SECRETOMA DE CÉLULAS-TRONCO**

Porto Alegre

2022

Juliana Girón Bastidas

**DESENVOLVIMENTO DE ESTRATÉGIAS PARA REGENERAÇÃO CUTÂNEA
COM BASE EM UM BIOMATERIAL NANOFIBROSO DE PLGA/FIBRINA E
SECRETOMA DE CÉLULAS-TRONCO**

Tese apresentada ao Programa de Pós- Graduação em Ciências Biológicas: Fisiologia do Instituto de Ciências Básicas da Saúde da Universidade Federal do Rio Grande do Sul como requisito parcial para a obtenção do título de doutora em Fisiologia.

Orientador(a): Patricia Pranke (Prof. Dra.)
Coorientador(a): Natasha Maurmann (Dra.)

Porto Alegre

2022

AGRADECIMENTOS

Aos meus pais, por todo o apoio, amor, e esforço para sempre ter a melhor educação.

Aos meus irmãos, por todo o carinho incondicional. Especialmente, agradeço ao meu irmão Juan Pablo que me ajudou com as ilustrações dos artigos publicados.

À minha Orientadora, Prof. Dra. Patricia Pranke que me abriu as portas desde o primeiro contato, e possibilitou-me a oportunidade de desenvolver o meu projeto. Muito obrigada pelo apoio e confiança no meu trabalho.

À minha co-orientadora, Dra. Natasha Maurmann, por tudo que me ensinou, pela paciência, pela parceria nos experimentos, pela orientação, pela amizade. Por sempre estar disposta para me auxiliar no que precisei.

Aos meus colegas de laboratório, especialmente ao Bruno Alcantara e Luiza Oliveira por terem me ajudado nos experimentos *in vivo*, sem vocês teria sido muito difícil.

À Daikelly Braghirolli, pela amizade e pelos conselhos importantes que me deu quando estava padronizando a solução de *electrospinning*.

À Laura Sperling, que tirou muitas das minhas dúvidas relacionadas com a escolha de anticorpos e fixação de tecidos.

À Rafaela Zimmermann, pela bela amizade, pela companhia nas horas de bancada, por ouvir meus desabafos, e fazer meus dias mais leves.

Aos alunos de iniciação científica que passaram pelo grupo de pesquisa e contribuíram de alguma forma no desenvolvimento dessa tese.

Aos amigos que fiz no Brasil, pelos maravilhosos momentos juntos, pelas risadas, pelos momentos de descontração, pelos desabafos e momentos de reflexões. Em especial a Ángel, Nathalia, Edwin, Maria Eduarda, Francielle e Javier.

Aos co-autores dos trabalhos gerados durante o doutorado, pela contribuição técnica e intelectual.

Ao PPG Ciências Biológicas – Fisiologia, pelo ensino de qualidade e pela oportunidade que me deram de fazer o doutorado através do programa de bolsas da OEA.

A todos os professores que contribuíram na minha formação.

À CAPES, pela bolsa de doutorado.

Às agências de fomento e amparo à pesquisa, pelos financiamentos concedidos e ao Instituto de Pesquisa com Células-tronco.

À banca avaliadora dessa tese, pelo interesse e tempo disponibilizado.

RESUMO

Introdução: Até os dias de hoje, as feridas crônicas e queimaduras representam um problema grave de saúde pública que trazem consequências devastadoras para os pacientes e resultam em grandes custos para os sistemas de saúde e para a sociedade. **Objetivo:** O presente trabalho teve como objetivo desenvolver estratégias para a regeneração cutânea com base em um biomaterial nanofibroso de PLGA/fibrina e secretoma de células-tronco. **Metodologia:** A primeira estratégia consistiu no desenvolvimento de um biomaterial (*scaffold*) nanofibroso eletrofiado composto pelos polímeros: ácido poli(lático-co-glicólico) (PLGA), fibrina e polietileno glicol. Os *scaffolds* foram caracterizados por meio de testes físicos e biológicos. Para a análise *in vivo*, à membrana de *electrospinning* gerada foi adicionada uma camada de hidrogel de fibrina para construir um substituto dermo-epidérmico que foi analisado em um modelo de lesão cutânea de espessura completa em ratos. Os fibroblastos e queratinócitos foram isolados de biopsias de pele de rato, os fibroblastos foram cultivados na camada do hidrogel de fibrina e os queratinócitos na membrana eletrofiada para gerar um substituto cutâneo. Os *scaffolds* sem e com incorporação de células foram implantados e os tecidos neoformados analisados. A segunda estratégia consistiu na avaliação dos efeitos do secretoma de células-tronco derivadas de dentes decíduos esfoliados humanos (SHED) em queratinócitos. As vesículas extracelulares (VEs) de SHED foram isoladas e caracterizadas. **Resultados:** A caracterização por microscopia eletrônica de varredura mostrou nanofibras depositadas aleatoriamente e a incorporação de fibrina reduziu o diâmetro médio de 1051.0 ± 290.2 nm nos *scaffolds* de PLGA para $639,8 \pm 241,8$ nm nas membranas de PLGA/fibrina. A análise de FTIR confirmou a presença de fibrina nas membranas e a incorporação de fibrina reduziu o ângulo de contato. A fibrina aumentou a tensão e diminuiu a deformação do biomaterial. Os *scaffolds* demonstraram compatibilidade sanguínea e a incorporação de fibrina melhorou a adesão e viabilidade celular. Os testes *in vivo* não indicaram sinais de infecção nas feridas. Não houve diferença entre os grupos sem e com células (grupos 1 e 2, respectivamente) quando analisadas a espessura epitelial, a espessura do tecido de granulação e o índice de colágeno. No entanto, se observou diferença significativa entre esses grupos e o grupo controle negativo. Também, observou-se aumento da deposição de colágeno nos grupos 1 e 2 no dia 14 e remodelação epitelial nos grupos 1 e 2 no dia 21. Os marcadores de cicatrização de feridas mostraram aumento da expressão de proteínas anti-inflamatórias e fator de crescimento epidérmico (EGF) no grupo 1. Em contrapartida, não houve diferença na expressão de fator de crescimento do endotélio vascular (VEGF) entre os grupos. As atividades de glutatona peroxidase e superóxido dismutase foram diminuídas em relação ao

controle positivo e negativo. As SHED-VEs revelaram uma morfologia em forma de taça, expressaram os marcadores clássicos para exossomos CD9 e CD63, e foram efetivamente internalizadas pelos queratinócitos. Os resultados também indicaram que 50% de meio condicionado (MC) e 0,4 µg/ml de VEs foram igualmente eficientes para melhorar a viabilidade, migração e atenuação da citotoxicidade induzida por H₂O₂ em queratinócitos. Além disso, a expressão de VEGF em queratinócitos aumentou quando tratados com secretoma e VEs de SHED. **Conclusões:** Os resultados sugerem que a incorporação de células nos *scaffolds* em bicamada não influenciou nas características histológicas do tecido de granulação e epitélio, bem como no índice de colágeno. Os *scaffolds* bicamada contribuíram para a formação do tecido de granulação e na deposição precoce de colágeno, mantendo um microambiente anti-inflamatório. Por outro lado, o secretoma e VEs de SHED mostraram ser eficientes para melhorar a viabilidade, migração e atenuação da citotoxicidade induzida por H₂O₂ em queratinócitos. Portanto, tanto o *scaffold* bicamada, quanto o secretoma de SHED podem ser ferramentas terapêuticas promissoras para acelerar a reepitelização e cicatrização de feridas.

Palavras-chave: biomateriais, células-tronco, engenharia tecidual, pele, secretoma, vesículas extracelulares.

ABSTRACT

Introduction: Until the present day, chronic wounds and burns represent a serious public health problem that has devastating consequences for patients and which contribute to high costs for healthcare systems and societies. **Objective:** The present work aimed to develop strategies for skin regeneration based on a nanofibrous biomaterial of PLGA/fibrin and stem cell secretome. **Methodology:** The first strategy consisted of the development of an electrospun hybrid nanofibrous scaffold composed of polymers: poly(lactic-co-glycolic) acid (PLGA), fibrin and polyethylene glycol. The scaffolds were characterized through physical and biological tests. For *in vivo* analysis, a layer of fibrin hydrogel was added to the generated *electrospinning* membrane to construct a dermo-epidermal substitute which was tested in a full-thickness skin lesion model in rats. Fibroblasts and keratinocytes were isolated from rat skin biopsies, fibroblasts were cultivated on the fibrin hydrogel layer and keratinocytes on the electrospun membrane to generate a skin substitute. Scaffolds with and without cells were implanted and the neoformed tissues were analyzed. The second strategy consisted of the evaluation of the stem cells from human exfoliated deciduous teeth (SHED) secretome in relation to viability, migration, and attenuation of the cytotoxicity induced by H₂O₂ in the keratinocytes. Extracellular SHED vesicles were isolated and characterized. **Results:** scanning electron microscopy (SEM) characterization showed randomly oriented nanofibers and the incorporation of fibrin reduced the mean diameter from 1051.0 ± 290.2 nm in PLGA scaffolds, to 639.8 ± 241.8 nm in PLGA/fibrin membranes. FTIR analysis confirmed the presence of fibrin in the membranes and the incorporation of fibrin reduced the contact angle. The fibrin increased tensile strength and decreased elongation at break. The scaffolds demonstrated blood compatibility and fibrin incorporation improved cell adhesion and viability. *In vivo* tests showed no signs of wound infection. There was no difference between the groups without and with cells (groups 1 and 2, respectively) when analyzing epithelial thickness, granulation tissue thickness, and collagen index. However, a significant difference was observed between these groups and the negative control group. In addition, increased collagen deposition was observed in groups 1 and 2 on day 14 and epithelial remodeling in groups 1 and 2 on day 21. Wound healing markers showed increased expression of anti-inflammatory proteins and epidermal growth factor in group 1. In contrast, there was no difference in vascular endothelial growth factor (VEGF) expression between the groups. The glutathione peroxidase and superoxide dismutase activities were decreased in relation to the positive and negative control. The SHED-VEs revealed a cup-shaped morphology, expressing the classic markers for the exosomes CD9

and CD63, and were effectively internalized by keratinocytes. The results also indicated that 50% conditioned medium (CM) and 0.4 $\mu\text{g/ml}$ EVs were equally efficient in improving viability, migration, and attenuation of H_2O_2 induced cytotoxicity in the keratinocytes. Furthermore, VEGF expression in keratinocytes increased when treated with SHED secretome and EVs. **Conclusions:** The results suggest that the incorporation of cells in the bilayer scaffolds did not influence the histological characteristics of the granulation tissue and epithelium, or the collagen index. The bilayer scaffolds contributed to the formation of granulation tissue and early collagen deposition, maintaining an anti-inflammatory microenvironment. On the other hand, the SHED secretome and EVs proved to be efficient in improving the viability, migration and attenuation of H_2O_2 induced cytotoxicity in the keratinocytes. Therefore, both the bilayer scaffold and the SHED secretome may be promising therapeutic tools for accelerating re-epithelialization and wound healing.

Keywords: biomaterials, extracellular vesicles, skin, stem cells, secretome, tissue engineering.

LISTA DE FIGURAS

Figura 1. Estrutura da pele. Camadas da pele.....	13
Figura 2. Camadas da epiderme.....	14
Figura 3. Estrutura do estrato córneo.....	15
Figura 4. Níveis e componentes da barreira cutânea.....	17
Figura 5. Estrutura do polímero PLGA.....	23
Figura 6. Configuração básica do método de produção de eletrofiação.....	24

LISTA DE TABELAS

Tabela 1. Substitutos cutâneos comercialmente disponíveis.....	21
---	----

LISTA DE ABREVIATURAS E SIGLAS

CT	Células-tronco
CM	Do inglês <i>conditioned medium</i>
DAMPs	Do inglês <i>Damage-associated molecular patterns</i> - Padrões moleculares associados a danos
EGF	Do inglês <i>Epidermal Growth Factor</i> - fator de crescimento epidérmico
ERO	Espécies Reativas de Oxigênio
EVs	Do inglês <i>Extracellular vesicles</i>
FTIR	Do inglês <i>Fourier-transform infrared spectroscopy</i> - Infravermelho por transformada de Fourier
GPx	Do inglês <i>Glutathione peroxidase</i>
HFIP	1,1,1,3,3,3-hexafluoro2-propanol
H ₂ O ₂	Peróxido de hidrogênio
IL-10	Interleucina 10
MC	Meio condicionado
MEC	Matriz extracelular
MTT	Do inglês <i>3-(4, 5-dimethylthiazol-2-yl)-2,5-diphenyl tetrazolium bromide</i>
PAMPs	Do inglês <i>Pathogen-associated molecular pattern</i> - Padrões moleculares associados a patógenos
PC	Ácido pirrolidona carboxílico
PEG	Polietilenoglicol
PLGA	Do inglês <i>Poly(lactic-co-glycolic acid)</i>
PLLA	Ácido poli-L-láctico
PTH	Paratormônio
ROS	Do inglês <i>Reactive oxygen species</i> - Espécies Reativas de Oxigênio
SHED	Do inglês <i>Stem cells from human exfoliated deciduous teeth</i> - células tronco de dentes decíduos esfoliados humanos
TGF-β1	Do inglês <i>Transforming growth factor beta 1</i> - fator de transformação do crescimento beta
SOD	Superóxido dismutase
UCA	Ácido urocânico
VEGF	Do inglês <i>Vascular endothelial growth factor</i> - fator de crescimento do endotélio vascular
VEs	Vesículas extracelulares

SUMÁRIO

1.	Introdução	13
1.1	A pele.....	13
1.2	Funções da pele.....	16
1.2.1.	Barreira microbiológica, química, física e imunológica.....	16
1.2.2.	Termorregulação.....	17
1.2.3.	Receptor sensorial.....	18
1.2.4.	Síntese de vitamina D	18
1.3	Feridas crônicas e queimaduras	18
1.4	Engenharia tecidual e biomateriais	19
1.5	Fibrina.....	22
1.6	Ácido poli(lático-co-glicólico) (PLGA)	22
1.7	<i>Electrospinning</i>	23
1.8	Células-tronco derivadas de dentes decíduos esfoliados humanos.....	24
1.9	Secretoma de células-tronco	25
1.10	Artigo de revisão: <i>The role of stem cell-derived exosomes in the repair of cutaneous and bone tissue</i>	27
2.	Hipóteses.....	44
3.	Objetivos.....	45
4.	Capítulo 1.....	46
5.	Capítulo 2.....	59
6.	Capítulo 3.....	76
7.	Discussão	93
8.	Conclusões	96
9.	Referências	98
10.	Anexos	104

10.1.	Parecer da Comissão de Ética no Uso de Animais	104
10.2.	Parecer da Plataforma Brasil	105
10.3.	Produção acadêmica durante o doutorado	106
10.4.	Resumos publicados em anais de congressos	106
10.5.	Prêmios	108

1. Introdução

1.1 A pele

A pele é um dos maiores e mais importantes órgãos do corpo e compreende aproximadamente 16% do peso do corpo humano com uma área aproximada de 2 m² no adulto (EYERICH *et al.*, 2018; MCKNIGHT; SHAH; HARGEST, 2022). A pele forma a interface entre o corpo e o meio ambiente e cumpre diferentes funções fisiológicas essenciais para a manutenção da homeostasia do organismo. Dentre as funções encontramos: garantir a proteção contra agressões externas, contribuir na regulação da temperatura e do equilíbrio hídrico corporal, servir como receptor para as sensações gerais (dor, pressão, tato, temperatura) e a síntese de vitamina D3 (EL-CHAMI *et al.*, 2014; MCKNIGHT; SHAH; HARGEST, 2022).

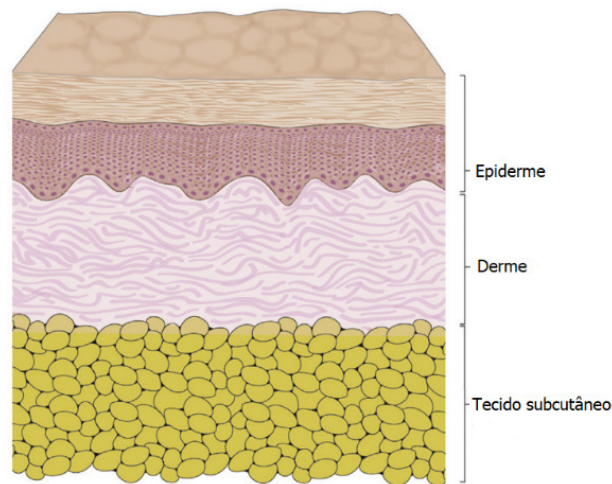


Figura 1. Estrutura da pele. Camadas da pele. Fonte: adaptado de MOAHAMED; HARGEST, 2022.

A pele consiste de duas camadas: epiderme e derme (Figura 1) (MICHAEL H. ROSS, 2016). A epiderme é a camada mais externa da pele, composta majormente por queratinócitos, e em menor proporção melanócitos, células de Langerhans e células de Merkel. A epiderme por sua vez é dividida em quatro camadas principais: o estrato córneo (camada mais externa), granular, espinhoso e basal (camada mais interna) (Figura 2).

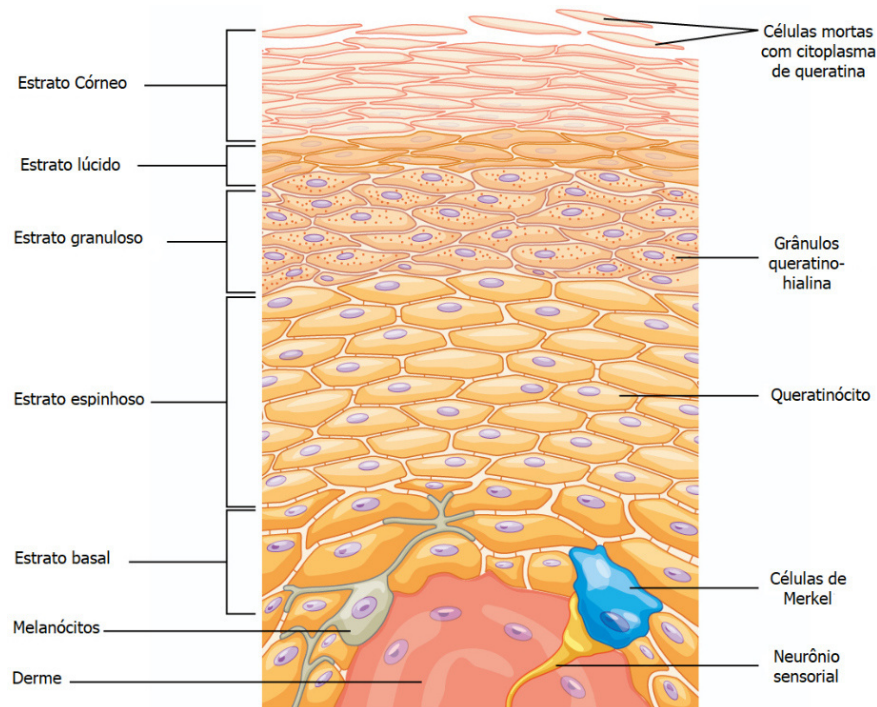


Figura 2. Camadas da epiderme. Fonte: adaptado de J GORDON, 2013.

A camada basal consiste em uma camada simples de queratinócitos unidos por desmossomos. Nessa camada se encontram os queratinócitos menos diferenciados e com maior capacidade de proliferação e migração. O processo de diferenciação dos queratinócitos, que ocorre à medida que as células migram da camada basal para a superfície da pele, resulta na queratinização. Na camada basal também se encontram melanócitos e células de Merkel (Figura 2). Os melanócitos produzem melanina para proteger as células dos danos produzidos pela radiação UV (KOBAYASHI *et al.*, 1998), enquanto que as células de Merkel desempenham uma função sensorial como mecanorreceptores, pois interagem com as terminações nervosas livres sensíveis ao toque (BARBIERI; WANAT; SEYKORA, 2014).

O estrato espinhoso é composto por queratinócitos que migraram da camada basal. Esses queratinócitos adotam uma morfologia poliédrica ao sofrer uma perda de água e manter as uniões intercelulares por desmossomos. Nessa camada também se encontram células de Langerhans, que são células dendríticas especializadas derivadas dos monócitos, que contribuem na apresentação antigênica (MOHAMED; HARGEST, 2022). O estrato espinhoso é característico da pele humana, mas não é encontrado na pele fina do rato (MAYNARD; DOWNES, 2019). Quando os queratinócitos entram no estrato granuloso, a síntese de proteínas que contribuem na cronificação do epitélio (pro-filagrina, filamentos de citoqueratina e lorricrina) se intensifica, sendo encapsuladas em grânulos basófilos de querato-hialina (BOUWSTRA; HELDER; EL GHALBZOURI, 2021). Além desses grânulos, os queratinócitos

também secretam os corpos lamelares, que contém uma mistura de ceramidas, colesterol e ácidos graxos livres (ADDOR; AOKI, 2010).

Finalmente, o estrato córneo é a camada mais externa, formada predominantemente por células anucleares e achatadas (corneócitos), com citoplasma formado por queratina. A superfície extracelular dos corneócitos está embebida pelo conteúdo lipídico dos corpos lamelares liberados no estrato granuloso, formando assim uma barreira semipermeável que serve como uma barreira de proteção contra os agentes externos, e evita a perda de fluidos e solutos do meio interno (BARBIERI; WANAT; SEYKORA, 2014) (Figura 3).

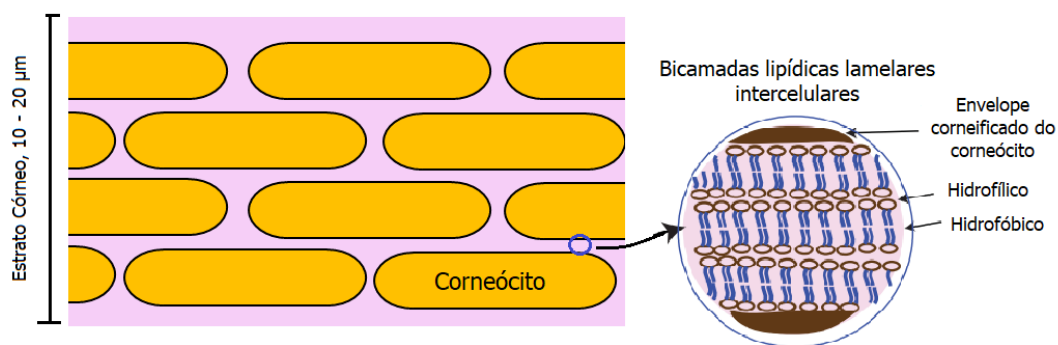


Figura 3. Estrutura do estrato córneo. No detalhe da esquerda estão ilustradas as bicamadas lipídicas lamelares entre os corneócitos. Fonte: adaptado de WOO, 2019.

A derme por sua vez, fornece suporte estrutural e nutricional à pele e é composta por tecido conjuntivo, contendo numerosos vasos sanguíneos, vasos linfáticos e nervos sensoriais (terminações nervosas livres e corpúsculos terminais como os corpúsculos de Pacini e Meissner) (LAI-CHEONG; MCGRATH, 2017). Adicionalmente, na derme encontram-se os anexos da pele, incluindo pelos, glândulas sudoríparas e glândulas sebáceas.

Histologicamente, a derme se divide em duas camadas: a camada papilar (mais superficial) constituída por tecido conjuntivo frouxo e a camada reticular (mais profunda) constituída por tecido conjuntivo denso não modelado (MOHAMED; HARGEST, 2022). Os quatro tipos principais de células residentes na derme são os fibroblastos, células dendríticas, macrófagos e mastócitos; sendo os fibroblastos dérmicos a principal fonte de matriz extracelular (MEC) da pele e os mais intimamente associados à MEC (LAI-CHEONG; MCGRATH, 2017).

A MEC da derme é composta principalmente por fibras estruturais de colágeno tipo I e III (70-80% do peso da pele seca), elastina e fibrilina (FRANTZ; STEWART; WEAVER, 2010). Também se compõe de moléculas não fibrosas como proteoglicanos (versicano e

decorina) e glicosaminoglicanos (ácido hialurônico, dermatan sulfato e sulfato de condroitina) que preenchem a maior parte do espaço intersticial extracelular e contribuem na hidratação e regulação do pH do tecido (HUANG *et al.*, 2022).

Sob a derme se encontra a hipoderme que consiste em um tecido conjuntivo frouxo que contém quantidades variáveis de tecido adiposo. Essa camada não faz parte da pele, não entanto atua como o principal suporte estrutural da pele e desempenha um papel vital na termorregulação, absorção de choques mecânicos e armazenamento de energia (BARBIERI; WANAT; SEYKORA, 2014; MICHAEL H. ROSS, 2016).

1.2 Funções da pele

1.2.1. Barreira microbiológica, química, física e imunológica.

Sendo a pele a nossa barreira mais externa, encontra-se colonizada por uma microbiota comensal proveniente do meio ambiente externo, incluindo bactérias, fungos e vírus (Figura 4). Essa microbiota constitui uma barreira contra a invasão por microrganismos patogênicos ao desenvolverem mecanismos para antagonizá-los por exclusão competitiva (HARRIS-TRYON; GRICE, 2022). Também, é capaz de transmitir sinais externos para a rede imune funcional da pele (EYERICH *et al.*, 2018) e secretar esfingomielinases, as quais processam os lipídios lamelares em ceramidas (um componente crítico do estrato córneo que reforça a barreira física) (HARRIS-TRYON; GRICE, 2022).

A barreira química da pele refere-se a diferentes fatores que contribuem com a manutenção da superfície ácida da pele para criar um ambiente químico que restringe a colonização bacteriana (EYERICH *et al.*, 2018) (Figura 4). Dentre esses fatores encontram-se o manto hidrolipídico, composto por aminoácidos, e derivados de aminoácidos, como ácido pirrolidona carboxílico (PCA) e ácido urocânico (UCA), além de ácido lático, açúcares, uréia, glicerol e uma variedade de íons (GUNNARSSON *et al.*, 2021). Um outro fator que contribui com a manutenção da superfície ácida da pele consiste na hidrólise de lipídios (triglicerídeos e colesterol) em ácidos graxos livres, efetuada por lipases secretadas pelas bactérias residentes. Esses ácidos graxos mantêm um pH baixo que inibe o crescimento de espécies patogênicas (COATES *et al.*, 2019). Adicionalmente, os queratinócitos produzem peptídeos antimicrobianos, os quais participam diretamente da eliminação de patógenos.

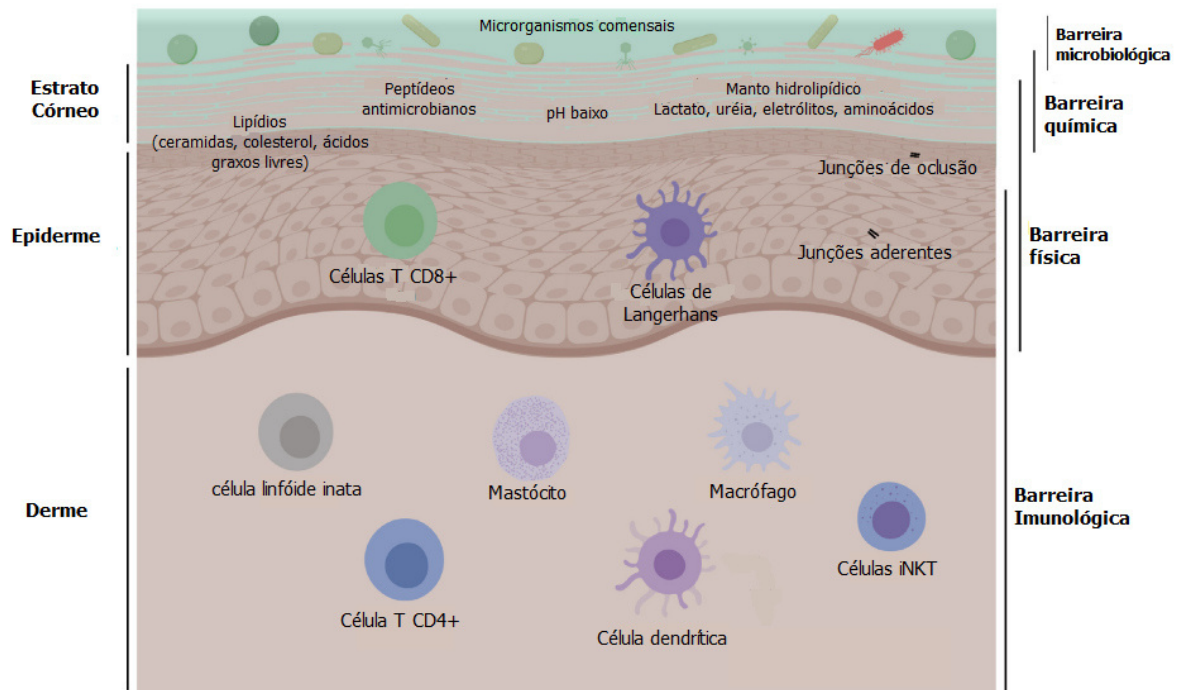


Figura 4. Níveis e componentes da barreira cutânea. Fonte: adaptado de EYERICH *et al.*, 2018.

A função de barreira física da pele é determinada pelo estrato córneo e as junções celulares presentes no epitélio, que impedem a penetração de substâncias potencialmente nocivas do ambiente externo, além de evitar a perda de água (EYERICH *et al.*, 2018). A prevenção da perda de água se explica graças à estrutura formada entre os corneócitos e a matriz lipídica intercelular apolar; enquanto que o envelope dos coneócitos (formado por filagrina, involucrina e outras proteínas) se conecta covalentemente com os lipídeos extracelulares e aporta resistência e resiliência à barreira (WOO, 2019) (Figura 3).

A barreira imune cutânea compreende uma variedade de células imunes inatas e adaptativas, residentes ou recrutadas, que povoam a epiderme e a derme (Figura 4). Essas células detectam com eficiência sinais de perigo através de padrões moleculares associados a patógenos e danos (PAMPs e DAMPs) e iniciam uma resposta imune adequada (EYERICH *et al.*, 2018).

1.2.2. Termorregulação

A pele participa de um sistema de feedback negativo que garante a manutenção de uma temperatura corporal estável em torno de 37°C. Esse sistema envolve a pele, os músculos esqueléticos, as glândulas sudoríparas e o hipotálamo. De forma geral, se a temperatura corporal cai, o hipotálamo envia sinais para contrair as arteríolas cutâneas e minimizar a perda de calor,

além de estimular os músculos esqueléticos a tremerem para gerar energia. Quando a temperatura corporal se normaliza, o sistema de feedback negativo detém os processos (MCKNIGHT; SHAH; HARGEST, 2022). Por outro lado, se a temperatura corporal aumenta, o hipotálamo aumenta a dilatação das arteríolas cutâneas, maximizando a perda de calor e estimulando as glândulas sudoríparas a produzirem suor.

1.2.3. Receptor sensorial

A pele também é um órgão sensorial, que contém um rico suprimento nervoso que informa ao cérebro sobre mudanças no ambiente de forma imediata. Na derme, as fibras nervosas mielínicas dos fascículos nervosos fornecem terminações nervosas para a epiderme e receptores sensitivos encapsulados na derme, incluindo os corpúsculos de Meissner (mecanorreceptores) e de Pacini (receptores para pressão profunda). As fibras nervosas que entram na epiderme perdem suas bainhas de mielina e se convertem em terminações nervosas livres ou se associam às células de Merkel, atuando como receptores táteis (OVALLE; NAHIRNEY, 2008).

1.2.4. Síntese de vitamina D

A epiderme é a principal fonte de vitamina D para o corpo. Como é bem conhecido, a vitamina D é produzida na pele a partir do 7-deidrocolesterol (7-DHC), hidroxilada primeiro no fígado (e outros tecidos) para 25 hidroxivitamina (25OHD), e depois no rim (e outros tecidos) para 1,25 dihidroxivitamina D (1,25(OH)₂D) (BIKLE, 2020). A forma ativa da vitamina D estimula a absorção intestinal de cálcio e fósforo, colabora com o paratormônio (PTH) na mobilização de cálcio do osso, e estimula a reabsorção de cálcio dependente de PTH nos túbulos distais renais. No entanto, sabe-se que os queratinócitos da epiderme possuem a maquinaria enzimática para metabolizar a vitamina D em seu metabólito ativo 1,25(OH)₂D. Essa molécula é capaz de regular o próprio metabolismo da pele ao controlar a proliferação celular na camada basal, favorecer a diferenciação e formação da barreira de permeabilidade, promover a imunidade inata e a regular o ciclo do folículo piloso (BIKLE, 2011).

1.3 Feridas crônicas e queimaduras

Globalmente as queimaduras são o quarto tipo de lesão mais frequente, depois de acidentes de trânsito, quedas e violência física (MARKIEWICZ *et al.*, 2022). Ainda, segundo a Organização Mundial da Saúde (OMS), estima-se que, a cada ano, aproximadamente 11 milhões de pessoas sofram queimaduras. Por outro lado, o ônus social e econômico causado

pelas feridas crônicas é subestimado e está crescendo devido ao envelhecimento da população e ao desenvolvimento precoce de doenças crônicas, como a diabetes (OLSSON *et al.*, 2019).

A excisão precoce do tecido lesado e a aplicação de autoenxertos/aloenxertos de pele parcial (*split-thickness skin grafts*) ou xenoenxertos é a base do tratamento de lesões dérmicas profundas e queimaduras de espessura total. Esse procedimento tem por objetivo reestabelecer a função de barreira da pele e evitar complicações comuns como sepse, hipotermia, e perda de proteínas e líquidos (CORUH; YONTAR, 2012; MARKIEWICZ *et al.*, 2022). No entanto, os autoenxertos de espessura parcial criam feridas no local doador semelhantes a queimaduras de segundo grau, aumentando ainda mais a morbidade. Além disso, a aplicação de enxertos de pele cadavérica ou xeno-enxertos acarreta riscos de resposta autoimune e de transmissão de doenças virais e bacterianas (CORUH; YONTAR, 2012; MARKIEWICZ *et al.*, 2022).

1.4 Engenharia tecidual e biomateriais

A engenharia tecidual consiste na associação de células, biomateriais ou *scaffolds* e substâncias bioativas, a fim de mimetizar o tecido nativo para restaurar, manter ou melhorar a sua função. Assim, os enxertos de pele gerados por engenharia tecidual podem ser produzidos usando diferentes polímeros naturais ou sintéticos. Dentre os polímeros naturais mais usados, encontram-se o colágeno, ácido hialurônico, quitosana e a fibrina. No caso dos polímeros sintéticos, os mais usados são o polietilenoglicol (PEG), poliuretano, ácido polilático-co-glicólico (PLGA), ácido poli-L-lático (PLLA), poliglactina e silicone (MARKIEWICZ *et al.*, 2022).

Os enxertos ainda podem ser celulares (*scaffolds* com incorporação de células) ou acelulares (*scaffolds* sem células) e, dependendo das camadas da pele que objetivam mimetizar, podem ser divididos em: epidérmicos, dérmicos ou dermo-epidérmicos. Assim, a engenharia tecidual da pele visa o desenvolvimento de enxertos de pele artificial que possam superar as limitações relacionadas ao uso de auto-enxertos e aloenxertos (OUALLA-BACHIRI *et al.*, 2020).

Atualmente, pode-se encontrar diversos substitutos cutâneos no mercado (ver Tabela 1) (OUALLA-BACHIRI *et al.*, 2020). No entanto, a maioria desses substitutos é produzida a partir de polímeros de origem xenogênica, alguns com células alogênicas, e outros com células autólogas (queratinócitos e fibroblastos). As principais desvantagens dos substitutos de origem xenogênico e alogênico, conforme relatado anteriormente, são os riscos relacionados à transmissão de doenças e à rejeição, respectivamente. Por outro lado, as limitações dos substitutos que contêm células autólogas consistem no longo tempo necessário para a cultura

de queratinócitos e o alto custo de processamento. Portanto, os pesquisadores na área da engenharia tecidual da pele continuam trabalhando com o intuito de fornecer uma solução integral e acessível para os pacientes.

Tabela 1. Substitutos de cutâneos comercialmente disponíveis.

Marca Comercial	Conteúdo celular	Fonte	Conformação	Estrutura anatômica	Tipo de Biomaterial	Descrição	Uso Clínico
AlloDerm®	Acelular	Alo	Bicamada	Dermal	Natural	Derme humana descélularizada e liofilizada com um lado “dérmico” e um lado de “membrana basal”	Aumento gengival, cobertura de raízes dentárias, queimaduras
Apligraf®	Celular	Xeno	Bicamada	Dermo-epidérmico	Natural	Queratinócitos e fibroblastos neonatais de prepúcio humano dentro de uma matriz de colágeno bovino tipo I	Licenciado apenas para úlceras de pé diabético (DFUs) e úlceras venosas de perna (VLUs)
Biobrane®	Acelular	Xeno	Bicamada	Dermal	Biossintético	Filme de silicone semipermeável parcialmente embutido em uma rede 3D de nylon funcionalizado com colágeno suíno tipo I	Queimaduras de espessura parcial superficial
Bioseed-S	Celular	Auto	Camada única	Epidermal	Natural	Queratinócitos autólogos suspensos em um <i>scaffold</i> de fibrina	Úlceras venosas crônicas resistentes à terapia
CryoSkin	Celular	Alo	Spray	Epidermal	Natural	Um spray celular feito de queratinócitos isolados de prepúcio de recém-nascido cultivados em silicone	Feridas superficiais
Dermagraft®	Celular	Alo	Camada única	Dermal	Sintético	Fibroblastos do prepúcio que secretam fatores de crescimento e MEC semeados em um andaime de malha de poliglactina bioabsorvível	Úlceras de pé diabético (DFUs), outras indicações clínicas
EPIBASE®	Celular	Auto	Camada única	Epidermal	Natural	Queratinócitos isolados de biópsia, cultivados e pulverizados sobre a ferida	Calcifilaxia cutânea, queimaduras
Epicel®	Celular	Auto	Camada única	Epidermal	Natural	Queratinócitos fixados a uma gaze com petróleo	Queimaduras dérmicas profundas
Epidex™	Celular	Auto	Camada única	Epidermal	Natural	Células precursoras de queratinócitos epidérmicos derivadas da bainha radicular externa do folículo piloso obtidas ao arrancar o cabelo do paciente. As células expandidas e depois cultivadas em um disco de membrana de silicone para produzir um equivalente epidérmico	Úlceras crônicas nas pernas
GraftJacket®	Acelular	Alo	Camada única	Dermal	Biossintético	Matriz de colágeno dérmico humano com canais vasculares	Lágrimas do manguito rotador
Hyalograft 3D®	Celular	Auto	Camada única	Dermal	Natural	Fibroblastos autólogos semeados em um <i>scaffold</i> de ácido hialurônico	Ferida de espessura total e parcial profunda
Integra®	Acelular	Xeno	Bicamada	Dermal	Biossintético	Matriz de fibras de colágeno de origem bovina e condroitina-6-sulfato, com uma membrana de silicone que atua como barreira	Queimaduras ou cirurgia reconstrutiva
Laserskin®	Celular	Auto	Camada única	Epidermal	Biossintético	Queratinócitos cultivados em uma membrana microperfurada de ácido hialurônico	Recapamento de feridas
Matriderm®	Acelular	Xeno	Camada única	Dermal	Biossintético	Um substituto dérmico com colágeno obtido da derme bovina e α -elastina hidrolisada	Para enxerto de pele de espessura parcial
OASIS®	Acelular	Xeno	Camada única	Composite	Natural	Matriz derivada da submucosa do intestino delgado suíno	Fechamento de feridas, úlceras de espessura total
OrCel®	Celular	Alo	Bicamada	Dermo-epidérmico	Natural	Queratinócitos epidérmicos e fibroblastos dérmicos co-cultivados em camadas separadas, em uma matriz esponjosa de colágeno bovino tipo I	Pacientes gravemente queimados
Permacol™ surgical implant	Acelular	Xeno	Camada única	Dermal	Natural	Matriz de colágeno derivado de derme suína e elastina	Especialmente usado para hérnia da parede abdominal e reconstrução dérmica
PolyActive®	Celular	Auto	Bicamada	Dermo-epidérmico	Natural	Componente macio de tereftalato de óxido de polietileno macio e um componente duro de tereftalato de polibutileno com queratinócitos e fibroblastos	Não especificado
Recell®	Celular	Auto	Camada única	Epidermal	Natural	Spray de queratinócitos e melanócitos	Queimaduras profundas
Suprathel®	Acelular	livre de células	Camada única	Epidermal	Sintético	Membrana porosa feita de um copolímero (terpolímero) de poli-dl-lactídeo, carbonato de trimetileno e ϵ -caprolactona	Queimaduras e abrasões de espessura parcial
SureDerm®	Acelular	Alo	Bicamada	Dermo-epidérmico	Biossintético	Derme humana descélularizada revestida com gelatina	Órbita exposta após exenteração
Terudermis®	Acelular	Xeno	Bicamada	Dermal	Natural	Esponja de colágeno bovino liofilizado reticulado com membrana de silicone	Queimaduras com exposição muscular ou óssea

Alogênico (Alo), autólogo (Auto), xenogênico (Xeno). Tabela adaptada de (OUALLA-BACHIRI *et al.*, 2020).

1.5 Fibrina

A fibrina é uma proteína fibrosa derivada da polimerização do fibrinogênio plasmático, que tem um papel importante nas etapas iniciais do processo de cicatrização ao contribuir com a formação do tampão hemostático para permitir a interação celular e deposição de matriz extracelular. Essa interação celular se deve principalmente ao fato da molécula de fibrina conter sítios Arg-Gly-Asp (RGD) para adesão celular, podendo se ligar também a vários tipos de células através de receptores de integrina. Dessa forma, os leucócitos ligam-se via receptores $\alpha M\beta 2$, as plaquetas via $\alpha IIb\beta 3$ e as células endoteliais e fibroblastos via $\alpha v\beta 3$, $\alpha v\beta 5$ e $\alpha 5\beta 1$ (SPROUL; NANDI; BROWN, 2017). Ainda, a fibrina possui sítios de ligação com proteínas da matriz extracelular, facilitando a regulação da adesão, proliferação e migração celular (HEHER *et al.*, 2018). Por outro lado, os produtos de degradação do fibrinogênio e/ou fibrina são capazes de modular a resposta inflamatória, afetando a migração de leucócitos e a produção de citocinas (ROBSON; SHEPHARD; KIRSCH, 1994; LAURENS; KOOLWIJK; DE MAAT, 2006; SPROUL; NANDI; BROWN, 2017).

Devido às propriedades biológicas desse polímero natural, o gel de fibrina tem sido amplamente investigado como agente hemostático em cirurgias, como *scaffolds* em engenharia tecidual, como promotor angiogênico na endotelização de enxertos vasculares e como sistema de liberação de drogas na cicatrização de feridas (AL KAYAL *et al.*, 2020).

Apesar dessas características, as fracas propriedades mecânicas do gel de fibrina tornam-se um fator limitante para as aplicações clínicas nas quais é necessário o fácil manuseio do biomaterial e o fornecimento de resistência mecânica, como por exemplo na cicatrização de feridas cutâneas. Devido a esses aspectos, torna-se necessário combinar a fibrina com polímeros sintéticos com propriedades mecânicas adequadas para preservar a integridade estrutural e a funcionalidade do biomaterial (*scaffold*) durante o momento da implantação e no longo prazo.

1.6 Ácido poli(lático-co-glicólico) (PLGA)

O PLGA é um copolímero sintético linear de ácido lático e ácido glicólico (Figura 5). É um biomaterial biodegradável e biocompatível, aprovado para aplicação clínica pela Agência Europeia de Medicamentos, bem como pela *Food and Drugs Administration* (FDA) dos EUA. O PLGA tem sido amplamente usado em todo o mundo para aplicações biomédicas e entrega de medicamentos, devido às suas vantagens proeminentes, como a facilidade de ajustar as taxas de degradação, boas propriedades mecânicas e excelente processabilidade (ZHAO *et al.*, 2016; MEKALA *et al.*, 2013). Ainda, seus produtos de degradação são facilmente metabolizados através do Ciclo de Krebs. No entanto, o PLGA é um polímero hidrofóbico e não possui sítios

naturais de reconhecimento de células. Para superar essas limitações, diferentes estratégias têm sido propostas, incluindo os tratamentos de superfícies ou combinando o PLGA com polímeros naturais e/ou moléculas bioativas, a fim de melhorar seu desempenho biológico (MEKALA *et al.*, 2013; ZHAO *et al.*, 2016).

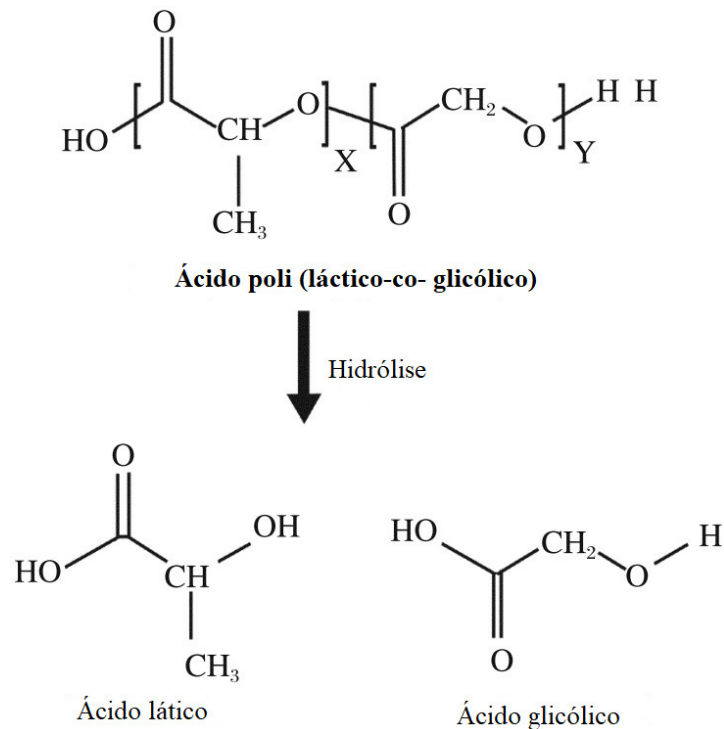


Figura 5. Estrutura do polímero PLGA e seus produtos de degradação (ácidos lático e glicólico) após hidrólise.

Fonte: adaptado de MEKALA *et al.*, 2013.

1.7 *Electrospinning*

O *electrospinning* ou eletrofição é uma técnica versátil que permite a fabricação de fibras contínuas em escala nanométrica a micrométrica. Dentre as vantagens dessa técnica está a sua simplicidade, baixo custo e obtenção de membranas com alta porosidade e alta relação superfície-volume, imitando a morfologia da matriz extracelular de um tecido. Por essa razão, as membranas fibrosas eletrofiadas têm sido amplamente investigados como potenciais *scaffolds* para aplicações biomédicas (RAMAKRISHNA *et al.*, 2005; MAURMANN; SPERLING; PRANKE, 2018).

O sistema compreende uma fonte de energia de alta tensão, uma bomba peristáltica, uma seringa com agulha e um coletor aterrado, conforme exemplificado na Figura 6. A técnica consiste na aplicação de um alto potencial elétrico entre dois eletrodos de polaridades opostas, um localizado na agulha e outro na placa coletora. A solução polimérica é acondicionada na

seringa, a qual será injetada pela bomba através da agulha, a uma determinada velocidade. Devido à alta tensão aplicada, a solução polimérica forma uma gota carregada eletrostaticamente na ponta da agulha. Posteriormente, a gota da solução polimérica forma um cone (cone de Taylor) devido a diferença de potencial entre a agulha e a placa coletora, gerando fios que saem da seringa em direção à placa coletora. As fibras são depositadas na placa, enquanto que o solvente usado para dissolver o polímero é evaporado durante o trajeto entre agulha e a placa coletora (XUE *et al.*, 2019).

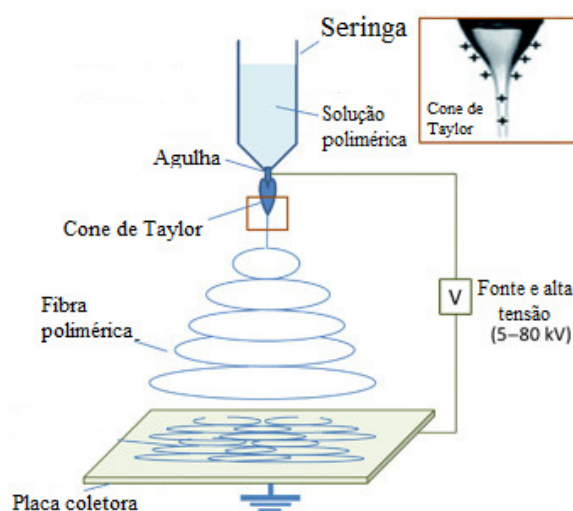


Figura 6. Configuração básica do método de eletrofiação. Fonte: adaptado de ZHENG, 2019.

Muitos parâmetros podem influenciar o processo de eletrofiação, incluindo as propriedades da solução (por exemplo, concentração, viscosidade, condutividade elétrica, tensão superficial, propriedades dielétricas), parâmetros do processo (por exemplo, voltagem, taxa de fluxo de fluido, distância da placa coletora) e parâmetros ambientais (como umidade e temperatura) (OKUTAN; TERZI; ALTAY, 2014). Sendo assim, é necessária a otimização dos parâmetros relacionados para a produção de fibras de boa qualidade.

1.8 Células-tronco derivadas de dentes decíduos esfoliados humanos.

Devido às propriedades regenerativas do secretoma e a sua capacidade de diferenciação em várias linhagens mesenquimais, as células-tronco (CT) têm sido aliadas importantes da engenharia tecidual e medicina regenerativa. Sendo incorporadas em *scaffolds*, injetadas por via intravenosa ou fazendo uso do seu secretoma para promover a reparação tecidual, as CT têm

mostrado resultados promissores em uma ampla gama de aplicações na engenharia de tecidos e medicina regenerativa (FITZSIMMONS *et al.*, 2018).

As células-tronco são células indiferenciadas, com capacidade de auto-renovação, e potencial de se diferenciar em diferentes tipos de células maduras. Essas células podem ser classificadas em: células-tronco embrionárias, células-tronco pluripotentes induzidas e células-tronco adultas (CTA) (ZAKRZEWSKI *et al.*, 2019). As CTA estão presentes na maioria dos tecidos e são responsáveis pela reposição desses ao longo da vida. Dentre as células-tronco adultas encontramos as células-tronco mesenquimais (CTM) e células-tronco hematopoiéticas (CTH). As CTM são uma população de células que originalmente foi identificada no estroma da medula óssea, e estão presentes em praticamente todos os tecidos (FRIEDENSTEIN, 1976; FRIEDENSTEIN; CHAILAKHYAN; GERASIMOV, 1987).

Em 2006 a Sociedade Internacional de Terapia Celular e Genética apresentou os critérios mínimos para definir as CTM. Segundo essa padronização, as células devem ser aderentes ao plástico, expressar os marcadores CD73, CD90 e CD105, e não expressar os marcadores hematopoiéticos e endoteliais CD11b, CD14, CD19, CD34, CD45, CD79a e HLA-DR. Também, devem ser células capazes de se diferenciar *in vitro* em adipócito, condrócitos e osteoblastos (DOMINICI *et al.*, 2006).

As células-tronco derivadas de dentes decíduos esfoliados humanos (*stem cells from human exfoliated deciduous* - SHED) são um tipo de CT adultas. Essas células foram inicialmente descritas em 2003 por Miura e colaboradores como sendo uma população de células multipotentes com uma alta capacidade de proliferação, auto-renovação e de diferenciação em uma variedade de tipos de células (incluindo células neurais, adipócitos e odontoblastos) (MIURA *et al.*, 2003). As SHED residem no nicho perivascular da polpa dentária e são consideradas uma ferramenta promissora para a medicina regenerativa ao ser uma fonte não invasiva de células multipotentes e apresentar menos implicações éticas do que outras fontes de células-tronco (KO; CHEN; SU, 2020).

Nos últimos anos, novos estudos têm sugerido que os fatores parácrinos secretados pelas CT seriam os principais responsáveis pelos seus efeitos terapêuticos. Assim, o estudo do secretoma dessas células, e em especial das vesículas extracelulares, ganharam muita atenção devido ao seu importante papel na comunicação célula-célula.

1.9 Secretoma de células-tronco

O secretoma é definido como o conjunto de substâncias liberadas pelas células para o seu entorno, incluindo fatores solúveis e vesículas extracelulares, que apresentam um amplo

espectro de ação biológica e potencial terapêutico. A fração solúvel do secretoma é abundante em moléculas imunomoduladoras, citocinas, quimiocinas e fatores de crescimento (MÚZES; SIPOS, 2022). Entretanto, a fração vesicular consiste em VEs que são classificadas em exossomos, microvesículas e corpos apoptóticos, de acordo com a biogênese, tamanho e composição. Essas vesículas carregam moléculas bioativas como proteínas, ácidos nucleicos e lipídios que estão envolvidas na comunicação célula a célula. Estudos tem sugerido que o perfil de RNAs das microvesículas e corpos apoptóticos poderia ser similar, enquanto que o perfil de RNAs dos exossomos é diferenciado (LÄSSER; JANG; LÖTVALL, 2018).

Os exossomos apresentam um diâmetro de 30 a 150 nm e se originam da via endocítica, sendo formados dentro dos corpos multivesiculares (KALRA; DRUMMEN; MATHIVANAN, 2016). Todavia, as microvesículas se originam a partir do brotamento e fissão da membrana plasmática, apresentando um diâmetro médio de 100 a 800 nm. Os corpos apoptóticos são vesículas heterogêneas que são conhecidas por serem liberadas de células em processo de apoptose e apresentam um diâmetro de 200 a 5000 nm (LÄSSER; JANG; LÖTVALL, 2018).

1.10 Artigo de revisão: *The role of stem cell-derived exosomes in the repair of cutaneous and bone tissue*

Artigo publicado no *Journal of Cellular Biochemistry* em 2022. Fator de impacto (2021) de 4,480

The role of stem cell-derived exosomes in the repair of cutaneous and bone tissue

Juliana Girón^{1,2}  | Natasha Maurmann^{1,2}  | Patricia Pranke^{1,2,3} 

¹Hematology & Stem Cell Laboratory, Faculty of Pharmacy, Universidade Federal do Rio Grande do Sul, Porto Alegre, Rio Grande do Sul, Brazil

²Post Graduate Program in Physiology, Universidade Federal do Rio Grande do Sul, Porto Alegre, Rio Grande do Sul, Brazil

³Stem Cell Research Institute, Porto Alegre, Rio Grande do Sul, Brazil

Correspondence

Juliana Girón, Hematology & Stem Cell Laboratory, Faculty of Pharmacy, Universidade Federal do Rio Grande do Sul, Porto Alegre, RS 90610-000, Brazil. Email: 00305205@ufrgs.br

Funding information

Fundação de Amparo à Pesquisa do Estado do Rio Grande do Sul (FAPERGS); Conselho Nacional de Desenvolvimento Científico e Tecnológico (CNPq); Coordenação de Aperfeiçoamento de Pessoal de Nível Superior (CAPES); Ministério da Ciência, Tecnologia, Inovações e Comunicações (MCTIC); Financiadora de Estudos e Projetos (FINEP)

Abstract

Exosomes are extracellular vesicles secreted by various cell types, which play important roles in physiological processes. In particular, stem cell-derived exosomes have been shown to play crucial functions in intercellular communication during the tissue healing process. This review summarizes the effects of exosomes derived from different stem cell sources on the repair of cutaneous and bone tissue, focusing on the different pathways that could be involved in the regeneration process. The biogenesis, isolation, and content of exosomes have also been discussed. The effectiveness of exosomes is broadly demonstrated for skin and bone regeneration in animal models, supporting the basis for clinical translation of exosomes as a ready-to-use cell-free therapeutic for skin and bone regeneration.

KEYWORDS

bone, exosomes, paracrine communication, skin, stromal cells, tissue regeneration

1 | INTRODUCTION

Stem cells (SCs) are an attractive alternative for the treatment of injured tissue, not only because of their differentiation potential but also because of their paracrine activity. SCs are able to release biologically active molecules such as microRNAs (miR), messenger RNAs (mRNAs), and proteins, which could modulate the activity of recipient cells involved in the wound repair process.¹ The microRNAs are posttranscriptional regulators that could influence the tissue regeneration

process by networking with cell signaling pathways and complex transcriptional programs.

Those biologically active molecules are commonly released through membrane vesicles of endosomal origin called exosomes. Exosomes (Exos) are a type of extracellular vesicle (EV) secreted by a variety of mammalian cell types, which are considered important mediators of cell-to-cell communication. Therefore, it is believed that SCs achieve an *in vivo* therapeutic effect mainly through paracrine signaling, using various mechanisms to interact with the target cells.

Exosomes can fuse with the plasma membrane of the target cells and then deposit their content. They can also be internalized by pinocytosis/phagocytosis or execute their functions by ligand-receptor binding, in which exosomes interact with surface molecules of the target cells to activate intracellular signaling.¹ Interestingly, the exosome membrane contributes to protecting the bioactive substances they carry from adverse conditions, such as high temperatures and pH variations.² Some examples of bioactive molecules found in Exos from different sources of SCs are presented in Table 1. Endothelial progenitor cells (EPCs) were included as the authors are categorizing them as unipotent SCs.¹⁷

Furthermore, SCs have demonstrated pro-regenerative properties when transplanted, despite their not being retained in organs for longer periods. In fact, studies have demonstrated that SCs, when implanted in the wound site, rarely differentiate, and their viability is limited, probably due to the harsh inflammatory microenvironment at the wound site.¹⁵ Hence, the paracrine ability of SCs is probably the key function of these cells.

SC Exos have been demonstrated to possess SC-like pro-regenerative properties, and for this reason, the use of such molecules has been proposed instead of using the SCs in their entirety for the treatment of injured tissue, thus, avoiding the adverse effects of SCs such as tumor formation, thrombosis, or immune responses. Furthermore, Exos present high stability and are easier to store and transport.

The present review summarizes the effects of SC-derived Exos on the repair of cutaneous and bone tissue, focusing on the different pathways that could be involved in the healing process. To begin with, the biogenesis and secretion of exosomes will be described, as well as the isolation methods and some strategies used to improve the impact of SC-Exos in tissue repair.

Following this, the effects of SC-exosomes in cutaneous regeneration and bone regeneration will be described, and finally, the use of biomaterials as exosome carriers.

2 | METHODS

The following formula was used for the initial search in the PubMed database: (exosome [MeSH terms]) AND (wound healing [MeSH terms]), using the 5-year filter. From this search, a total of 104 articles were obtained, and after applying the exclusion/inclusion criterials, a total of 37 articles were used. For the second search, the formula (exosome [MeSH terms]) AND (bone regeneration [MeSH terms]) was used, also with the 5-year filter. From this search 20 articles were obtained, from which 8 articles were used. Some additional articles were taken from referenced studies in the previous articles and used for this review.

Only articles in English using SC-derived exosomes or EPC-derived exosomes were selected because EPCs have been considered by some authors as unipotent SCs, which present asymmetric cell division and promising therapeutic effects.¹⁷ Articles using exosomes from other cell sources were discarded. No review papers were selected. Papers with the aim of studying the regeneration of tissue, aside from bone and cutaneous tissue, were also discarded.

3 | BIOGENESIS OF EXOSOMES

Exos are 30–150 nm, and are generated in endosomal multivesicular compartments. Exos are surrounded by a bilayer of phospholipids enriched with cholesterol, sphingomyelin, and hexosylceramids, besides some

Stem cell source	Exosome cargo	References
ADSCs	Nrf2, Wnt-3a	[3,4]
BSCs	miR-21-5p	[5]
BMMSCs	miR-214, miR-21, miR-126, miR-125b, miR-27b, and miR-19b, VEGF, miR-26a, Stat3	[6-9]
ESCs	miR-200a	[10]
EPCs	lncRNA-MALAT1, miR-126	[11,12]
UCMSCs	miR-21, miR-23a, miR-125b, and miR-145, AKT, PDGF-D, Wnt4, miR-126	[2,13-15]
USCs	DMBT1	[16]

TABLE 1 Examples of stem and endothelial progenitor cell-derived exosome cargo

Abbreviations: ADSC, adipose-derived stem cell; BSC, bone stem cell; BMMSC, bone marrow mesenchymal stem cell; DMBT1, malignant brain tumors 1; ESC, embryonic stem cell; EPC, endothelial progenitor cell; lncRNA, long noncoding RNA; MALAT1, Metastasis associated lung adenocarcinoma transcript 1; miR, microRNA; Nrf2, nuclear factor erythroid 2; PDGF-D, platelet-derived growth factor D; VEGF, vascular endothelial cell growth factor; USC, urine-derived stem cell; UCMSC, umbilical cord-derived mesenchymal stem cell.

proteins involved in cell recognition and binding such as tumor susceptibility gene 101 (TSG101), Alix, flotillin 1, tetraspanins (CD9, CD63, and CD81), integrins, and cell adhesion molecules.¹⁸

These small EVs are formed by the inward budding of the plasma membrane, generating an early endosome. The membrane from the early endosome then invaginates and buds into the endosome, forming the intraluminal vesicles (ILVs), as shown in Figure 1.

The generation of ILVs can occur through different mechanisms. The ESCRT is the best-described mechanism, which is composed of four separate protein complexes that interfere in multivesicular body (MVB) formation, vesicle budding, and cargo sorting.¹⁹ Additionally, ESCRT-independent machineries can also be involved in the formation of MVB, such as the ceramide-dependent pathway and the tetraspanin-dependent pathway. The ceramide-dependent pathway is based on the formation of lipid rafts that cluster the sphingomyelin of the endosomal membrane; the sphingomyelin is then converted into ceramide by sphingomyelinases.²⁰ These ceramide-enriched domains are able to coalesce and then form the ILVs. On the other hand, tetraspanin-enriched domains together with CD81 could also play a key role in sorting target receptors and intracellular components toward exosomes.²¹ Therefore, it is believed that several mechanisms could be involved for ensuring the sorting of bioactive molecules into

exosomes; however, to bring to light the specific SC-related mechanisms, more studies will be required.

Finally, through ESCRT-dependent machinery or ESCRT-independent machinery, proteins and RNAs are packed into the ILVs, and the formed structure is called an MVB. A portion of MVBs could be digested by fusion with lysosomes, while others fuse to the plasma membrane mediated by RAB and SNARE proteins, allowing for the release of the ILVs to the extracellular space, thereby liberating the exosomes.²²

Although many publications have adopted the term “exosome,” the use of this term is in fact not appropriate as the common isolation protocols are not able to separate the different subpopulations of EVs or the non-vesicular entities with similar density or size. Thus, the isolated sample generally contains a mixture of EVs together with exosomes, microvesicles, and apoptotic bodies. Therefore, the International Society for Extracellular Vesicles endorses the use of the terms “small EVs” (<100 nm or <200 nm) and “large EVs” (>200 nm).²³ However, as the cited studies in this review adopted the term exosome, we will refer to the small EVs as exosomes.

4 | EXOSOME ISOLATION

Among the isolation methods, the most commonly used is differential ultracentrifugation (UC), in which the conditioned medium, obtained after the cultivation of the cells, is

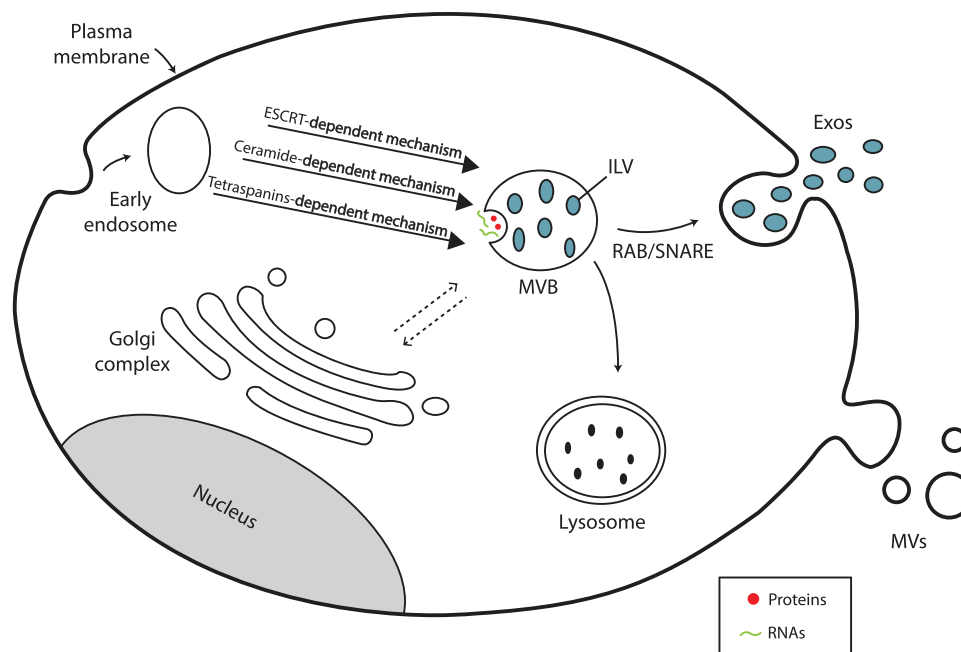


FIGURE 1 Biogenesis and secretion of exosomes. ESCRT, endosomal sorting complex required for transport; Exos, exosomes; ILV, intraluminal vesicles; MVs, microvesicles; MVB, multivesicular body; RAB, Ras-related proteins in brain; SNARE, soluble N-ethylmaleimide-sensitive factor attachment protein receptor.

subjected to a series of centrifugations with a sequential increase in centrifugal force, which can start at 300g and finish with over 100 000g. The objective of this method is to separate the larger vesicles from the smaller ones to obtain the exosomes. However, the limitations of this technique are the aggregation of the EVs, their possible damage as a consequence of the high speed, and the contamination with other structures with similar size ranges such as exomers²⁴ and high-density lipoproteins.

The density gradient centrifugation (DGC), on the other hand, is a method that provides a more purified separation, which combines the size and the density isolation method in which a gradient made by sucrose or iodixanol is used.

Ultrafiltration (UF) is a size-based isolation method in which the conditioned medium of the SCs is filtered through a membrane with a specific pore size by pressure or centrifugation. This is a rapid and efficient method; however, filters usually get easily jammed due to the trapping of vesicles.²⁵

In the method of polymer-based precipitation (PP), a polymer solution is used, such as polyethylene glycol, which decreases EV solubility, leading to precipitation at low-speed centrifugation. A disadvantage of this method is that EVs are not exclusively isolated, being coisolated by other molecules, including RNA-protein complexes.¹⁸

Immunoaffinity isolation is a technique in which EV surface protein antibodies are associated with beads or other matrices, allowing for the physical separation by low-speed centrifugation or magnetic techniques.²⁶ The used antibodies could be specific for the isolation of specific EV subpopulations or could also be designed to trap unwanted EV populations.

Size exclusion chromatography is a size-based separation technique that uses a stationary phase column filled with a porous matrix. In this case, small particles such as proteins, smaller than the pore size, are retained in the matrix by entering the pores, thus, taking longer to pass through the column. On the other hand, EV, bigger than the pore size, get eluted first.²⁶

In terms of efficiency, DGC and size exclusion chromatography have been reported to obtain the purest exosome preparations, followed by UC. However, these techniques are time-consuming and require special equipment.²⁷ In contrast, precipitation solution-based techniques like ExoQuick-TC™ and Total Exosome Isolation™ are easy to execute, but kits are expensive and co-isolate contaminating factors, which can interfere with the results of experiments.²⁷ Moreover, precipitation techniques present a higher protein yield, but as a consequence of contaminating nonexosomal proteins.^{27,28} Hence, the composition of proteins and RNAs from the isolated sample can be different and depends on the used purification method.

From the papers used to conduct this review, 47% used UC, 22% used two steps isolation with a UF followed by DGC for further purification. The 20% used precipitation kits, the 6% used two steps isolation with a UF followed by UC, 4% used only DGC and 2% used only UF. Table 2 describes the percentage distribution of the commercially available isolation kits used for each technique in the analyzed papers. Table 2 shows that ExoQuick-TC™ was the most used for PP, while the Centrifugal Filters Amicon (Millipore) were used in all papers with the UF technique. In the case of DGC, there was a preference for 30% sucrose/D₂O cushions prepared in laboratory, probably due to the high cost of commercially available density gradient mediums. No papers with the immunoaffinity isolation technique were found.

5 | NANOVESICLES ENGINEERED FROM STEM CELLS

As the yield of SC-exosomes is a limiting factor for large-scale production for cell-free therapies, the generation of cell-derived nanovesicles (CDNs) by extruding living SCs through microfilters has been reported.²⁹ The resulting plasma membrane fragments can convert into nanovesicles due to the self-assembling property of the lipid membrane in the aqueous phase. Jeong and colleagues obtained CDNs by

Isolation methods	Commercially available isolation kits	%
DGC	OptiPrep™ Density Gradient Medium	15
	30% sucrose/D ₂ O cushion (prepared in laboratory)	85
UF	Amicon Ultra-15 Centrifugal Filter Unit (Millipore)	100
PP	ExoQuick-TC™	70
	Exosome Isolation Reagent (RiboBio)	20
	Total Exosome Isolation Reagent (Thermo)	10

TABLE 2 Percentage distribution of the commercially available isolation kits used in analyzed papers

extruding murine embryonic stem cells (ESCs) and collecting them by density-gradient centrifugation.²⁹ The generated exosomes were shown to have a spherical morphology similar to exosomes secreted from ESCs, and also to contain RNAs and proteins from the origin cells. The CDNs were able to enhance migration and proliferation into fibroblasts. Furthermore, the fibroblasts increased expression levels of vascular endothelial cell growth factor (VEGF)- α , transforming growth factor (TGF)- β , proliferating cell nuclear antigen (PCNA), Ki-67, and the phosphorylated form of mitogen-activated protein kinase (MAPK) (p-MAPK), suggesting that these membrane proteins of the nanovesicles could trigger the MAPK signal pathway when they make contact with the cell plasma membrane.²⁹

Similarly, Lee and colleagues generated CDNs from induced pluripotent stem cells (iPSCs) by the serial extrusion technique and collected them by density-gradient UC using iodixanol.³⁰ The iPSC-CDNs showed similar physicochemical features to exosomes from iPSCs (iPSC-Exos), but with an increased production yield, an important advantage for clinical applications. Treatment with iPSCs-CDNs significantly reduced the activity of a typical senescence marker, the senescence-associated- β -galactosidase, in senescent fibroblasts.³⁰ Furthermore, iPSCs-CDNs suppressed the expression of p53 and p21, key factors involved in cell cycle arrest, apoptosis, and cellular senescence signaling pathways.

6 | STRATEGIES TO IMPROVE THE IMPACT OF SC-EXOSOMES IN TISSUE REPAIR

Some studies have reported the use of strategies to enhance the beneficial effect of SC exosomes in the regulation of tissue repair. The transfection of SCs with specific noncoding RNA or protein genes has, therefore, been proposed. Then, SC-derived exosomes overexpressing such molecules will be able to enhance tissue repair.^{31,32} While gene editing is a promising technique that could enhance the expression of important molecules involved in the tissue regeneration process, these technologies still present limitations like off-target effects and possible safety issues, making them difficult to apply in humans today.

Another reported strategy is based on the preconditioning of SCs before the isolation of the derived exosomes to enhance their biological functions. Various preconditioning strategies have been reported, such as the precondition with magnetic nanoparticles;⁵ subjecting SCs to hypoxic conditions or hypoxic-mimetic agents;^{33,34} and also preconditioning with tumor necrosis factor-alpha (TNF- α) concentrations, simulating an inflammatory ambient.⁴

Additionally, the preconditioning of SCs could be used not only to enhance their biological functions but also to increase the exosome production as SCs have a limited capacity for releasing exosomes. Wang and colleagues found that the preconditioning of MSCs with a combination of N-methyltyrosine and norepinephrine significantly increased exosome production three-fold, probably by enhancing metabolic activity.³⁵ It is important to note that the treatment did not alter the ability of the MSC exosomes to induce angiogenesis, polarize macrophages to an anti-inflammatory phenotype or downregulate collagen expression. However, exosome secretion is a cell-specific process and molecule modulators do not necessarily have the same effects on all cell types.

Moreover, the conjugation of specific aptamers to SC-exosomes has also been reported. Aptamers are single-stranded DNA/RNA oligonucleotides, capable of binding to target molecules with high affinity and specificity.^{8,36} Aptamers could, therefore, be used for driving the SC-exosomes to the injured site, where a target molecule is localized.

7 | EFFECTS OF SC-EXOSOMES IN CUTANEOUS REGENERATION

Skin lesions are very common occurrences with a high rate of mortality and morbidity, often involving significant consequences such as barrier function destruction and alterations in the perception of pain, temperature, and touch. Thus, alternatives for wound healing treatment are urgently required.

A number of studies have analyzed the effects of SC-Exos on cutaneous wound healing, using different cell sources and routes of administration. Local subcutaneous injections are common, but also, intravenous injections have demonstrated that exosomes can be recruited to the wound area and contribute to accelerating cutaneous wound healing.³⁷ The congregation of intravenously injected exosomes in the wound area could likely be related to the homing function of SCs. Recently, a study demonstrated that a combined topical application and intravenous administration of ADSC-Exos is more effective in promoting wound healing.³⁸

7.1 | Exosomes from Bone Marrow Stem Cells (BMSC-Exos)

In vitro BMSC-Exos have been shown to contribute to fibroblast migration and proliferation through AKT, STAT3, and ERK 1/2 signaling pathways.⁹ Furthermore,

BMMSCs are enriched with transcriptionally active STAT3, a transcription factor involved in migration, proliferation, angiogenesis, and growth factor production.⁹

Wu and colleagues isolated exosomes from bone mesenchymal stem cells (BSCs) preconditioned with Fe₃O₄ magnetic nanoparticles and a static magnetic field. BSC-Exos showed a higher expression of miR-21-5p, a microRNA able to downregulate SPRY2, a protein with antiangiogenic properties and related with cell migration and proliferation inhibition. BSC-Exos significantly improved fibroblast migration and tube formation in human umbilical vein endothelial cells (HUVEC), *in vitro*, and were able to activate the PI3K/AKT and ERK 1/2 signaling pathways on fibroblast and endothelial cells by transferring miR-21-5p. *In vivo*, BSC-Exos induced a higher wound closure rate, less scar formation, and more collagen deposition.⁵

As it is an established fact that hypoxic preconditioning in SCs improves their regenerative properties, Ding and colleagues preconditioned BMMSCs with deferoxamine, a classical hypoxic-mimetic that mimics the oxygen deprivation effects.⁶ The authors isolated the exosomes from the deferoxamine preconditioned cells and found a marked upregulation of miR-126 when compared with normal exosomes. The miR-126, which is involved in the angiogenesis process, was able to induce the activation of the PI3K/AKT pathway in HUVECs and promote neovascularization.

Recently, another method for enhancing the biological functions of BMMSCs was proposed by Qiu and colleagues through the pretreatment of these cells with exosomes from neonatal mice serum.³³ In the study, exosomes from pretreated BMMSCs were isolated and analyzed in a full-thickness mice model. *In vitro*, exosomes were able to promote endothelial cell proliferation, migration, and tube formation. Furthermore, the endothelial cells treated with the exosomes highly expressed AKT and endothelial nitric oxide synthase (eNOS), suggesting that the promotion of angiogenesis could take place via regulating the AKT/eNOS pathway. The authors noted that exosomes significantly increased wound healing by inducing angiogenesis, which was confirmed by quantification of the expression of the endothelial marker CD31 in the skin tissue samples.³³

7.2 | Exosomes from Human Umbilical Cord Stem Cells (UCMSC-Exos)

UCMSC-Exos have been demonstrated to accelerate wound healing, reduce scar formation, and also to reduce the expression of α -smooth muscle actin (α -SMA).² Hence, UCMSC-Exos may be able to reduce scarring and

in situ myofibroblast formation as they express specific microRNAs (miR-21, miR-23a, miR-125b, and miR-145), which could suppress the activation of the TGF- β /smad2 pathway involved in myofibroblast differentiation.² Furthermore, UCMSC-Exos are able to parallelly activate Wnt/ β -catenin and AKT signaling pathways in keratinocytes to prompt wound healing. The Wnt4 protein (which is expressed in UCMSCs-Exos) leads to the activation of β -catenin, and thus, improves keratinocyte proliferation and migration.³⁹ Furthermore, UCMSC-Exos were able to improve vascularization at the wound site.¹³ This occurs through the Wnt4 protein being present in UCMSC-Exos, which can activate Wnt/ β -catenin in endothelial cells.

Additionally, the AKT protein transfection into SCs could be a good strategy for improving the angiogenesis properties of exosomes.¹⁴ AKT plays an important role in promoting cell proliferation and inhibiting cell apoptosis. Ma and colleagues demonstrated that exosomes from UCMSCs overexpressing AKT (AKT-Exos) were able to promote endothelial cell proliferation, migration, and tube formation *in vitro*, and increased blood vessel formation when the chick allantoic membrane assay was developed.¹⁴ Moreover, AKT-Exos highly expressed the platelet-derived growth factor D (PDGF-D), a protein with proangiogenic activity. When the expression of PDGF-D was knockdown in AKT-Exos, the promotion of tube formation was markedly absent in the endothelial cells.¹⁴

7.3 | Exosomes from Induced Pluripotent Stem Cell (iPSCs-Exos)

iPSCs have exhibited similar properties to ESCs with the advantage of not presenting ethical concerns. iPSCs-Exos stimulated the proliferation and migration of human dermal fibroblasts and HUVECs in a dose-dependent manner *in vitro*.^{37,40} In addition, iPSC-Exos are able to promote accelerated reepithelialization, induce collagen deposition, promote higher vessel densities, and a higher number of mature vessels *in vivo*.⁴⁰ Similarly, Lu and colleagues found that iPSC-Exos *in vivo*, could contribute to accelerating wound healing, epithelialization, and angiogenesis, with no risk of teratoma formation, and having a similar wound closure speed when compared to living iPSCs.⁴¹ Autologous iPSC-Exos more effectively accelerated wound healing, epithelialization, and angiogenesis. However, the performance of allogenic exosomes was still better than the control, consisting of phosphate buffered saline (PBS) without Exos. Additionally, allogenic iPSC-Exos did not generate a host immune response. Thus, the mass-production of allogenic iPSC-

Exos could be an interesting alternative for wound healing therapeutics.

7.4 | Exosomes from adipose tissue-derived stem cells (ADSCs-Exos)

ADSCs are an interesting exosome source as a remarkable number of proteins involved in various biological processes are packed in such vesicles. Proteomic analysis of ADSC-Exos has revealed their potential role as a therapeutic strategy. Xing and colleagues identified 1185 proteins in ADSC-Exos, which participate in metabolic pathways, focal adhesion, regulation of actin cytoskeleton, microbial metabolism, and interestingly, in some tissue repair-related signaling pathways such as MAPK, VEGF, and Jak-STAT.⁴²

Furthermore, ADSC-Exos were also able to enhance keratinocytes migration and proliferation by the Wnt/ β -catenin signaling pathway.⁴³ Moreover, these exosomes have demonstrated the ability to upregulate the expression of extracellular matrix (ECM) markers such as Collagen I (Col 1), Collagen III (Col 3), α -SMA, and matrix metalloproteinase-1 (MMP1) in fibroblast, by the PI3K/AKT signaling pathway *in vitro*, and increase the number of blood vessels.⁴⁴ The angiogenesis-inducing activity of ADSC-Exos has also been shown to serve therapeutic functions in the wound healing of diabetic animals.

He and colleagues established a skin lesion model by exposing HaCaT and fibroblast to H₂O₂ *in vitro*.⁴⁵ ADSC-Exos were, therefore, isolated to elucidate the mechanism of exosomes in wound healing. They confirmed the expression of metastasis associated lung adenocarcinoma transcript 1 (MALAT1) on ADSC-Exos. MALAT1 is a long noncoding RNA that could be involved in the regulation of cell migration and cell cycle. ADSC-Exos were able to reduce the apoptotic rate of impaired HaCaT and fibroblast. In addition, exosomes significantly attenuated H₂O₂-induced suppression of cell proliferation and migration by downregulating miR-124 and activating the Wnt/ β -catenin pathway.⁴⁵ When MALAT1 was knockdown in ADSC-Exos, these protective effects were lost in HaCaT and fibroblast.

Moreover, some researchers have proposed modifying exosomes by overexpressing important molecules involved in the tissue regeneration process as a strategy for enhancing the biological properties of such vesicles. Shi and colleagues observed that ADSC-Exos with the overexpression of the noncoding circular RNA 0000250 (ADSCs-circ_0000250-exos) enhanced cell proliferation and tube formation of EPCs submitted to high glucose conditions.³¹ The *in vivo* assay in diabetic rats showed

that ADSC-circ_0000250-exos were able to accelerate wound closure and significantly improve vascularization. These exosomes also significantly suppressed the expression of miR-128-3 (a proinflammatory molecule) and promoted sirtuin 1 expression, which has anti-inflammatory and antioxidant properties.³¹ Additionally, Li and colleagues demonstrated that ADSC-Exos expressed Nrf2, a protein-related to cell migration, proliferation, apoptosis, and differentiation, along with the regulation of adaptative responses to oxidative stress.⁴⁶ ADSC exosomes were able to accelerate cutaneous wound healing in diabetic mice by reducing reactive oxygen species (ROS) and the inflammatory cytokine level. Furthermore, ADSC-Exos prevented the senescence of the EPCs subjected to a high glucose environment (as occurs with diabetic patients), in addition to improving vascularization. When Nrf2 were overexpressed in ADSC-Exos, the results were potentiated.

7.5 | Exosomes from human urine-derived stem cells (USC-Exos)

USCs are a noninvasive and low-cost exosomes source, with relatively easy isolation, multipotent differentiation, and telomerase activity without presenting teratoma formation. Exosomes from USCs have also shown their ability to stimulate angiogenesis. Chen and colleagues demonstrated that USC-Exos were able to promote angiogenesis by transferring DMBT1, a protein that is highly expressed in this type of exosome.¹⁶ DMBT1 can increase the expression of VEGF-A, which activates the PI3K-AKT pathway. USC-Exos also promoted a faster wound closure in diabetic mice, with a higher rate of re-epithelialization, lower level of scar formation, a larger amount of blood vessels, and collagen deposition.¹⁶ Such characteristics were attenuated when the expression of DMBT1 in USCs was knockdown, showing the importance of the role of DMBR1 in the wound healing process.

7.6 | Exosomes from Embryonic Stem Cells (ESC-Exos)

ESCs present attractive therapeutic properties due to their pluripotency; however, ethical concerns and associated tumorigenesis and immune rejection risks make them difficult to use in wound healing treatments. Until now, an only one study was reported with ESC-Exos. Chen and colleagues analyzed the effects of ESC-Exos in HUVECs with D-galactose-induced senescence and found that chronic ESC-Exos treatment could reduce the aging

hallmarks and recover the compromised function, such as proliferation, migration and tube formation by transferring miR-200a.¹⁰ ESC-Exos treatment also restored the oxidative stress balance, reduced ROS intensity and restored Nrf2 levels. Additionally, the authors found a high expression of miR-200a in ESC-Exos, which can down-regulate Keap1 expression, and therefore activate Nrf2. In vivo, ESC-Exos accelerated the wound healing process and promoted local angiogenesis at the wound site in aged mice by rejuvenating endothelial senescence.¹⁰

7.7 | Exosomes from menstrual blood stem cells (MenSCs-Exos)

MenSCs-Exos have also been analyzed as menstrual blood is an accessible, noninvasive, rich source of MSCs.⁴⁷ These exosomes were able to promote a faster re-epithelialization and wound closure in diabetic wounds by enhancing angiogenesis and inducing the transition of the phenotype M1 macrophages to M2 macrophages.

7.8 | Exosomes from Endothelial Progenitor Cells (EPCs-Exos)

EPCs-Exos contribute to wound healing by positively modulating vascular endothelial cell function as EPC exosomes are able to upregulate the expression of proangiogenic molecules in vascular endothelial cells, including fibroblast growth factor-1 (FGF-1), VEGFA, VEGFR-2, angiopoietin-1 (ANG-1), E-selectin, chemokine-16 (CXCL-16), eNOS, and interleukin-8 (IL-8).⁴⁸ These findings are in agreement with other studies, showing that EPC-Exos significantly enhance endothelial cell proliferation, migration, and angiogenic tubule formation in vitro.⁴⁹ Additionally, EPC-Exos remarkably enhance the amount of total and mature blood vessels at the wound site, being directly proportional to the exosome concentration. Those actions are carried out by the activation of ERK 1/2 signaling in endothelial cells, favoring wound repair. Furthermore, it was observed that inhibition of this signaling process significantly blocked the proangiogenic effects of exosomes.⁴⁹

To sum up, SC-derived exosomes can activate different signaling pathways involved in the skin regeneration process, among which can be mentioned PI3k/AKT, ERK 1/2, Wnt/ β -catenin, and nuclear factor-kappa B. These mechanisms contribute principally to enhancing cell properties of keratinocytes, fibroblasts, and endothelial cells. Additionally, exosomes could contribute to the

regulation of ROS and cytokine levels, such as in macrophage transition into an anti-inflammatory profile M2 (Figure 2).

Examples of SC-derived exosome sources, isolation method, and use in skin regeneration are shown in Table 3.

8 | EFFECTS OF SC-EXOSOMES IN BONE REGENERATION

Bone healing is an intricate process in which the regulation of migration, proliferation, and differentiation of local mesenchymal SCs or progenitor cells is crucial.

SC-derived exosomes are able to promote osteogenesis, principally through four mechanisms: reducing apoptosis; recruiting mesenchymal SCs and promoting their proliferation; creating an osteoinductive environment to promote the osteogenic differentiation of SCs; and promoting angiogenesis and bone vascularization.³

8.1 | Exosomes from EPC

Bone healing is closely coupled with the angiogenesis process during neo-osteogenesis, in which EPCs contribute to the formation of new blood vessels, besides being able to regulate bone formation by secretion of various trophic factors, such as SDF-1, an important factor for MSC and EPC migration.⁵¹ Furthermore, it has been demonstrated that EPCs may enhance osteogenic properties of MSCs in a paracrine form. Xu and colleagues demonstrated that when MSCs were cocultivated with EPC, MSCs showed increased alkaline phosphatase (ALP) activity, besides significantly enhanced expression of the osteogenic genes osteopontin (OPN), bone sialoprotein (BSP), and runt-related transcription factor 2 (Runx2). The study also confirmed that EPCs may have positive paracrine effects on osteogenic differentiation of MSCs by activating the p38 MAPK signaling pathway.⁵²

Bone remodeling is the final phase of bone healing and occurs through a process that includes initial hard callus resorption by the osteoclasts, followed by the formation of the bone matrix through the osteoblasts, which subsequently become mineralized. Interestingly, a study showed that EPC-derived exosomes (EPCs-Exos) promoted osteoclastogenesis through the LncRNA-MALAT1/miR-124 pathway.¹¹ Exosomes from EPC highly expressed LncRNA-MALAT1, and when their effect was analyzed in bone marrow-derived macrophages (BMMs), exosomes negatively controlled miR-124 activity and upregulated the expression of integrin β 1 (ITGB1). ITGB1 is a protein involved in the osteoclast

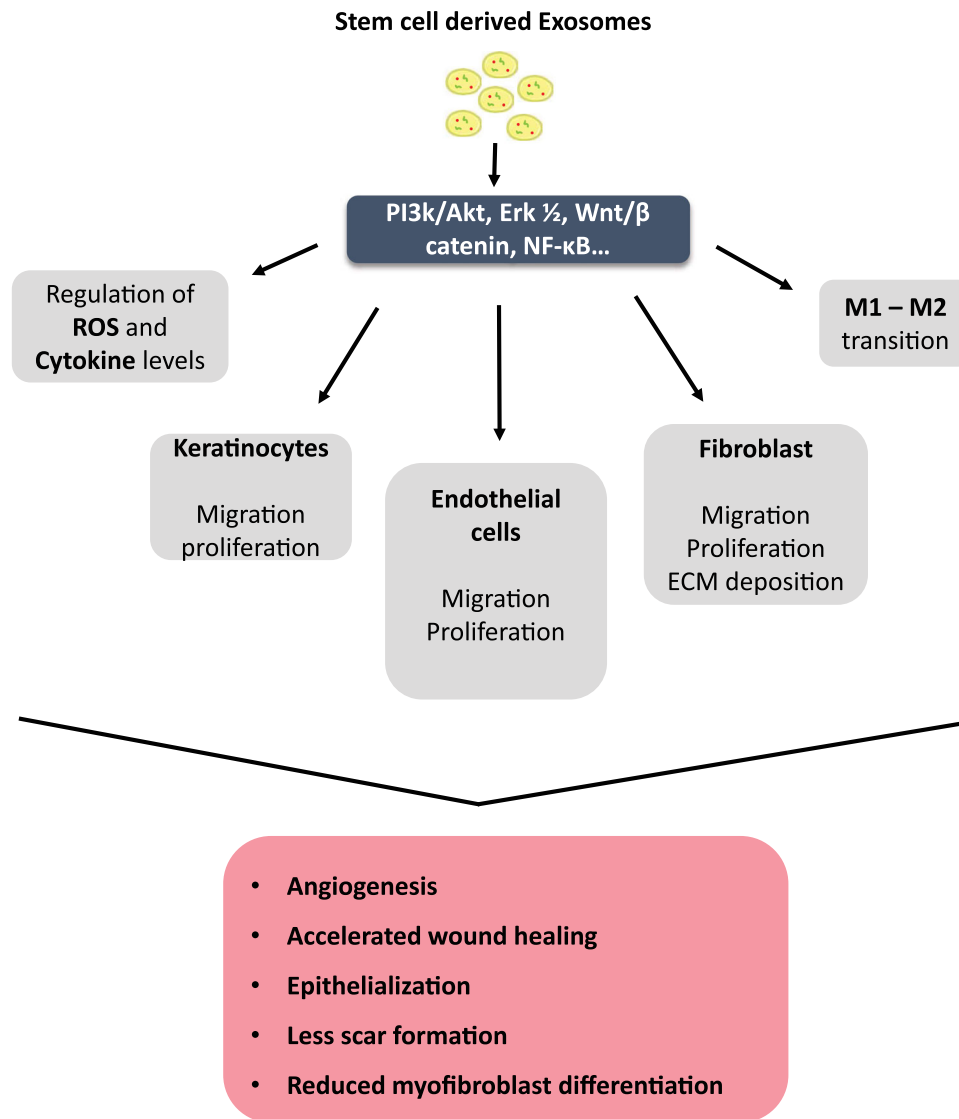


FIGURE 2 Mechanisms involved in cutaneous regeneration induced by stem cell-derived exosomes. M1, proinflammatory macrophages; M2, anti-inflammatory macrophages

differentiation process, while miR-124 downregulates osteoclastogenesis by suppressing the nuclear factor of the activated T cell, cytoplasmic (1NFATc1) expression.⁵³ Furthermore, BMMs treated with the EPCs-Exos expressed osteoclast markers such as MMP9, CTSK, TRAP, and CAR2.¹¹ The authors concluded that EPCs-Exos could promote bone repair by enhancing the recruitment and differentiation of osteoclast precursors through LncRNA-MALAT1.¹¹ Similar findings were reported by Furuta and colleagues, who reported TRAP-positive cells in the calluses of femur fractures treated with BMMSC-Exos, 10 days after surgery.⁵⁴

Moreover, the generation of new blood vessels in healing bone is crucial for providing nutrition, gas exchange, and systemic circulation factors. Importantly, exosomes from SCs and progenitor cells have been

proven to contribute to angiogenesis induction. Jia and colleagues found a marked expression of miR-126 in EPC-Exos, which was able to downregulate SPRED-1 (a Ras/ERK inhibitor) and activate the Ras/ERK signaling pathway on HUVECs in vitro.¹² EPC-Exos also enhanced proliferation, migration, and tube formation of HUVECs, besides increasing the expression of angiogenesis-related genes: VEGF-A, basic FGF (bFGF), TGF-β1, and ANG. In vivo, EPC-Exos significantly accelerated callus formation and mineralization, improved bone formation, and increased the vessel density in a tibial distraction osteogenesis model.¹²

EPC-Exos were also able to accelerate reendothelialization in rat models of balloon-induced vascular injury when 30 μg of exosomes were intravenously injected.⁵⁵ Additionally, EPC-Exos promoted proliferation and migration

TABLE 3 Examples of stem and endothelial progenitor cell-derived exosome-mediated skin regeneration

Source	Isolation method	Model	Dose	Effect	Pathway	References
ADSCs	PP	In vitro HaCaT cells exposed to H ₂ O ₂ to simulate a skin lesion model	-	Promoted cell proliferation, migration, and inhibited cell apoptosis of HaCaT	Wnt/ β -catenin	[43]
ADSCs	PP	In vitro skin lesion model by exposing HaCaT and fibroblast to H ₂ O ₂	-	Attenuated the suppression of cell proliferation, migration, and apoptotic rate induced by H ₂ O ₂	Wnt/ β -catenin	[45]
ADSCs	PP	Full-thickness excisional wound models in mice	200 μ g	Exos intravenous injections were superior to local injections, promoting collagen expression at the early stage, thereby accelerating wound healing	-	[37]
ADSCs	UC	Full-thickness excisional wound models in mice	200 μ g	Increased gene expression and protein levels of Col 1, Col 3, α -SMA, and MMP1 in fibroblasts. Enhanced number of blood vessels	PI3K/AKT	[44]
BMSCs	UC	Full-thickness excisional wound models in rats	25 μ g	Accelerated wound closure, narrower scar widths, and higher vessel densities	PI3K/AKT and ERK 1/2	[5]
BMMSCs	UC	In vitro	10 μ g/ml	Enhanced fibroblast proliferation and migration	AKT, STAT3, ERK 1/2	[9]
ESCs	UC	Pressure-induced ulcer model in aged mice	1×10^{10} particles	Accelerate wound healing and higher vessel densities	Nrf2	[10]
EPCs	UF \rightarrow DGC	Full-thickness excisional wound models in diabetic rats	1×10^{11} particles	Higher vessel densities, faster wound closure, higher reepithelialization, and collagen deposition and less scar formation	ERK 1/2	[50]
iPSCs	PP	Full-thickness excisional wound models in macaques	50 μ g	Accelerated wound healing, epithelialization, and angiogenesis. No teratomas formation. Similar wound closure speed between iPSCs and their Exos	-	[41]
iPSCs	UC	In vitro	40 μ g	Larger collagen deposition. Higher vessel densities and numbers of mature vessels. Stimulation of the proliferation and migration of fibroblasts and HUVECs in a dose-dependent manner	-	[13]
UCMSCs	UF \rightarrow DGC	Second-degree burn injury in rats	200 μ g	Accelerated re-epithelialization	Wnt/ β -catenin and AKT	[13]
USCs	PP	Full-thickness excisional wound models in diabetic mice	200 μ g	Higher amount of blood vessels and collagen deposition.	PI3K/AKT by increasing the VEGF-A levels	[16]

Abbreviations: ADSC, adipose-derived stem cell; BMMSC, bone marrow mesenchymal stem cell; BMSC, bone marrow stem cell; Col 1, Collagen I; Col 3, Collagen III; DGC, density gradient centrifugation; EPC, endothelial progenitor cell; ESC, embryonic stem cell; iPS, induced pluripotent stem cell; MMP1, matrix metalloproteinase-1; PP, polymer-based precipitation; UCMSC, umbilical cord-derived mesenchymal stem cell; UF, ultrafiltration; USC, urine-derived stem cell; VEGF-A, vascular endothelial cell growth factor A; α -SMA, α -smooth muscle actin.

of endothelial cells *in vitro* and stimulated endothelial cells to express angiogenesis-related molecules, including eNOS, IL-8, ANG-1, E-selectin, HIF-1 α , VEGF-A, and VEGFR-2. These results suggest that EPC-Exos promote vascular repair by upregulating endothelial cell function.⁵⁵

8.2 | Exosomes from UCMSC

Zhang and colleagues used a commercial hydrogel (HyStem-HP hydrogel) to deliver UCMSC exosomes in a rat model of femoral fracture.⁵⁶ The administration of UCMSC-Exos led to a statistically significant increase in bone mineral density, bone volume, and vessel volume. *In vitro*, HUVECs treated with UCMSC-Exos exhibited remarkable increases in VEGF and HIF-1 α levels, in addition to enhancing proliferation, migration, and angiogenic tube formation ability. On the other hand, the authors did not find a significant difference in the osteogenesis-related genes of osteoblasts treated with the UCMSC-Exos or those incubated in differentiation medium. Therefore, the results suggest that UCMSC-Exos did not regulate the expression of osteogenesis-related genes, and subsequently, the promotion of fracture healing could be related to the promotion of angiogenesis and not to the acceleration of osteogenic differentiation.⁵⁶

However, another study found that UCMSC-Exos were able to promote the expression levels of β -catenin and Wnt3a in healing bone at the fracture site and to promote osteoblast differentiation by increasing the expression levels of osteogenic marker genes COL-1, OPN, and Runx2.⁵⁷ Thus, UCMSC-Exos probably participate in fracture repair through the Wnt signaling pathway.

Furthermore, Liu and colleagues compared the effect of exosomes derived from UCMSCs under hypoxia (hypo-UCMSC-Exos) and those derived under normoxia (UCMSC-Exos) in a bone fracture model.¹⁵ Hypoxia preconditioning mediated enhanced production of exosomal miR-126 through the activation of Hypoxia-inducible factor-1 α (HIF-1 α). Hypo-UCMSCs-Exos, highly enriched with miR-126, promoted angiogenesis, proliferation, and migration in HUVECs by transferring miR-126.³⁴ Furthermore, miR-126 was able to downregulate the activity of the SPRED1 protein, thereby activating the Ras/ERK pathway. When miR-126 was knockdown in hypo-UCMSC-Exos, the beneficial effects of these exosomes were absent. *In vivo*, transplantation of hypo-UCMSC-Exos caused a significant increase in the ratio callus volume/tissue volume and blood vessel density at Day 7.³⁴

8.3 | Exosomes from ADSCs

Exosomes from ADSCs have also been analyzed for bone regeneration purposes. Chen and colleagues overexpressed the miR-375 in ADSCs, a positive regulator in the osteogenic differentiation of MSCs.⁵⁸ The isolated exosomes (miR-375-ADSC-Exos) improved the osteogenic differentiation of BMSCs and the ALP activity was significantly enhanced. The mRNA expression of osteogenesis-related genes: Runx2, ALP, COL1, and OCN in BMSCs with osteogenic induction was upregulated. It was determined that miR-373 could downregulate the insulin-like growth factor-binding protein-3 (IGFBP3) expression.⁵⁸ IGFBP3 is an osteoblast differentiation inhibitor that is able to suppress the bone morphogenetic protein 2 (BMP-2) signaling.⁵⁹ *In vivo*, miR-375-ADSC-Exos were incorporated in a commercial hydrogel, exhibiting an enhanced bone regenerative capacity in a rat model of calvarian defect.⁵⁸

On the other hand, exosomes from ADSCs preconditioned with TNF- α (mimicking the acute inflammatory phase), were able to enhance the proliferation and osteogenic differentiation in human primary osteoblastic cells (POC) *in vitro*.⁴ Furthermore, exosomes from preconditioned cells presented an elevated Wnt-3a content, and parallelly, POC cultivated with such exosomes showed a significant increase in β -catenin expression. Later, the inhibition of Wnt signaling resulted in a significant decrease in osteogenic gene expression levels.⁴ The results suggest that TNF- α preconditioning on ADSCs potentiate the trophic function from released exosomes by increasing the Wnt-3a content in exosomes.

8.4 | Exosomes from bone BMSCs

BMSCs have been widely used in bone regeneration strategies due to their osteogenic capacity,⁶⁰ and in recent years, BMSC-derived exosomes have shown promising results. Zhang and colleagues found that exosomes from BMMSCs, analyzed in a rat model of femoral nonunion, enhanced bone formation, increased the expression of osteogenesis-related genes (BMP-2, Smad1, Runx2, osteoglycin, and osteoprotegerin), and angiogenesis-related genes (HIF-1 α and VEGF).⁶¹ Moreover, the expression of Smad and Runx2 was significantly reduced in mouse embryo osteoblast precursor cells when incubated with BMMSC-Exos in the presence of a BMP-2 inhibitor *in vitro*. The results above suggest that BMMSC-Exos could contribute to the fracture healing process by activating osteogenic differentiation through the BMP-2/Smad1/Runx2 signaling pathway, but also

improve vascularization through the HIF-1 α /VEGF pathway.⁶¹

Moreover, pro-osteogenic properties of SC exosomes could be affected by aging. Xu and colleagues found a marked overexpression of miR-128-3p on BMMSC-Exos derived from older rats.⁶² The overexpression of miR-128-3p could suppress the osteogenic differentiation of MSCs by Smad5 downregulation. Smad5 participates in BMP-induced osteogenesis. BMP receptor mediates their signals through Smad proteins like Smad5 and regulate gene transcription during osteoblastic differentiation and bone formation. Thus, the osteogenic effects of BMMSC-Exos derived from aged rats could be attenuated by up-regulated miR-128-3p.⁶²

In agreement with other studies, Takeuchi and colleagues demonstrated that BMMSC-Exos are able to promote bone regeneration by enhancing angiogenesis.⁷ In vitro, BMMSC-Exos enhanced osteogenic and angiogenic gene expression in MSCs. Additionally, researchers found that BMMSC-Exos are charged with the VEGF proangiogenic protein, and are also able to induce VEGF secretion from the recipient cells. Furthermore, BMMSC-Exos promoted larger bone formation and a higher number of blood vessels in vivo.⁷ In contrast, when exosomes with an angiogenesis inhibitor (Exo-anti VEGF) were administered, the results were the opposite.

Enhanced bone regeneration by inducing angiogenesis was also reported by Liang and colleagues. They evaluated exosomes derived from BMMSCs preconditioned with a low dose of dimethylxylglycine (DMOG), a hypoxic-mimetic agent.⁶³ DMOG-MSC-Exos were able to significantly downregulate PTEN, an endogenous negative regulator of the PI3 kinase signal pathway, activating the AKT/mTOR (mammalian target of rapamycin) pathway to stimulate angiogenesis in HUVECs in vitro. This contributed to obtaining a significantly larger new bone area and mineralization parameter, such as enhanced blood vessel area in a critical-sized calvarial defect rat model in vivo.⁶³ Interestingly, both the MSC-Exos and DMOG-MSC-Exos groups significantly enhanced the expression of molecules, critical for proliferation, and migration in HUVECs, including, p65, Hippo-YAP, JAK-STAT, and β -catenin. However, PTEN exhibited the most significant change, suggesting that different mechanisms could be involved in angiogenesis promotion.

Systemic administration of SC-derived exosomes directed toward the treatment of bone injuries is not considered an option as the majority of exosomes are accumulated in the liver and lungs. Considering this factor, Luo and colleagues conjugated a BMMSC-specific aptamer to Exos (BMMSCs-Exos-apt) to improve the

accumulation of such exosomes in the injured bone where BMMSCs are present.⁸ The results showed that the BMMSC-Exos-apt were able to enhance the osteoblastic differentiation of BMMSCs in vitro, as well as the accumulation of BMMSC-Exos-apt at the injury site in vivo when were systemically administered. Additionally, the BMMSC-Exos-apt promoted higher bone formation in a femur fracture model when compared with normal Exos and the control group.⁸

Moreover, because characteristics of the micro-environment of parental cells may influence the function of released exosomes, Zhu and colleagues analyzed the bone regenerative effect of exosomes secreted by BMMSCs from diabetic type I rats (dBMMSC-Exos) and compared this with exosomes secreted by BMMSCs derived from normal rats (nBMMSC-Exos).⁶⁴ They found that the bone regenerative effect of exosomes derived from BMMSCs is impaired in diabetes mellitus type I, probably due to the high levels of advanced glycation end products (AGEs). Although dBMMSC-Exos and nBMMSC-Exos enhanced the osteogenic differentiation of BMMSCs and promoted the angiogenic activity of HUVECs, nBMMSC-Exos had a greater effect. These findings were confirmed in vivo in rat calvarial defects, when more extensive bone regeneration was seen in the nBMMSC-Exos group than the dBMMSC-Exos group. Similarly, a greater new capillary formation was found in the nBMMSC-Exos group than in the dBMMSC-Exos group.⁶⁴ Thus, exosomes from diabetic patients may not be appropriate for therapeutic purposes.

To sum up, exosomes derived from different sources of stem and progenitor cells can activate different signaling pathways involved in the bone regeneration process, such as Wnt/ β -catenin/Runx2, Bmp-2/Smad/Runx2, P38 MAPK, Ras/ERK, VEGF, AKT/mTOR, JAK-STAT, and β -catenin (Figure 3). The activated mechanisms could contribute to enhancing cell properties of MSCs, endothelial cells, and osteoclasts, allowing for osteoblast proliferation and differentiation, enhanced angiogenesis, and regulation of osteoclast activity. SPRED1 and miR-124 can be downregulated by SC-Exos to allow for the activation of tissue regeneration-related mechanisms.^{12,34,53}

Examples of SC-derived exosome sources, isolation method, and use in bone regeneration are shown in Table 4.

9 | EXOSOMES AND BIOMATERIALS

In recent years, a proposal has been made for the incorporation of SC-derived exosomes with scaffolds to provide a sustained release of these bioactive molecules,

Stem cell derived Exosomes

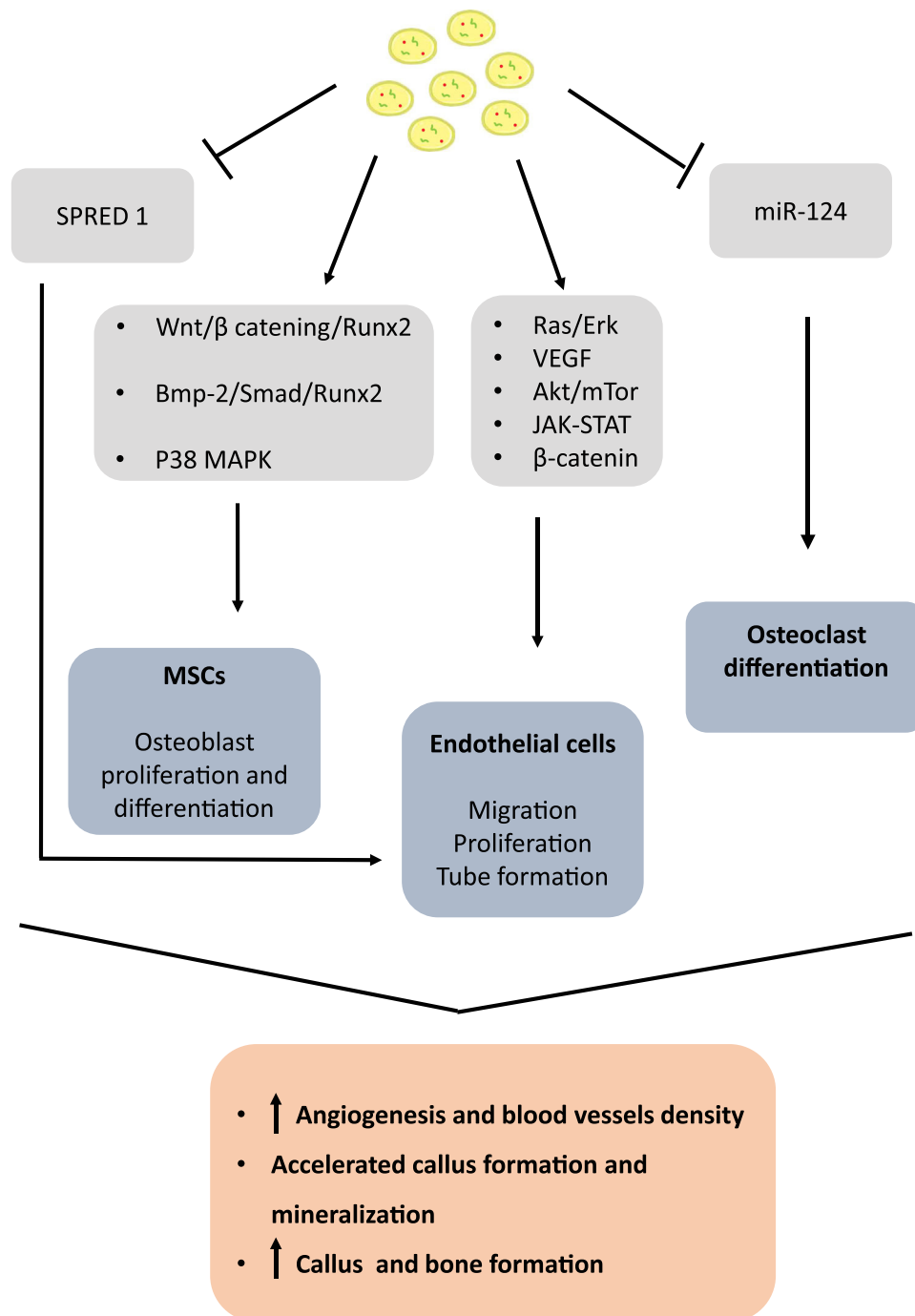


FIGURE 3 Mechanisms involved in bone regeneration induced by stem cell-derived exosomes

avoiding the rapid clearance rate when administrated by injection.⁶⁵

Wang and colleagues elaborated an injectable adhesive thermosensitive multifunctional polysaccharide-based dressing with sustained release of ADSC-Exos.⁶⁶ The scaffold maintained the exosome bioactivity and showed angiogenic properties, allowing for more collagen deposition and a faster reepithelialization process

in diabetic wounds, with less scar formation and appearance of skin appendages. Furthermore, the incorporation of ADSC-Exos on a hyaluronic acid scaffold has also been reported for the promotion of ECM deposition by fibroblast, as well as reepithelialization and vascularization in wound healing.⁶⁷

Li and colleagues incorporated ADSC-Exos with a PLGA scaffold coated with polydopamine (pDa).³ The

TABLE 4 Examples of stem and endothelial progenitor cell-derived exosome-mediated bone regeneration

Cell source	Isolation method	Model	Dose	Effect	Pathway	References
BMMSCs	UC	Femur fracture model in mice	-	Accelerated fracture repair	-	[54]
BMMSCs	UC	Femoral nonunion rat model	10 ¹⁰ particles	Enhanced osteogenesis, angiogenesis, and bone healing processes	BMP-2/Smad1/Runx2 HIF-1 α /VEGF	[61]
BMMSCs	UF→DGC	Femoral fracture model	200 μ g	Enhanced bone formation and higher expression of osteogenesis-related genes	Smad5/Runx2	[62]
BMMSC	UC	Calvarial defects	100 μ g	Superior proangiogenic properties and bone regeneration	AKT/mTOR	[63]
EPCs	UF→DGC	Femur fracture model in mice	-	Enhanced osteoclastogenesis and fracture repair	LncRNA-MALAT1/ miR-124	[11]
EPCs	UF→DGC	Tibial distraction osteogenesis model	10 ¹¹ Exos	Accelerated bone regeneration and higher vessel density	SPRED1/Ras/ERK	[12]
Hypoxic UCMSCs	UF→DGC	Femoral fracture model	200 μ g	Significant increase in callus volume/tissue volume, and blood vessel volume, and number	SPRED1/Ras/ERK	[15]

Abbreviations: BMMSC, bone marrow mesenchymal stem cell; BMP-2, bone morphogenetic protein 2; DGC, density gradient centrifugation; EPC, endothelial progenitor cell; HIF-1 α , hypoxia-inducible factor-1 α ; lncRNA, long noncoding RNA; miR, micro RNA; mTOR, mammalian target of rapamycin; PP, polymer-based precipitation; Runx2, Runt-related transcription factor 2; UCMSC, umbilical cord-derived mesenchymal stem cell; UF, ultrafiltration; VEGF, vascular endothelial cell growth factor.

pDa was added to adhere and carry the exosomes. The addition of the exosomes significantly promoted more new bone tissue in a critical-sized bone defect. Additionally, it was found that the number of host MSCs recruited on the implanted scaffolds with exosomes was approximately two-fold higher compared with those without exosomes. The results suggest that other mechanisms could be involved for MSC recruitment to enhance bone regeneration through SC exosomes.³

Wang and colleagues developed an injectable, self-healing, and antibacterial polypeptide-based hydrogel formed by Pluronic F127, (F127), oxidative hyaluronic acid (OHA), and poly- ϵ -L-lysine (EPL) with a pH-responsive for long-term ADSC-Exos release.⁶⁸ In the hydrogel, OHA was selected because of its water-retaining ability and biocompatibility; EPL provided antibacterial activity and adhesive ability, while the F127 offered thermal-responsive gelation. The scaffold presented an efficient antibacterial and adhesive activity and significantly improved the proliferation, migration, and tube formation ability of HUVECs *in vitro*. Additionally, the scaffold significantly enhanced the wound closure rate, allowing for fast angiogenesis, reepithelization, and collagen deposition within the wound site in diabetic full-thickness cutaneous wounds.⁶⁸

Wang and colleagues demonstrated that a methylcellulose-chitosan injectable hydrogel loaded with placental mesenchymal stem cell-derived exosomes (PMSC-Exos) could be appropriate for treating wounds in diabetic patients.⁶⁹ The addition of PMSC-Exos on the hydrogel allowed for a denser collagen and vessel distribution, besides presenting significantly increased VEGF expressions on the 10th and 15th days. Bcl-2, a protein involved in cell apoptosis inhibition, was also significantly upregulated on the 10th day.

Tao and colleagues used the overexpression technology, in which the miR-126-3p, which presents angiogenic activity, was overexpressed in synovium mesenchymal stem cells (SMSCs).³² Thus, they obtained exosomes with a significantly increased expression of miR-126-3p (SMSC-126-Exos), which were incorporated in a chitosan hydrogel to allow for a sustained release of these bioactive particles. The increased expression of the miR-126-3p strongly promoted angiogenesis by the activation of PI3K/AKT and MAPK/ERK pathways, which play key roles in cell proliferation, migration, and angiogenesis. Additionally, a controlled release of SMSC-126-Exos increased reepithelization, collagen deposition, and blood vessel number at wound sites of diabetic rats.³²

Yang and colleagues used an F127 hydrogel to deliver UCMSC-derived exosomes.⁷⁰ The scaffold was able to maintain the biological activity of exosomes, and a significantly accelerated wound closure rate in diabetic rats

was also observed. Furthermore, a significantly increased expression of CD31 in the UCMSC-Exos-F127 and UCMSC-Exos groups was observed. The protein Ki67 was highly expressed in the UCMSC-Exos-F127 group when compared with the UCMSC-Exos, F127 hydrogel, and PBS groups. Additionally, the UCMSC-Exos-F127 upregulated the expression of VEGF and TGF- β 1. This study suggests that loading exosomes on scaffolds could enable the continuous release of exosomes and potentiate their effects.⁷⁰

Tricalcium phosphate (β -TCP) is a widely employed osteoconductive biomaterial used clinically for bone repair and regeneration purposes. Zhang and colleagues combined iPSC-Exos with β -TCP scaffolds to repair critical-sized calvarial bone defects.⁵⁰ The exosomes released from β -TCP scaffolds were internalized by BMMSCs. Additionally, BMMSCs cultivated on the scaffolds presented enhanced proliferation, migration, and osteogenic differentiation through the activation of the PI3K/AKT signaling pathway. Similarly, expression levels of ALP were significantly enhanced. *In vivo*, observation was made of a large amount of new bone formation in the defects with the implantation of the β -TCP scaffolds loaded with exosomes, as well as a higher osteocalcin expression.⁵⁰ Thus, exosomes were able to enhance the osteoinductive activity of the β -TCP scaffolds.

Furthermore, the incorporation of exosomes from SCs from human exfoliated deciduous teeth (SHED) with β -TCP scaffolds has also reported benefits for bone regeneration, enhancing angiogenesis, and the osteogenesis process.⁷¹

10 | CONCLUSIONS

SC-derived exosomes exhibit properties for cell-free therapies with novel mechanisms and applications in tissue regeneration and repair. Various protocols for the isolation and purification of exosomes have been used for each research group, and the lack of standard methods is a challenge to obtain highly pure and well-characterized exosomes for clinical application.

As the yield of pure SC-exosomes is low, nanovesicles engineered from SC by the extrusion technique are an option for large-scale production of SC-Exos. However, more studies are required to determine the proteomic profile and their similarities with native SC-exosomes.

Additionally, have been reported different strategies to improve the impact of SC-Exos in tissue repair, such as the edition of SC genes for the overexpression of important molecules in the derived exosomes, the conjugation of specific aptamers to facilitate the SC-Exos delivery on the injured site, and SC preconditioning

strategies to enhance biological functions and exosomes yield.

In regard to the role of SC-Exos on cutaneous and bone tissues, scientific literature demonstrates that SC-Exos contain important mediators, such as RNAs (micro and long noncoding) and growth factors (VEGF, Nrf2, Wnt-3a, Stat3, PDGF-D and AKT) that work like cell-to-cell messengers. In particular, it has been demonstrated that exosomes generated by ADSCs, BSCs, BMSCs, BMMSCs, ESCs, EPCs, iPSCs, USCs, and UCMSCs contribute to the regulation of the healing process by the activation of different pathways, which, for example, are able to modulate the inflammation state, angiogenesis promotion, cell proliferation, and migration, but also the ECM synthesis. Some of the possible pathways involved in exosome-mediated bone regeneration include Wnt/ β -catenin/Runx2, Bmp-2/Smad/Runx2, P38 MAPK, Ras/ERK, AKT/mTOR, and JAK-STAT, and, in the skin, PI3k/AKT, ERK 1/2, and Wnt/ β -catenin. It is important to note that comparing Exos from different SC sources, the “cargo” can vary, which means different modulatory properties, thus, the standardization of the SC-source and its culture conditions for a particular tissue disorder is required.

Overall, the efficacy of exosomes strongly suggests promising therapeutics for injured bone and skin tissue, with the possibility of their being incorporated into scaffolds for a sustained release and the potentiation of results.

ACKNOWLEDGMENTS


This study was supported by Ministério da Ciência, Tecnologia, Inovações e Comunicações (MCTIC); Financiadora de Estudos e Projetos (FINEP); Conselho Nacional de Desenvolvimento Científico e Tecnológico (CNPq); Fundação de Amparo à Pesquisa do Estado do Rio Grande do Sul (FAPERGS); Coordenação de Aperfeiçoamento de Pessoal de Nível Superior (CAPES).

CONFLICT OF INTERESTS

The authors declare that there are no conflict of interests.

ORCID

Juliana Girón  <http://orcid.org/0000-0003-3131-5067>

Natasha Maurmann  <https://orcid.org/0000-0001-5103-6394>

Patricia Pranke  <https://orcid.org/0000-0003-4698-6314>

REFERENCES

- Valadi H, Ekström K, Bossios A, Sjöstrand M, Lee JJ, Lötvald JO. Exosome-mediated transfer of mRNAs and microRNAs is a novel mechanism of genetic exchange between cells. *Nature Cell Biol.* 2007;9(6):654-659. <https://doi.org/10.1038/ncb1596>
- Fang S, Xu C, Zhang Y, et al. Umbilical cord-derived mesenchymal stem cell-derived exosomal microRNAs suppress myofibroblast differentiation by inhibiting the transforming growth factor- β /SMAD2 pathway during wound healing. *Stem Cells Transl Med.* 2016;5(10):1425-1439. <https://doi.org/10.5966/sctm.2015-0367>
- Li W, Liu Y, Zhang P, et al. Tissue-engineered bone immobilized with human adipose stem cells-derived exosomes promotes bone regeneration. *ACS Applied Mater Interfaces.* 2018;10:5240-5254. <https://doi.org/10.1021/acsami.7b17620>
- Lu Z, Chen Y, Dunstan C, Roohani-Esfahani S, Zreiqat H. Priming adipose stem cells with tumor necrosis factor-alpha preconditioning potentiates their exosome efficacy for bone regeneration. *Tissue Engineering Part A.* 2017;23(21-22):1212-1220. <https://doi.org/10.1089/ten.tea.2016.0548>
- Wu D, Kang L, Tian J, et al. Exosomes derived from bone mesenchymal stem cells with the stimulation of Fe₃O₄ nanoparticles and static magnetic field enhance wound healing through upregulated miR-21-5p. *Int J Nanomedicine.* 2020;15:7979-7993. <https://doi.org/10.2147/IJN.S275650>
- Ding J, Wang X, Chen B, Zhang J, Xu J. Exosomes derived from human bone marrow mesenchymal stem cells stimulated by deferoxamine accelerate cutaneous wound healing by promoting angiogenesis. *BioMed Res Int.* 2019;2019:9742765. <https://doi.org/10.1155/2019/9742765>
- Takeuchi R, Katagiri W, Endo S, Kobayashi T. Exosomes from conditioned media of bone marrow-derived mesenchymal stem cells promote bone regeneration by enhancing angiogenesis. *PLoS One.* 2019;14(11):0225472. <https://doi.org/10.1371/journal.pone.0225472>
- Luo ZW, Li FXZ, Liu YW, et al. Aptamer-functionalized exosomes from bone marrow stromal cells target bone to promote bone regeneration. *Nanoscale.* 2019;11(43):20884-20892. <https://doi.org/10.1039/c9nr02791b>
- Shabbir A, Cox A, Rodriguez-Menocal L, Salgado M, Van Badiavas E. Mesenchymal stem cell exosomes induce proliferation and migration of normal and chronic wound fibroblasts, and enhance angiogenesis in vitro. *Stem Cells Dev.* 2015;24(14):1635-1647. <https://doi.org/10.1089/scd.2014.0316>
- Chen B, Sun Y, Zhang J, et al. Human embryonic stem cell-derived exosomes promote pressure ulcer healing in aged mice by rejuvenating senescent endothelial cells. *Stem Cell Res Ther.* 2019;10(1):142. <https://doi.org/10.1186/s13287-019-1253-6>
- Cui Y, Fu S, Sun D, Xing J, Hou T, Wu X. EPC-derived exosomes promote osteoclastogenesis through LncRNA-MALAT1. *J Cell Mol Med.* 2019;23(6):3843-3854. <https://doi.org/10.1111/jcmm.14228>
- Jia Y, Zhu Y, Qiu S, Xu J, Chai Y. Exosomes secreted by endothelial progenitor cells accelerate bone regeneration during distraction osteogenesis by stimulating angiogenesis. *Stem Cell Res Ther.* 2019;10(1):12. <https://doi.org/10.1186/s13287-018-1115-7>
- Zhang B, Wu X, Zhang X, et al. Human umbilical cord mesenchymal stem cell exosomes enhance angiogenesis through the Wnt4/ β -catenin pathway. *Stem Cells Transl Med.* 2015;4(5):513-522. <https://doi.org/10.5966/sctm.2014-0267>
- Ma J, Zhao Y, Sun L, et al. Exosomes derived from Akt-modified human umbilical cord mesenchymal stem cells

- improve cardiac regeneration and promote angiogenesis via activating platelet-derived growth factor D. *Stem Cells Transl Med*. 2017;6(1):51-59. <https://doi.org/10.5966/sctm.2016-0038>
15. Liu H, Liu S, Qiu X, et al. Donor MSCs release apoptotic bodies to improve myocardial infarction via autophagy regulation in recipient cells. *Autophagy*. 2020;16(12):2140-2155. <https://doi.org/10.1080/15548627.2020.1717128>
 16. Chen CY, Rao SS, Ren L, et al. Exosomal DMBT1 from human urine-derived stem cells facilitates diabetic wound repair by promoting angiogenesis. *Theranostics*. 2018;8(6):1607-1623. <https://doi.org/10.7150/thno.22958>
 17. Wang L, Wei J, Da Fonseca Ferreira A, et al. Rejuvenation of senescent endothelial progenitor cells by extracellular vesicles derived from mesenchymal stromal cells. *JACC: Basic Transl Sci*. 2020;5(11):1127-1141. <https://doi.org/10.1016/j.jacbs.2020.08.005>
 18. Hu W, Song X, Yu H, Sun J, Zhao Y. Therapeutic potentials of extracellular vesicles for the treatment of diabetes and diabetic complications. *Int J Mol Sci*. 2020;21(14):1-24. <https://doi.org/10.3390/ijms21145163>
 19. Henne WM, Buchkovich NJ, Emr SD. The ESCRT pathway. *Dev Cell*. 2011;21(1):77-91. <https://doi.org/10.1016/j.devcel.2011.05.015>
 20. Trajkovic K, Hsu C, Chiantia S, et al. Ceramide triggers budding of exosome vesicles into multivesicular endosomes. *Science*. 2008;319(5867):1244-1247. <https://doi.org/10.1126/science.1153124>
 21. Colombo M, Raposo G, Théry C. Biogenesis, secretion, and intercellular interactions of exosomes and other extracellular vesicles. *Annu Rev Cell Dev Biol*. 2014;30:255-89.
 22. Zhang Y, Liu Y, Liu H, Tang WH. Exosomes: biogenesis, biologic function and clinical potential. *Cell Biosci*. 2019;9:1-18.
 23. Théry C, Witwer KW. Minimal information for studies of extracellular vesicles 2018 (MISEV2018): a position statement of the International Society for Extracellular Vesicles and update of the MISEV2014 guidelines. *J Extracell Vesicles*. 2018;7(1):1535750. <https://doi.org/10.1080/20013078.2018.1535750>
 24. Zhang H, Freitas D, Kim HS, et al. Identification of distinct nanoparticles and subsets of extracellular vesicles by asymmetric flow field-flow fractionation. *Nature Cell Biol*. 2018;20(3):332-343. <https://doi.org/10.1038/s41556-018-0040-4>
 25. Tiwari S, Kumar V, Randhawa S, Verma SK. Preparation and characterization of extracellular vesicles. *Am J Reprod Immunol*. 2021;85(2):e13367. <https://doi.org/10.1111/aji.13367>
 26. Witwer KW, Buzás EI, Bemis LT, et al. Standardization of sample collection, isolation and analysis methods in extracellular vesicle research. *J Extracell Vesicles*. 2013;2(1):20360. <https://doi.org/10.3402/jev.v2i0.20360>
 27. Deun JVan, Mestdagh P, Sormunen R, et al. The impact of disparate isolation methods for extracellular vesicles on downstream RNA profiling. *J Extracell Vesicles*. 2014;3(1). <https://doi.org/10.3402/JEV.V3.24858>
 28. Veerman RE, Teeuwen L, Czarnewski P, et al. Molecular evaluation of five different isolation methods for extracellular vesicles reveals different clinical applicability and subcellular origin. *J Extracell Vesicles*. 2021;10(9):e12128. <https://doi.org/10.1002/JEV2.12128>
 29. Jeong D, Jo W, Yoon J, et al. Nanovesicles engineered from ES cells for enhanced cell proliferation. *Biomaterials*. 2014;35(34):9302-9310. <https://doi.org/10.1016/j.biomaterials.2014.07.047>
 30. Lee H, Cha H, Park JH. Derivation of cell-engineered nanovesicles from human induced pluripotent stem cells and their protective effect on the senescence of dermal fibroblasts. *Int J Mol Sci*. 2020;21(1):343. <https://doi.org/10.3390/ijms21010343>
 31. Shi R, Jin Y, Hu W, et al. Exosomes derived from mmu_circ_0000250-modified adipose-derived mesenchymal stem cells promote wound healing in diabetic mice by inducing miR-128-3p/SIRT1-mediated autophagy. *Am J Physiol Cell Physiol*. 2020;318(5):C848-C856. <https://doi.org/10.1152/ajpcell.00041.2020>
 32. Tao S-C, Guo S-C, Li M, Ke Q-F, Guo Y-P, Zhang C-Q. Chitosan wound dressings incorporating exosomes derived from microRNA-126-overexpressing synovium mesenchymal stem cells provide sustained release of exosomes and heal full-thickness skin defects in a diabetic rat model. *Stem Cells Transl Med*. 2017;6(3):736-747. <https://doi.org/10.5966/sctm.2016-0275>
 33. Qiu X, Liu J, Zheng C, et al. Exosomes released from educated mesenchymal stem cells accelerate cutaneous wound healing via promoting angiogenesis. *Cell Prolif*. 2020;53(8):e12830. <https://doi.org/10.1111/cpr.12830>
 34. Liu W, Li L, Rong Y, et al. Hypoxic mesenchymal stem cell-derived exosomes promote bone fracture healing by the transfer of miR-126. *Acta Biomater*. 2020;103:196-212. <https://doi.org/10.1016/j.actbio.2019.12.020>
 35. Wang J, Bonacquisti EE, Brown AD, Nguyen J. Boosting the Biogenesis and secretion of mesenchymal stem cell-derived exosomes. *Cells*. 2020;9(3):660. <https://doi.org/10.3390/cells9030660>
 36. Hosseini Shamili F, Alibolandi M, Rafatpanah H, et al. Immunomodulatory properties of MSC-derived exosomes armed with high affinity aptamer toward myelin as a platform for reducing multiple sclerosis clinical score. *J Controlled Release*. 2019;299:149-164. <https://doi.org/10.1016/j.jconrel.2019.02.032>
 37. Hu L, Wang J, Zhou X, et al. Exosomes derived from human adipose mesenchymal stem cells accelerates cutaneous wound healing via optimizing the characteristics of fibroblasts. *Sci Rep*. 2016;6:32993. <https://doi.org/10.1038/srep32993>
 38. Zhou Y, Zhao B, Zhang XL, et al. Combined topical and systemic administration with human adipose-derived mesenchymal stem cells (hADSC) and hADSC-derived exosomes markedly promoted cutaneous wound healing and regeneration. *Stem Cell Res Ther*. 2021;12(1):257. <https://doi.org/10.1186/s13287-021-02287-9>
 39. Zhang B, Wang M, Gong A, et al. HucMSC-exosome mediated-Wnt4 signaling is required for cutaneous wound healing. *Stem Cells*. 2015;33(7):2158-2168. <https://doi.org/10.1002/stem.1771>
 40. Zhang J, Guan J, Niu X, et al. Exosomes released from human induced pluripotent stem cells-derived MSCs facilitate cutaneous wound healing by promoting collagen synthesis and angiogenesis. *J Transl Med*. 2015;13(1):49. <https://doi.org/10.1186/s12967-015-0417-0>
 41. Lu M, Peng L, Ming X, et al. Enhanced wound healing promotion by immune response-free monkey autologous iPSCs and exosomes vs. their allogeneic counterparts. *EBioMedicine*. 2019;42:443-457. <https://doi.org/10.1016/j.ebiom.2019.03.011>

42. Xing X, Han S, Cheng G, Ni Y, Li Z, Li Z. Proteomic analysis of exosomes from adipose-derived mesenchymal stem cells: a novel therapeutic strategy for tissue injury. *BioMed Res Int*. 2020;2020:6094562. <https://doi.org/10.1155/2020/6094562>
43. Ma T, Fu B, Yang X, Xiao Y, Pan M. Adipose mesenchymal stem cell-derived exosomes promote cell proliferation, migration, and inhibit cell apoptosis via Wnt/ β -catenin signaling in cutaneous wound healing. *J Cell Biochem*. 2019;120(6):10847-10854. <https://doi.org/10.1002/jcb.28376>
44. Zhang W, Bai X, Zhao B, et al. Cell-free therapy based on adipose tissue stem cell-derived exosomes promotes wound healing via the PI3K/Akt signaling pathway. *Exp Cell Res*. 2018;370(2):333-342. <https://doi.org/10.1016/j.yexcr.2018.06.035>
45. He L, Zhu C, Jia J, et al. ADSC-Exos containing MALAT1 promotes wound healing by targeting miR-124 through activating Wnt/ β -catenin pathway. *Biosci Rep*. 2020;40(5). <https://doi.org/10.1042/BSR20192549>
46. Li Xue, Xie X, Lian W, et al. Exosomes from adipose-derived stem cells overexpressing Nrf2 accelerate cutaneous wound healing by promoting vascularization in a diabetic foot ulcer rat model. *Exp Mol Med*. 2018;50(4):1-14. <https://doi.org/10.1038/s12276-018-0058-5>
47. Dalirfardouei R, Jamialahmadi K, Jafarian AH, Mahdipour E. Promising effects of exosomes isolated from menstrual blood-derived mesenchymal stem cell on wound-healing process in diabetic mouse model. *J Tissue Eng Regen Med*. 2019;13(4):555-568. <https://doi.org/10.1002/term.2799>
48. Li Xiacong, Jiang C, Zhao J. Human endothelial progenitor cells-derived exosomes accelerate cutaneous wound healing in diabetic rats by promoting endothelial function. *J Diabetes Complications*. 2016;30(6):986-992. <https://doi.org/10.1016/j.jdiacomp.2016.05.009>
49. Zhang J, Chen C, Hu B, et al. Exosomes derived from human endothelial progenitor cells accelerate cutaneous wound healing by promoting angiogenesis through Erk1/2 signaling. *Int J Biol Sci*. 2016;12(12):1472-1487. <https://doi.org/10.7150/ijbs.15514>
50. Zhang J, Liu X, Li H, et al. Exosomes/tricalcium phosphate combination scaffolds can enhance bone regeneration by activating the PI3K/Akt signaling pathway. *Stem Cell Res Ther*. 2016;7(1):136. <https://doi.org/10.1186/s13287-016-0391-3>
51. Tamari T, Kawar-Jaraisy R, Doppelt O, Giladi B, Sabbah N, Zigdon-Giladi H. The paracrine role of endothelial cells in bone formation via CXCR4/SDF-1 pathway. *Cells*. 2020;9(6). <https://doi.org/10.3390/cells9061325>
52. Xu C, Liu H, He Y, Li Y, He X. Endothelial progenitor cells promote osteogenic differentiation in co-cultured with mesenchymal stem cells via the MAPK-dependent pathway. *Stem Cell Res Ther*. 2020;11(1):537. <https://doi.org/10.1186/s13287-020-02056-0>
53. Lee Y, Kim HJ, Park CK, et al. MicroRNA-124 regulates osteoclast differentiation. *Bone*. 2013;56(2):383-389. <https://doi.org/10.1016/j.bone.2013.07.007>
54. Furuta T, Miyaki S, Ishitobi H, et al. Mesenchymal stem cell-derived exosomes promote fracture healing in a mouse model. *Stem Cells Transl Med*. 2016;5(12):1620-1630. <https://doi.org/10.5966/sctm.2015-0285>
55. Li Xiacong, Chen C, Wei L, et al. Exosomes derived from endothelial progenitor cells attenuate vascular repair and accelerate reendothelialization by enhancing endothelial function. *Cytotherapy*. 2016;18(2):253-262. <https://doi.org/10.1016/j.jcyt.2015.11.009>
56. Zhang Yuntong, Hao Z, Wang P, et al. Exosomes from human umbilical cord mesenchymal stem cells enhance fracture healing through HIF-1 α -mediated promotion of angiogenesis in a rat model of stabilized fracture. *Cell Proliferation*. 2019;52(2):e12570. <https://doi.org/10.1111/cpr.12570>
57. Zhou J, Liu HX, Li SH, et al. Effects of human umbilical cord mesenchymal stem cells-derived exosomes on fracture healing in rats through the Wnt signaling pathway. *Eur Rev Med Pharmacol Sci*. 2019;23(11):4954-4960. https://doi.org/10.26355/eurrev_201906_18086
58. Chen S, Tang Y, Liu Y, et al. Exosomes derived from miR-375-overexpressing human adipose mesenchymal stem cells promote bone regeneration. *Cell Proliferation*. 2019;52(5):e12669. <https://doi.org/10.1111/cpr.12669>
59. Eguchi K, Akiba Y, Akiba N, Nagasawa M, Cooper LF, Uoshima K. Insulin-like growth factor binding protein-3 suppresses osteoblast differentiation via bone morphogenetic protein-2. *Biochem Biophys Res Commun*. 2018;507(1-4):465-470. <https://doi.org/10.1016/j.bbrc.2018.11.065>
60. Liao H-T. Osteogenic potential: comparison between bone marrow and adipose-derived mesenchymal stem cells. *World J Stem Cells*. 2014;6(3):288-295. <https://doi.org/10.4252/wjsc.v6.i3.288>
61. Zhang L, Jiao G, Ren S, et al. Exosomes from bone marrow mesenchymal stem cells enhance fracture healing through the promotion of osteogenesis and angiogenesis in a rat model of nonunion. *Stem Cell Res Ther*. 2020;11(1). <https://doi.org/10.1186/s13287-020-1562-9>
62. Xu T, Luo Y, Wang J, et al. Exosomal miRNA-128-3p from mesenchymal stem cells of aged rats regulates osteogenesis and bone fracture healing by targeting Smad5. *J Nanobiotechnology*. 2020;18(1):47. <https://doi.org/10.1186/s12951-020-00601-w>
63. Liang B, Liang JM, Ding JN, Xu J, Xu JG, Chai YM. Dimethylxaloylglycine-stimulated human bone marrow mesenchymal stem cell-derived exosomes enhance bone regeneration through angiogenesis by targeting the AKT/mTOR pathway. *Stem Cell Res Ther*. 2019;10(1):335. <https://doi.org/10.1186/s13287-019-1410-y>
64. Zhu Y, Jia Y, Wang Y, Xu J, Chai Y. Impaired bone regenerative effect of exosomes derived from bone marrow mesenchymal stem cells in type 1 diabetes. *Stem Cells Transl Med*. 2019;8(6):593-605. <https://doi.org/10.1002/sctm.18-0199>
65. Riau AK, Ong HS, Yam GHF, Mehta JS. Sustained delivery system for stem cell-derived exosomes. *Front Pharmacol*. 2019;10:1368. <https://doi.org/10.3389/fphar.2019.01368>
66. Wang M, Wang C, Chen M, et al. Efficient angiogenesis-based diabetic wound healing/skin reconstruction through bioactive antibacterial adhesive ultraviolet shielding nanodressing with exosome release. *ACS Nano*. 2019;13(9):10279-10293. <https://doi.org/10.1021/acs.nano.9b03656>
67. Liu K, Chen C, Zhang H, Chen Y, Zhou S. Adipose stem cell-derived exosomes in combination with hyaluronic acid accelerate wound healing through enhancing re-epithelialization and vascularization. *Br J Dermatol*. 2019;181(4):854-856. <https://doi.org/10.1111/bjd.17984>

68. Wang Chenggui, Wang M, Xu T, et al. Engineering bioactive self-healing antibacterial exosomes hydrogel for promoting chronic diabetic wound healing and complete skin regeneration. *Theranostics*. 2019;9(1):65-76. <https://doi.org/10.7150/thno.29766>
69. Wang Chunyao, Liang C, Wang R, et al. The fabrication of a highly efficient self-healing hydrogel from natural biopolymers loaded with exosomes for the synergistic promotion of severe wound healing. *Biomater Sci*. 2020;8(1):313-324. <https://doi.org/10.1039/c9bm01207a>
70. Yang J, Chen Z, Pan D, Li H, Shen J. Umbilical cord-derived mesenchymal stem cell-derived exosomes combined pluronic F127 hydrogel promote chronic diabetic wound healing and complete skin regeneration. *Int J Nanomedicine*. 2020;15:5911-5926. <https://doi.org/10.2147/IJN.S249129>
71. Wu J, Chen L, Wang R, et al. Exosomes secreted by stem cells from human exfoliated deciduous teeth promote alveolar bone defect repair through the regulation of angiogenesis and osteogenesis. *ACS Biomater Sci Eng*. 2019;5(7):3561-3571. <https://doi.org/10.1021/acsbiomaterials.9b00607>

How to cite this article: Girón J, Maurmann N, Pranke P. The role of stem cell-derived exosomes in the repair of cutaneous and bone tissue. *J Cell Biochem*. 2021;1-19. <https://doi.org/10.1002/jcb.30144>

2. Hipóteses

Hipótese 1: A produção de um biomaterial híbrido composto pelo polímero sintético PLGA e o polímero natural fibrina teria melhores propriedades mecânicas e biológicas.

Hipótese 2: O Secretoma de SHED contribuiria com a viabilidade e migração de queratinócitos.

3. Objetivos

3.1. Objetivo Geral

Desenvolver estratégias para a regeneração cutânea com base em um biomaterial nanofibroso de PLGA/fibrina e secretoma de células-tronco.

3.2. Objetivos específicos - Subprojeto 1

- Realizar a produção, caracterização e testes de *scaffolds* de PLGA contendo fibrina.
- Estabelecer culturas primárias de queratinócitos e fibroblastos.
- Construir um substituto cutâneo de espessura total.
- Realizar a implantação do substituto cutâneo em um modelo animal e avaliar a sua funcionalidade *in vivo* por meio de estudos histológicos e imunoenzimáticos.

3.3. Objetivos específicos do subprojeto 2

- Isolar as vesículas extracelulares (VEs) do meio condicionado (MC) de culturas de SHED, com o método de ultracentrifugação sequencial, e caracterizá-las.
- Avaliar a viabilidade de queratinócitos cultivados com diferentes concentrações de MC e VEs.
- Avaliar o efeito do MC e VEs na migração de queratinócitos.
- Explorar um possível mecanismo de ação do secretoma de SHED.

4. Capítulo 1

Development of fibrous PLGA/fibrin scaffolds as a potential skin substitute

Artigo publicado no periódico *Biomedical Materials*. Fator de impacto 4,103 (2021)

Biomedical Materials



PAPER

Development of fibrous PLGA/fibrin scaffolds as a potential skin substitute

RECEIVED
1 May 2020

REVISED
22 June 2020

ACCEPTED FOR PUBLICATION
26 June 2020

PUBLISHED
22 July 2020

Juliana Girón Bastidas^{1,2,5} , Natasha Maurmann^{1,2} , Mauro Ricardo da Silveira³ ,
Carlos Arthur Ferreira³  and Patricia Pranke^{1,2,4} 

¹ Hematology and Stem Cell Laboratory, Faculty of Pharmacy, Universidade Federal do Rio Grande do Sul, Porto Alegre, RS 90610-000, Brazil

² Post Graduate Program in Physiology, Universidade Federal do Rio Grande do Sul, Porto Alegre, RS 90050-170, Brazil

³ Engineering School, Universidade Federal do Rio Grande do Sul, Porto Alegre, RS, Brazil

⁴ Stem Cell Research Institute, Porto Alegre, RS 90020-10, Brazil

⁵ Author to whom any correspondence should be addressed.

E-mail: 00305205@ufrgs.br

Keywords: electrospinning, poly(lactic-co-glycolic) acid, fibrin

Abstract

The aim of this study has been to fabricate a hybrid electrospun nanofibrous scaffold composed of poly(lactic-co-glycolic) acid (PLGA)/fibrin polymers to be used as a skin substitute and analyze its physical and biological properties. Fibrin was obtained from rat blood plasma, characterized and solubilized in formic acid. The final electrospinning solution concentration was 40% PLGA (w/v) and 1% fibrin (w/v). To improve spinnability, 3% PEG (w/v) was added. The scaffolds were characterized by scanning electron microscopy (SEM) and Fourier transform infrared spectroscopy (FTIR). Water contact angle, maximum elongation, thermal stability, degree of swelling, blood compatibility, cytotoxicity and cell viability were analyzed. The characterization by SEM showed randomly oriented nanofibers with a mean diameter of 639.8 ± 241.8 nm for the PLGA/fibrin and 1051.0 ± 290.2 nm for the PLGA. FTIR spectra confirmed the presence of fibrin in the mats. Fibrin incorporation reduced the water contact angle from 118.9 ± 2.9 to 111.1 ± 2.8 . The fibrin increased tensile strength and decreased elongation at break. The scaffolds demonstrated blood compatibility and fibrin incorporation improved cell adhesion and viability when direct and indirect MTT analyses were carried out. Thus, it can be concluded that the PLGA/fibrin mat is a promising material for use as a skin substitute.

1. Introduction

Skin is the largest organ of the body, with a surface of 2 m², this being a physical barrier between external and internal environments. It offers protection from dehydration, external damage, infections, UV radiation and environmental toxins. Furthermore, skin acts as a sensory organ, which transmits sensation to pain, temperature and deep pressure, playing an important role in the balance of body temperature and water content and, consequently, in the maintenance of physiological homeostasis [1]. Skin is also one of the most immune active organs and interferes in vitamin D production, essential for calcium absorption and normal bone metabolism [2].

Skin disease prevalence has rapidly increased since 2005, with chronic wounds being a growing

problem worldwide [3]. Due to the importance of preserving skin integrity, tissue engineering has become an alternative to the conventional treatments for full-thickness wounds, which consist of the use of autografts, allografts or xenografts. These conventional treatments have some disadvantages, such as the risk of disease transmission, high cost and donor site morbidity [4].

One of the elements of tissue engineering which are of important relevance are the scaffolds, consisting of biomaterials fabricated from polymers of natural or synthetic origin which support the cell. Their importance lies in the fact that the composition and structure of such biomaterials can provide appropriate conditions for the tissue regeneration process. Therefore, scaffolds act as an extracellular matrix (ECM) analog; capable of guiding cell adhesion,

proliferation and differentiation and also the promotion of angiogenesis. Such cell functions are influenced by polymer composition and related mechanical properties, including thickness and pore size [5].

Although tissue engineering of the skin has been widely studied, an ideal skin substitute has still not been developed. For a skin substitute to be considered ideal, it must have characteristics such as water loss prevention because a moist wound environment is required to facilitate the healing process [6]. However, adequate moisture balance is necessary. The water absorption capacity of the scaffolds, therefore, should be in agreement with the quantity of the wound exudate, it being possible to maintain a healthy physiological level of moisture [7]. Thereby, dry wounds will require a hydrating scaffold, and in contrast, wounds with excessive exudate will require an absorptive scaffold able to prevent the maceration of the surrounding skin. Absorptive scaffolds should be able to transmit moisture vapor away from the wound bed towards the upper surface and allow the moisture to evaporate into the air. The transmission of moisture vapor is directly proportional to the porosity of the scaffold [8]. Therefore, the scaffold should prevent dehydration and also the accumulation of extra exudates, such as seroma. For these reasons, the election of the scaffolds should be in agreement with the characteristics of the wound. On the other hand, complications like hematomas should be avoided by having good homeostasis before applying the substitute.

Besides water loss balance, characteristics such as a wide availability of the polymer, biodegradability, support for cellular adhesion, infection resistance, presence of epidermal and dermal components, low antigenicity, high shear strength, easy storage, long shelf life and good cost-benefit are desirable [5]. These characteristics are dependent on the polymer properties and the technique used for scaffold fabrication. In this study, electrospinning was applied, which is a versatile technique widely used for fabricating fibers ranging from the nano- to the microscale.

In addition, the use of hybrid materials has been suggested in order to take advantage of the physical properties of synthetic polymers as well as the biological ones of natural polymers [9]. Fibrin is a natural polymer composed of fibrinogen monomers present in blood plasma, with interesting properties to be used in tissue engineering which play an important role in the wound healing process. Fibrin acts as a support for the hemostatic plug and it is also considered to be a preliminary matrix within the wound space [10]. Fibrin can interact with cells such as leukocytes, platelets, endothelial cells and fibroblast via integrin receptors. Arg-Gly-Asp (RGD) motif is the principal integrin-binding domain of ECM proteins, which play an important role in cell adhesion [11]. It has been shown that the fibrinogen molecules

themselves (constituent A alpha and B beta chains) promote fibroblast proliferation [12].

Fibrin not only interacts with cells but also contains motifs that allow for the interaction with other ECM proteins, providing an adequate environment for cell adhesion, proliferation and migration [13]. Native collagen I has binding sites that are common for fibrin, fibronectin and metalloproteinase 1 [14]. This fact presupposes that a scaffold containing fibrin could provide a functional articulation between itself and the native tissue, therefore facilitating cell migration. Moreover, there are other ECM proteins capable of binding fibrin and regulating cell adhesion, proliferation and migration, such as fibronectin, vitronectin and thrombospondin [11, 13].

Furthermore, fibrin is an important signaling molecule, being a potent vascular endothelial cell activator, inducing the expression of the IL8, which influence leukocyte migration and activation [11]. It has also been reported that fibrin degradation product D-dimer induces synthesis and the release of IL-1 β , IL-6 and plasminogen activator inhibitors from monocytes *in vitro*, which are regulators of hepatic response. IL-6 stimulates transcription of acute-phase proteins genes and fibrinogen synthesis, meanwhile, IL-1 down-regulates fibrinogen synthesis; which means that fibrin plays an active role in the tissue regeneration/repair processes [15].

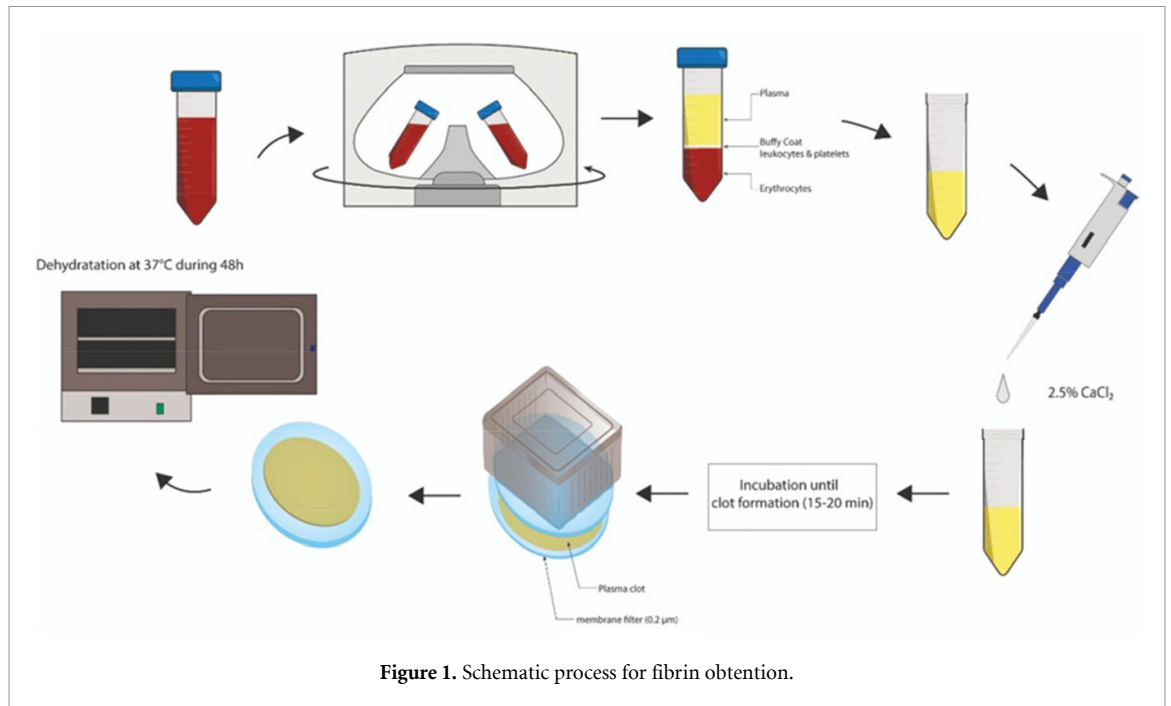
Additionally, poly(lactic-co-glycolic) acid (PLGA) is a synthetic polymer approved by the European Medicine Agency as well as the US Food and Drugs Administration. PLGA is frequently used worldwide for biomedical applications and drug delivery as it is biodegradable, biocompatible and its degradation products are easily metabolized through the Krebs Cycle [16].

The aim of this study has been to produce electrospun nanofibrous scaffolds composed of PLGA/fibrin polymers and to analyze their physical and biological properties.

2. Materials and methods

2.1. Materials

The products used from Sigma-Aldrich were 1,1,1,3,3,3-hexafluoro-2-propanol (HFIP), 3-(4,5-dimethylthiazol-2-yl)-2,5-diphenyl tetrazolium bromide (MTT), 4,6-diamidino-2-phenylindole (DAPI), Dulbecco's Modified Eagle's Medium (DMEM/HEPES)—low glucose and high glucose, paraformaldehyde (PFA), rhodamine-phalloidin, trypsin-EDTA solution 10x and Triton X-100. Formic acid was purchased from Labsynth. Collagenase and penicillin/streptomycin were purchased from Gibco, PLGA 75:25 from PURAC, fetal bovine serum (FBS) heat-inactivated from Cultilab, Campinas/SP and dimethyl sulfoxide (DMSO) from Nuclear.



2.2. Fibrin obtention and characterization

Seven male Wistar rats aged four months (300–450 g body weight) were obtained from the Animal House of the Institute of Basic Health Sciences of the Federal University of Rio Grande do Sul. All the procedures were performed following authorization from the Ethics Committee (Number 36484, approved on 16 May 2019).

The blood was collected after anesthesia with citrate-phosphate-dextrose anticoagulant in a 9:1 proportion by cardiac puncture. The harvested blood was centrifuged (800g, 13 min at 4 °C) and the blood plasma was removed by aspiration, figure 1. Fibrinogen polymerization was induced by adding 2.5% CaCl₂ to the plasma (1:9). The plasma was incubated until clot formation; the clot was placed between two 0.2 μm pore size membranes and weight was applied until the formation of a thin sheet of fibrin. The fibrin was dehydrated at 37 °C for 48 h. The dehydrated product was analyzed by Fourier transform infrared spectroscopy (FTIR).

2.3. Preparation of electrospinning solution

Fibrin was dissolved in formic acid at room temperature with continuous stirring overnight at 1000 rpm. Once fibrin was dissolved, HFIP was added at the proportion of formic acid:HFIP 1:1. The solution was stirred for 15 min before adding the PLGA in a final solution concentration of 40% PLGA (w/v), 1% fibrin (w/v) and 3% PEG (w/v). To dissolve the PLGA, the solution was stirred for 2 h at room temperature until homogenization was reached. The electrospinning solution for the control scaffolds was prepared with the same solvents and solute concentration, with the exception of the fibrin.

2.4. Fabrication of PLGA and PLGA/fibrin electrospun nanofibers

The polymeric solution was loaded in a 2 ml plastic syringe fitted with a 23 G needle. The electrospinning parameters were fixed as applied high-voltage of 17 kV (18 kV at the positive and 1 kV at the negative) the flow rate of 0.48 ml h⁻¹ controlled by a syringe pump (electrospinning model homemade) and a tip-collector distance of 20 cm. Random fibers were electrospun on round glass coverslips of 13 mm diameter and were fixed using the same polymeric solution prepared for the nanofibers fabrication on the underside of the glass coverslips so that they could be manipulated without distorting the microstructure. The scaffolds were sterilized with UV light for 1 h at each site in a laminar flow hood.

2.5. Characterization

2.5.1. Scanning electron microscopy.

The scaffold morphology and PLGA/fibrin fiber diameter, together with the cell presence, were performed by the SEM model Pro X (Phenom-World—Thermo Fisher Scientific, the Netherlands). The samples were washed with phosphate buffer (PBS, pH 7.4), fixed in 4% PFA for 30 min, rinsed in buffer PBS and dehydrated in ethanol series. The dried samples were metalized with a thin layer of gold and placed on stubs using adhesive carbon disks. Images were acquired using an accelerating voltage of 15 kV and a magnification range of 500–5000×. The average fiber diameter was determined by SEM through the measurement of a total of 200 fibers of PLGA and PLGA/fibrin, selected randomly from seven images for each, using the ImageJ software.

2.5.2. Thermal stability and water contact angle.

Thermal stability of the scaffolds and residual solvent content was evaluated by a thermogravimetric analyzer (TGA Q50, TA Instruments, USA), at a heating rate of 20 °C min⁻¹, in a temperature range of 30 °C–800 °C under a nitrogen atmosphere. To analyze hydrophilicity, the water drop contact angle was carried out by Phoenix Mini (Surface and Electro-Optics Co., South Korea) using a sessile drop method (between 0.03 ml and 0.05 ml of drop volume), and a minimum of 15 drop images were recorded for each sample.

2.5.3. Mechanical testing.

Maximum elongation and stress were determined by dynamic mechanical analysis (DMA) in a DMA 2980 (TA Instruments, USA) using the tension film clam. The scaffolds were cut into rectangular shapes (10 × 6 mm). The assays were carried out at a constant temperature (37 °C) with a ramp force of 0.1 N min⁻¹ until 13 N maximum loads. Data from the stress-strain curves were recorded and the tensile stress at maximal load was obtained from this data for each sample. The analyses were made using the TA Universal Analysis software.

2.5.4. FTIR

Influences of fibrin in the PLGA scaffolds were analyzed in the fingerprint region in the range of 2000 and 750 cm⁻¹ in a FTIR spectrometer Spectrum 1000 (PerkinElmer, Inc., USA) by averaging 32 scans at a resolution of 4 cm⁻¹. The horizontal ATR (HATR) accessory (Pike Technologies, USA) was used for the PGLA and PLGA/fibrin films; the fibrin powder was mixed with potassium bromide (KBr) (Sigma-Aldrich, USA) and pressed into a disk shape.

2.5.5. Swelling test.

The scaffolds were cut into quadrangular shapes (1 cm × 1 cm) and weighed (W_i). To calculate the swelling degree, the membranes were immersed in PBS at 37 °C. After 1 h and 24 h, the scaffolds were removed and the surface water blotted out by filter paper to be weighed after swelling (W) [8]. The swelling degree was calculated as follows:

$$\text{Degree of Swelling (\%)} = \frac{W - W_i}{W} \times 100$$

2.5.6. Blood compatibility test.

To test the compatibility of the scaffolds with blood, the hemolysis assay was performed. Citrated rat blood (4 ml) was diluted with 5 ml of normal saline 0.9%. For the positive control, 10 ml of Milli-Q water was used and 10 ml of normal saline 0.9% was taken as the negative control. Scaffolds of diameter 1 cm were submerged in 10 ml of normal saline. Following this, 0.2 ml of citrated diluted blood was added to each group and incubated at 37 °C for 60 min, followed by centrifugation at 1500 rpm for 10 min.

Subsequently, the absorbance of the supernatant was taken at 570 nm. The hemolysis percentage was calculated as follows:

$$\% \text{hemolysis} = \frac{A_s - A_{NC}}{A_{PC} - A_{NC}}$$

where A_s is the absorbance of the sample, A_{NC} is the absorbance of the negative control, A_{PC} is the absorbance of the positive control.

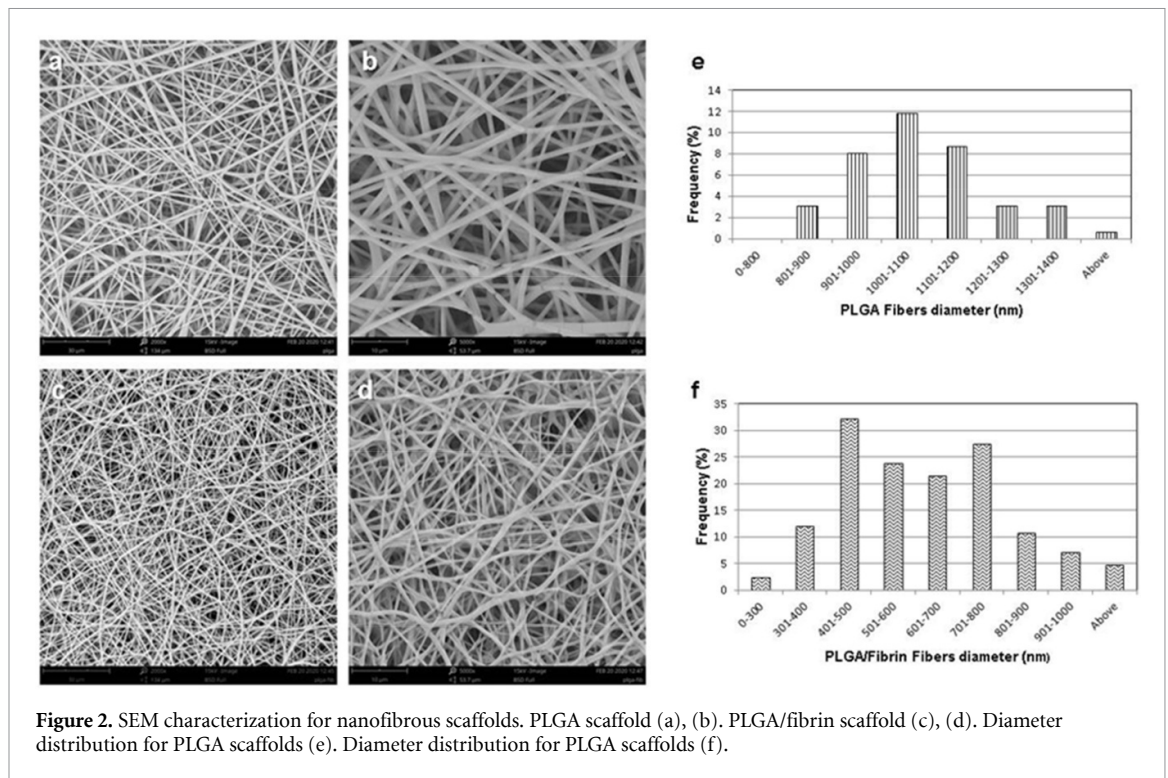
2.5.7. In vitro cell culture studies.

Stem cells were isolated from exfoliated human deciduous teeth (SHED) [17] after approval by the Brazilian National Research Ethics Committee (Protocol number CAAE 12892419.0.0000.5347). SHED characterizations were performed by morphological analysis, flow cytometry, and differentiation assay *in vitro* [17–19].

To analyze cell viability on the scaffolds, the membranes were placed into a 24 well plate. SHED and HaCaT cells were seeded at a density of 25×10^3 cells per well and incubated at 37 °C with 5% CO₂. The culture media DMEM (low and high glucose for SHED and HaCaT, respectively) were supplemented with 10% fetal bovine serum and 1% penicillin/streptomycin. After 1 and 6 d, the cells were treated with 0.25 μg ml⁻¹ of MTT for 4 h at 37 °C. The supernatant was removed and 200 μl DMSO was added per well to dissolve the formed formazan crystals. The last procedure was made twice to obtain a good dissolution of the crystals. Absorbance was measured at 560 nm and 630 nm with the equipment Multiskan™ FC Microplate Photometer (Thermo Scientific™).

Cytotoxicity of the PLGA/fibrin scaffolds was also analyzed by indirect MTT. The scaffolds were placed in a sterile tube and 1 ml of the culture medium with 1% antibiotic without fetal bovine serum was added to each sterile sample. The scaffolds were incubated and after 7 d, the scaffold incubated medium (SIM) was removed and supplemented with FBS 10%. DMEM high glucose supplemented with FBS 10% was considered as the control medium (CM). The cells (1600 HaCat per well) were seeded and cultivated in a 96-well plate and incubated for 8 h to allow for the cells to adhere to the plate. After the incubation period, the culture medium was removed and 200 μl of SIM or CM was added to each well.

After 24 h, the cell culture medium was removed and 50 μl of MTT with a concentration of 0.5 g ml⁻¹ was added to each well. The plate was placed in a 5% CO₂ incubator at 37 °C for 2 h. The media was then discarded and 200 μl DMSO was added to each well to dissolve the formazan crystals. The absorbance was measured at 570 nm. The toxicity and cell viability of the scaffold was calculated as follows:



$$\text{Toxicity}\% = \left(1 - \frac{\text{mean of } A_{\text{SIM}}}{\text{mean of } A_{\text{CM}}}\right) \times 100$$

$$\text{Viability}\% = 100 - \text{Toxicity}\%$$

where A_{SIM} is the absorbance of the cells treated with SIM and A_{CM} is the absorbance of the cells treated with the control medium.

2.5.8. Cell adhesion and morphology.

The presence of cells attached to the nanostructured scaffolds was confirmed by fluorescence microscopy. The scaffolds were analyzed on the first and sixth days after the keratinocytes and SHED were seeded on the membranes. The membranes were washed in PBS, fixed in 4% paraformaldehyde buffer for 30 min, rinsed in buffer PBS and the cell nuclei were blue stained with $0.5 \mu\text{g ml}^{-1}$ of DAPI (1 min). To evaluate the morphology, the cells were stained with phalloidin ($30 \mu\text{g ml}^{-1}$) for actin filaments. The photographs were obtained by fluorescence microscope Leica DMi8 (Leica Microsystems).

3. Results and discussion

3.1. Morphology and diameter of the nanofibrous scaffolds

Figure 2 shows by SEM the formation of randomly oriented nanofibers with heterogeneous diameters. The SEM images of the PLGA scaffolds are illustrated in figures 2(a) and (b); the mean diameter of the fibers was $1051.0 \pm 290.2 \text{ nm}$ (figure 2(e)).

The PLGA/fibrin scaffolds presented a diameter ranging from 200 nm to 1300 nm, with a mean

of $639.8 \pm 241.8 \text{ nm}$. Approximately 77% of the fiber diameter was located between 300 and 800 nm (figures 2(c), (d), (f)). The smaller diameter in the PLGA/fibrin scaffolds is probably related to the addition of CaCl_2 salt to the plasma, improving the electrical conductivity of the polymeric solution and, consequently, decreasing the fibers diameter [20].

It is important to highlight that fibers with concentrations of PLGA lower than 40% presented beads and it was necessary to increase their concentration for obtaining uniform fibers and to counteract the acidic hydrolytic effect of formic acid. Formic acid could be responsible for maintaining a higher percentage of fibers with a diameter in the nano-scale [21]. On the other hand, it was observed that by increasing the concentration of the natural polymer, the fibers also presented beads; for this reason it was necessary to maintain a 1% fibrin concentration. Formic acid has been used to improve the solubilization of natural polymer and to develop hybrid scaffolds; the presented results are consistent with the findings of other investigations when formic acid was used. Shalumon and colleagues developed a hybrid scaffold of chitosan and PCL using formic acid as a solvent, and to avoid the formation of beads, it was necessary to increase the concentration of the synthetic polymer and decrease the concentration of the natural one [22]. However, studies using low concentrations of the natural polymer have already reported efficient results [23–26], and in this study, it is demonstrated that the incorporation of 1% fibrin increases cell viability.

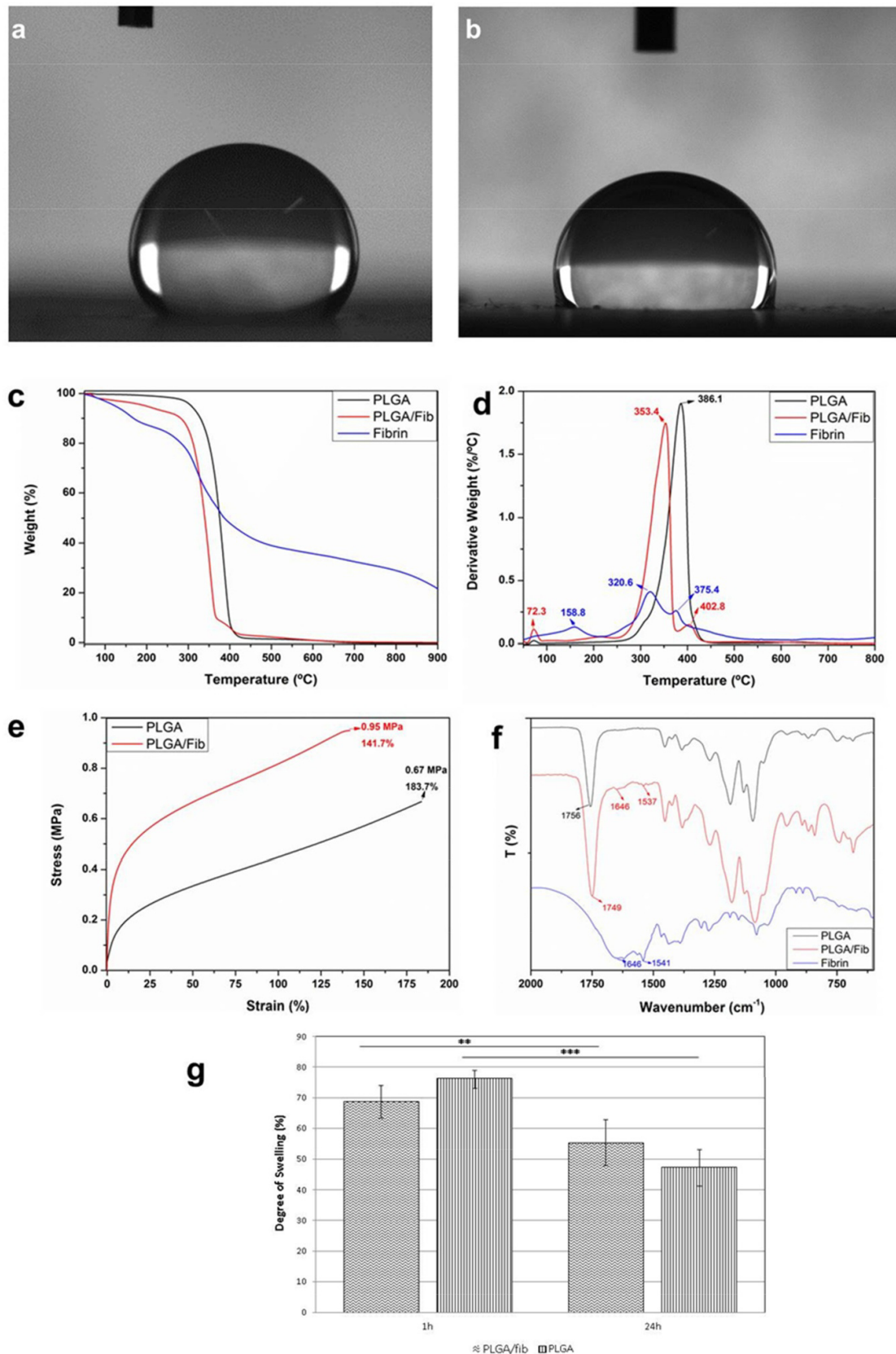


Figure 3. Water contact angle for PLGA scaffold (a) and PLGA/fibrin scaffold (b). TGA thermograms (c). Derivative of the TGA curve (d). Stress–strain curves (e). FTIR (f). Degree of swelling for scaffolds (g).

3.2. Thermal stability and water contact angle

The hydrophilicity of the nanofibrous membranes was analyzed by contact angle determination. The

water contact angle of the PLGA scaffolds was 118.9 ± 2.9 (figure 3(a)); however, with the incorporation of fibrin, the water contact angle of the

Table 1. Characteristic degradation temperatures of PLGA/fibrin (Fib) scaffolds and fibrin substrate.

Sample	Events	Temperature		Weight loss (%)	Weight (%)				
		range (°C)	T max (°C)		100 °C	300 °C	500 °C	700 °C	Residue at 800 °C
PLGA	1	30–100	72.3	0.32					
	2	100–500	386.1	98.29	99.68	96.08	1.38	0.02	0.0
	3	500–800	–	1.39					
PLGA/Fib	1	30–100	72.1	2.31					
	2	100–380	353.4	89.31	97.69	85.63	2.26	0.26	0.1
	3	380–450	402.8	5.56					
Fib	4	450–800	–	2.72					
	1	30–200	158.8	12.60					
	2	200–360	320.6	30.88	96.92	76.40	39.02	32.52	28.94
	3	360–550	375.4	19.28					
	4	550–800	–	8.30					

PLGA/fibrin scaffolds decreased to 111.1 ± 2.8 (figure 3(b)). Although fibrin presents a moderated hydrophobic nature after fibrinogen polymerization, which is determined by acid-base and Van der Waals interactions, the water contact angle of the PLGA/fibrin scaffolds was reduced [27]. While it can still be considered hydrophobic, a lower water contact angle could influence the improvement of cell-scaffold interaction.

To investigate the thermal stability of the PLGA/fibrin scaffolds, TGA analysis was carried out. On the TGA curves (figure 3(c)) it is possible to see a shift of the curve to the left, which signifies that the incorporation of fibrin facilitates scaffold degradation.

The PLGA scaffold showed two decomposition events, the first between 30 °C–100 °C, probably related to residual solvent evaporation (table 1, figure 3(d)). The second event occurred between 100 °C–500 °C when 98.3% of the scaffold weight was lost; this is associated with thermal degradation of the polymer backbone, as seen in other investigations [28, 29].

The PLGA/fibrin scaffold showed four degradation events. The first event, related to the residual solvent, appears again between 30 °C–100 °C, and 89.3% of the scaffold weight had been lost between 100 °C–380 °C. The third degradation event for the PLGA/fibrin scaffold occurred between 380 °C–450 °C, when 5.6% of the weight was lost. This event is probably related to fibrin degradation.

The fibrin substrate presented slower degradation kinetics, with four degradation events. In this case, weight loss occurred gradually, without big peaks of degradation. The polymer had lost 62.8% of its weight at 550 °C, and above this temperature, the final decomposition phase or carbonization of the polymer was observed [30]. A residual product of 28.9% at 800 °C was seen (table 1, figure 3(d)). The result shows that isolated fibrin is a stable product with important intermolecular forces, and explains why in the PLGA/fibrin scaffold there was a residual

mass at 800 °C of 0.1%, which is related to the natural polymer and its final carbonization phase (table 1).

Furthermore, based on the experience of our research group working with PLGA 75:25, it has been observed that the molecular weight of electrospun PLGA scaffolds decreased about 32% after 45 d of incubation in PBS [31] and an *in vivo* partial degradation of the PLGA scaffold after six weeks was also observed [32]. On the other hand, biodegradation of fibrin is mediated by plasmin and it is subject to a variety of factors such as tissue metabolism rate, tissue depth, presence of cells and fibrinogen concentration [33]. Wolbank and colleagues reported that the subcutaneous degradation kinetic for fibrin was of approximately 16 d [34]. Similarly, other authors have reported fibrin degradation in between one and two weeks, depending on the addition or not of cells [35–37]. It has therefore been suggested that, due to the degradation characteristics of PLGA spun scaffolds, they should be used for chronic wounds [38]. However, future studies should be made to determine the influence on the scaffold degradation behavior when 1% of fibrin is incorporated on PLGA mats.

3.3. Mechanical properties of nanofiber scaffolds

Stress-strain curves of PLGA and PLGA/fibrin scaffolds are presented in figure 3(e). The tensile strength of the scaffold increased when fibrin was incorporated, meanwhile, elongation at break decreased from 183.7 to 141.7%. The increment of the tensile strength and decrease of elongation at break could be attributed to the fibrin's intramolecular hydrogen bonding properties, inducing bundle formation by reinforcing the PLGA fibers [23]. Studies have found values of higher tensile strength and lower elongation at break for PLGA scaffolds, even with a lower concentration of the polymer [28, 39, 40], which indicates that the effect of formic acid on the polymer should be further studied.

Thus, it can be concluded that fibrin incorporation enhances the mechanical properties of the scaffold and such properties are expected to improve with

the incorporation of cells and the gradual deposition of the ECM.

3.4. FTIR of scaffolds

Influences of fibrin in the PLGA scaffolds were analyzed in the range between 2000 and 750 cm^{-1} . FTIR results are shown in figure 3(f). The fibrin presented characteristic amide absorption peaks (N–H), including 1541 cm^{-1} (Amide II bond) and 1646 cm^{-1} (Amide I bond) [41, 42]. PLGA displayed a characteristic absorption carbonyl (C=O) peak in 1756 cm^{-1} as well as a characteristic absorption band between 1100–1250, which represents the esters groups (C–O) [43]. On the other hand, the PLGA/fibrin scaffold showed similar peaks of both fibrin and PLGA.

Although the association of fibrin with synthetic polymers using the electrospinning technique for the development of scaffolds has already been reported, these studies used commercial fibrinogen [44, 45] or purified fibrinogen [46], which incurs higher production costs. Some studies have supported the use of blood plasma, but in these cases, the intention has been of coating the electrospinning mats with fibrin [47, 48], and not including the natural polymer in the electrospinning solution.

The method used in this present study, therefore, is advantageous because of its simplicity and low-cost, it being possible to construct the mat with autologous plasma without the risk of rejection induced by the natural polymer.

3.5. Swelling behavior

The ability to absorb water is a relevant characteristic of a skin substitute because of the importance of preventing severe fluid loss in full-thickness injuries. This study calculated the swelling degree of the mats, to evaluate if the incorporation of fibrin could contribute to decreasing the swelling degree of the scaffold, taking into account that fibrin from a plasma blood clot is moderately hydrophobic [27]. The results showed no statistically significant difference at the first hour for the PLGA and PLGA/fibrin scaffold, with a swelling degree of $76 \pm 3\%$ and $69 \pm 5\%$, respectively, figure 3(g). However, after 24 h, both mats presented a reduction in the swelling capacity of $55 \pm 7\%$ for the PLGA/fibrin and $47 \pm 6\%$ for the PLGA. Although the PLGA/fibrin swelling degree was better, the difference was not significant. The behavior of the membranes was expected due to the phenomenon of contraction that PLGA spun fibers undergo when mats are incubated in PBS at 37 °C, a phenomenon that has been widely reported [49, 50]. The contraction forces of the polymer fibers could thus hinder the scaffold expansion caused by water absorption.

3.6. Blood compatibility

To evaluate if the PLGA/fibrin scaffold was compatible with blood, the hemolysis percentage was calculated. The hemolysis percentage denotes the ratio of

erythrocytes, whose cell membrane is broken down when it comes into contact with the mat. Thus, a lower hemolysis percentage suggests good hemocompatibility of the scaffold. Figure 4(a) illustrates the absorbance of the hemolysis assay. Absorbance for the positive control was 0.432 ± 0.012 . Absorbance for the negative control, PLGA scaffold and PLGA/fibrin scaffolds was: 0.006 ± 0.001 ; 0.006 ± 0.001 , and 0.006 ± 0.001 , respectively, with hemolysis percentage for the PLGA and PLGA/fibrin scaffolds of 0.117 and 0.088, respectively. It can be concluded that both scaffolds were highly hemocompatible.

3.7. Indirect MTT assay

To test the cytocompatibility and toxicity of the mats, an indirect MTT assay was performed. Figure 4(b) shows increased cell viability of $107.2 \pm 6.8\%$ in the cells cultivated with the SIM of PLGA/fibrin mats compared with the control (cells cultivated with DMEM supplemented with FBS 10%). The results suggest that the SIM of the PLGA/fibrin scaffold contributed to improving the viability of the HaCaT cells, perhaps due to the fibrin release from the scaffold. On the other hand, the toxicity percentage of the PLGA/fibrin scaffold was: -7.2% . A negative result was obtained due to the mean of the absorbance in the group of cells cultivated with SIM from the PLGA/fibrin scaffold being greater than that of the control.

3.8. Direct MTT assay

MTT assay was used to evaluate the cell viability of the HaCaT and SHED cells on the scaffolds after 1 and 6 d. The tissue culture plate (TCP) was taken as control. Figures 4(c) and (d) illustrate absorbances for each group at different times.

The results showed similar viability of the HaCaT cells on the PLGA/fibrin scaffolds compared with the TCP on the first day (figure 4(c)). In contrast, the PLGA scaffold promoted significantly reduced viability compared with the PLGA/fibrin scaffolds. On the sixth day, there was a significant difference in the HaCaT cell viability cultivated on the PLGA/fibrin scaffold compared with the PLGA scaffold, although, it was inferior to the TCP. The results suggest that the incorporation of fibrin influenced initial HaCaT adhesion and proliferation. Although it was described that keratinocytes are not able to bind to fibrin due to the lack of integrin $\alpha v \beta 3$ [51], it has also been described that migration and proliferation of keratinocytes is dependent on fibrinogen concentration [52]; fibrinogen concentration, therefore, ranging from 17–33 mg ml^{-1} in fibrin 3D constructs provides an appropriate proliferation for keratinocytes. On the other hand, in the protein composition of a fibrin clot, fibronectin has been identified [42, 53], which has adhesion sites for $\alpha 5 \beta 1$ integrins, expressed in keratinocytes, being important for keratinocyte migration [54]. Besides this, it

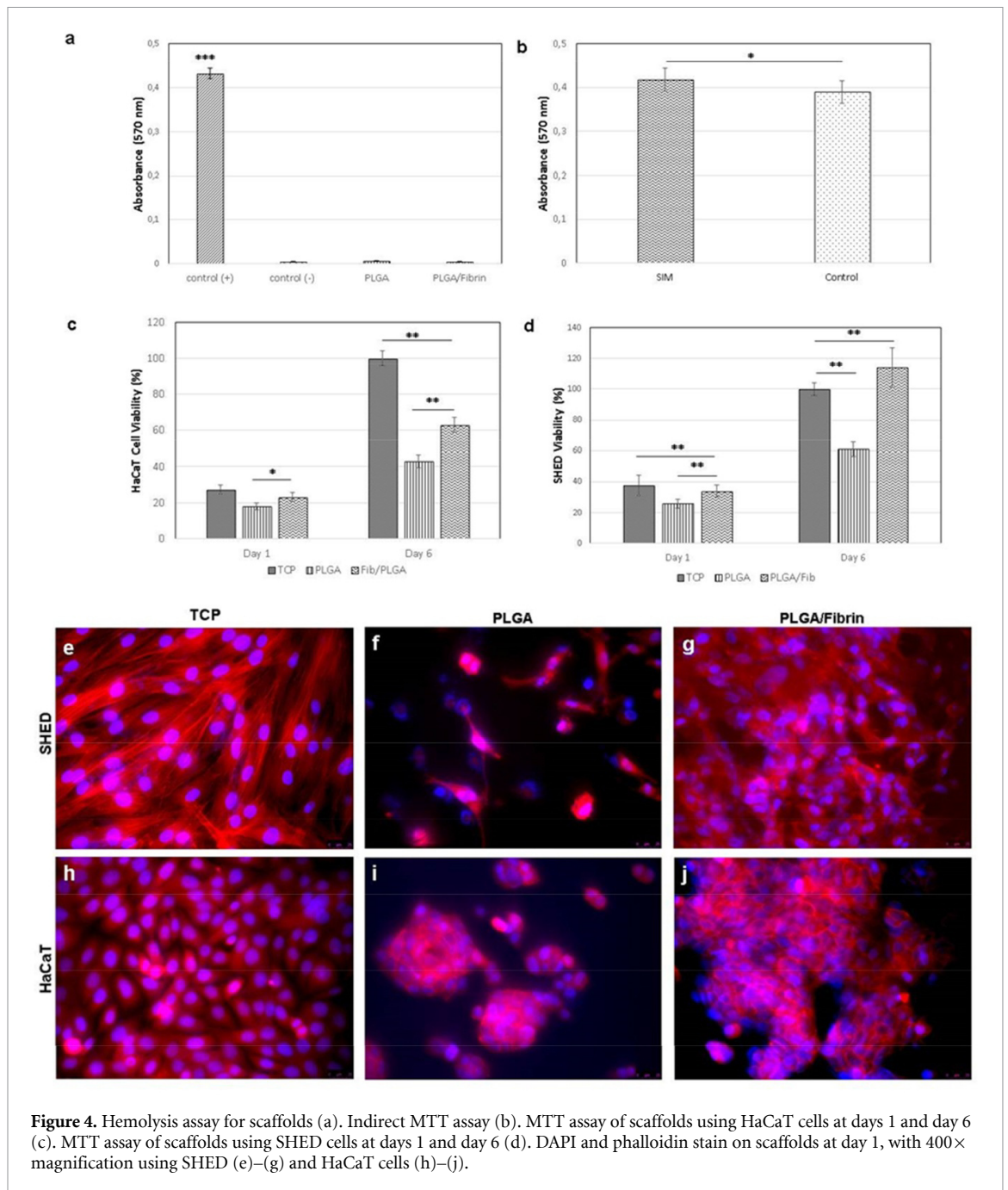


Figure 4. Hemolysis assay for scaffolds (a). Indirect MTT assay (b). MTT assay of scaffolds using HaCaT cells at days 1 and day 6 (c). MTT assay of scaffolds using SHED cells at days 1 and day 6 (d). DAPI and phalloidin stain on scaffolds at day 1, with 400 \times magnification using SHED (e)–(g) and HaCaT cells (h)–(j).

has been suggested that fibrin stimulates keratinocytes to secrete TGF- α , which in turn increases cell proliferation and EGF receptor capacity, supporting the proliferation of keratinocytes in an autocrine fashion [55].

When SHED viability was evaluated, the results showed a significant difference between all the groups, both on day 1 and day 6 (figure 4(d)). On the first day, there was a significantly increased viability of SHEDs on the PLGA/fibrin scaffold compared to the PLGA scaffold; however, the viability in the TCP was superior. In contrast, on day 6, the PLGA/fibrin scaffold had a significantly increased viability compared to the TCP as well as the PLGA scaffold. The PLGA scaffold viability was significantly reduced when compared to the PLGA/fibrin scaffold and the TCP.

The results suggest that the incorporation of fibrin in the mats improved the biological properties of the PLGA polymer, and viability on the mats is cell type-dependent.

3.9. Cell adhesion and morphology

The nuclei of the cells were stained with DAPI to evaluate if the cells were able to adhere to the scaffolds after 1 d and, to evaluate the morphology, actin filaments were stained with phalloidin (figures 4(e)–(j)). The SHED cultivated on the PLGA/fibrin scaffolds (figure 4(g)) presented a similar conformation of their morphology comparable with the control group (figure 4(e)). Meanwhile, the SHED culture in the PLGA scaffolds stills exhibited rounded

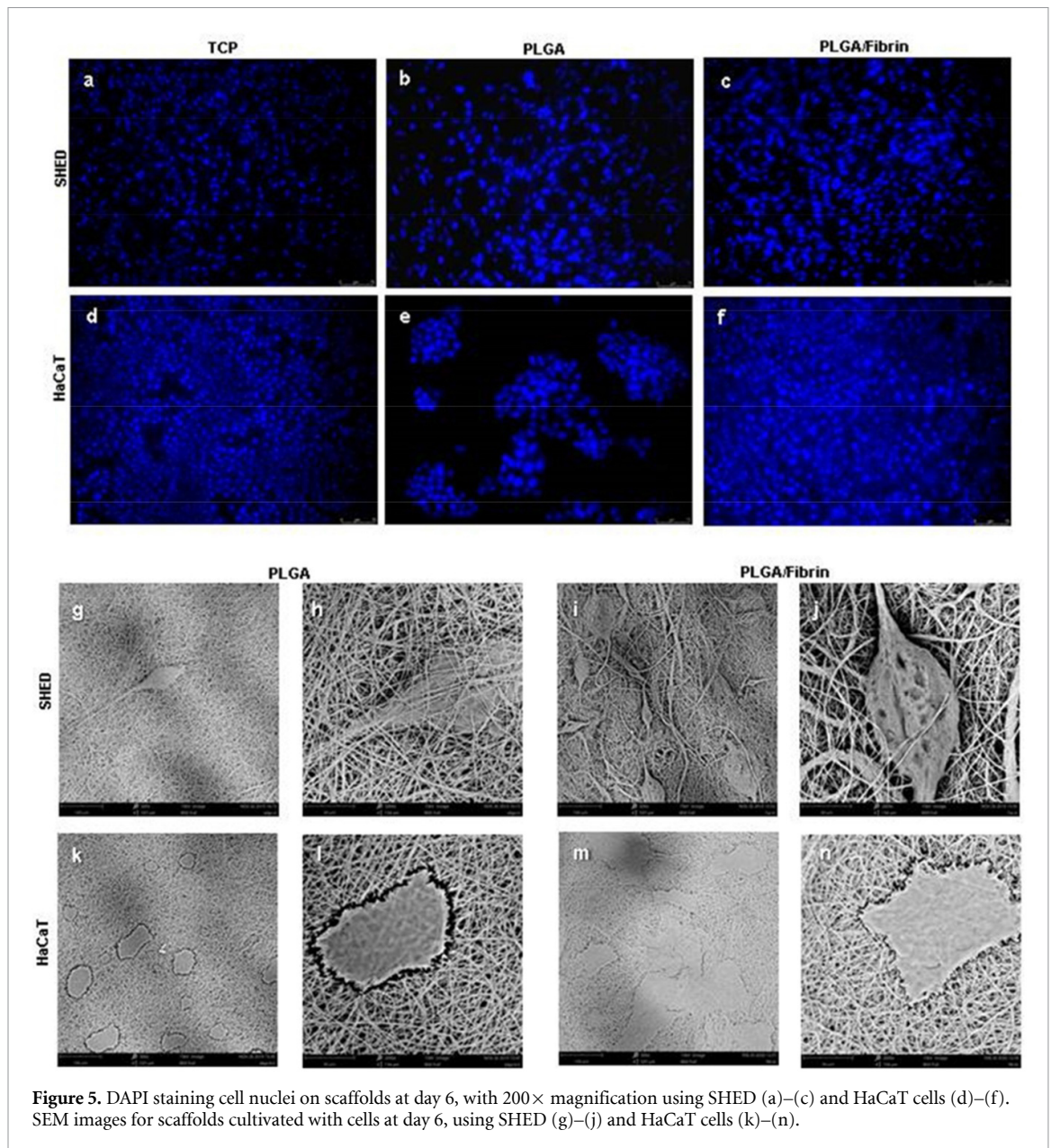


Figure 5. DAPI staining cell nuclei on scaffolds at day 6, with $200\times$ magnification using SHED (a)–(c) and HaCaT cells (d)–(f). SEM images for scaffolds cultivated with cells at day 6, using SHED (g)–(j) and HaCaT cells (k)–(n).

morphology (figure 4(f)). The HaCaT cells presented a similar cytoskeleton conformation in both the PLGA and PLGA/fibrin scaffolds (figure 4(i) and (j), respectively), being evident the presence of a higher cell density on the scaffold with fibrin incorporation. Images were taken in sites of greater cellular confluence.

The images taken at day 6 with DAPI stain are shown in figures 5(a)–(f). Magnification $200\times$ shows an overview of cell density on day 6, which confirms the results shown in the MTT assay. A higher nuclei density for both cell types in the PLGA/fibrin scaffolds can be seen compared with the PLGA scaffolds (figures 5(c) and (f)).

As seen in the DAPI stain images, the SEM images of $500\times$ magnification (figures 5(g), (i), (k), and (m)) showed a greater cell number in both cell types cultivated in the scaffolds with fibrin incorporation. It is even possible to see a layer of HaCaT cells

on the PLGA/fibrin scaffold (figure 5(m)), meanwhile, scattered cells are seen in the PLGA scaffolds (figure 5(k)). The images with $2000\times$ magnification (figures 5(h), (j), (l), (n)) show a normal morphology of both cell types at day six, on both the PLGA and PLGA/fibrin scaffolds.

4. Conclusion

In the present investigation, nanofibrous hybrid scaffolds of PLGA synthetic polymer and fibrin natural polymer were produced. It was demonstrated that the incorporation of 1% fibrin allows for the production of material with enhanced mechanical properties and cell viability as well as good blood compatibility. Furthermore, the isolation method of fibrin was shown to be a simple and efficient method for the obtainment of fibrin and probably other plasma proteins, which improve the biological properties of

PLGA scaffolds. It can therefore be suggested that fibrin could be used for spinning other synthetic polymers, considering the poor biological properties of such materials. Finally, it can be concluded that the PLGA/fibrin scaffold is a promising material to be used as a skin substitute.

Acknowledgments

This work was supported by Coordenação de Aperfeiçoamento de Pessoal de Nível Superior (CAPES) for PhD fellowship, Brazil (Grant No. 88882.439513/2019-01, 2019); Ministry of Science, Technology, Innovations and Communications (MCTIC)/FEEG/FURGS, Brazil (Grant No. 23078.010846/2019-78); Financiadora de Estudos e Projetos (FINEP), (Grant No. 0114013500); Fundação de Amparo à Pesquisa do Estado do Rio Grande do Sul (FAPERGS), (Grant No. 17/255/0001271-2) and Research the Stem Cell Research Institute.

ORCID iDs

Juliana Girón Bastidas  <https://orcid.org/0000-0003-3131-5067>

Natasha Maurmann  <https://orcid.org/0000-0001-5103-6394>

Mauro Ricardo da Silveira  <https://orcid.org/0000-0001-9717-3036>

Carlos Arthur Ferreira  <https://orcid.org/0000-0002-5707-8517>

Patricia Pranke  <https://orcid.org/0000-0003-4698-6314>

References

- [1] Matejuk A 2018 Skin immunity *Arch. Immunol. Ther. Exp.* **66** 45–54
- [2] Guttman-Yassky E, Zhou L and Krueger J G 2019 The skin as an immune organ: tolerance versus effector responses and applications to food allergy and hypersensitivity reactions *J. Allergy Clin. Immunol.* **144** 362–74
- [3] Vos T and Allen C 2016 Global, regional, and national incidence, prevalence, and years lived with disability for 310 diseases and injuries, 1990–2015: a systematic analysis for the Global Burden of Disease Study 2015 *Lancet* **388** 1545–602
- [4] Paggiaro A O, Bastianelli R, Carvalho V F, Isaac C and Gemperli R 2019 Is allograft skin, the gold-standard for burn skin substitute? A systematic literature review and meta-analysis *J. Plastic Reconstr. Aesthetic Surg.* **72** 1245–53
- [5] Nicholas M N, Jeschke M G and Amini-Nik S 2016 Methodologies in creating skin substitutes *Cell. Mol. Life Sci.* **73** 3453–72
- [6] Winter G D 1962 Formation of the scab and the rate of epithelization of superficial wounds in the skin of the young domestic pig *Nature* **193** 293–4
- [7] Jaffe L, Wu S C and Dressings T T 2019 Negative pressure wound therapy *Clin. Podiatr. Med. Surg.* **36** 397–411
- [8] Sobhanian P, Khorram M, Hashemi S S and Mohammadi A 2019 Development of nanofibrous collagen-grafted poly(vinyl alcohol)/gelatin/alginate scaffolds as potential skin substitute *Int. J. Biol. Macromol.* **130** 977–87
- [9] Pina S *et al* 2019 Scaffolding strategies for tissue engineering and regenerative medicine applications *Materials* **12** 1824
- [10] Kordestani S S 2019 Wound healing process *Atlas of Wound Healing: A Tissue Regeneration Approach* (Amsterdam: Elsevier) ch 3, pp 11–22
- [11] Sproul E, Nandi S and Brown A 2018 Fibrin biomaterials for tissue regeneration and repair *Peptides and Proteins as Biomaterials for Tissue Regeneration and Repair* (Cambridge: Woodhead Publishing) pp 127–50
- [12] Gray A J, Bishop J E, Reeves J T and Laurent G J 1993 A alpha and B beta chains of fibrinogen stimulate proliferation of human fibroblasts *J. Cell. Sci.* **104** 409–13
- [13] Heher P, Mühleder S, Mittermayr R, Redl H and Slezak P 2018 Fibrin-based delivery strategies for acute and chronic wound healing *Adv. Drug Deliv. Rev.* **129** 134–47
- [14] Reyhani V, Seddigh P, Guss B, Gustafsson R, Rask L and Rubin K 2014 Fibrin binds to collagen and provides a bridge for $\alpha V\beta 3$ integrin-dependent contraction of collagen gels *Biochem. J.* **462** 113–23
- [15] Robson S C, Shephard E G and Kirsch R E 1994 Fibrin degradation product D-dimer induces the synthesis and release of biologically active IL-1 β , IL-6 and plasminogen activator inhibitors from monocytes *in vitro Br. J. Haematol.* **86** 322–6
- [16] Maurmann N, Sperling L E and Pranke P 2018 Electrospun and electrosprayed scaffolds for tissue engineering *Advances in Experimental Medicine and Biology* vol 1078, ed H J Chun, C H Park, I K Kwon and G Khang (Berlin: Springer) pp 79–100
- [17] Bottezini P A 2018 Efeito da remoção seletiva de tecido cariado nas características imunofenotípicas apresentadas por células-tronco mesenquimais da polpa de dentes decíduos humanos *Master's Thesis* Universidade Federal do Rio Grande do Sul http://oasisbr.ibict.br/vufind/Record/URGS_244b5d1cd1810559e5320b1fde9b64b8/Description#tabnav (accessed 24 February 2020)
- [18] Maurmann N, Pereira D P, Burguez D, Pereira F D A D S, Neto P I, Rezende R A, Gamba D, da Silva J V L and Pranke P 2017 Mesenchymal stem cells cultivated on scaffolds formed by 3D printed PCL matrices, coated with PLGA electrospun nanofibers for use in tissue engineering *Biomed. Phys. Eng. Express* **3** 045005
- [19] Siqueira R L *et al* 2017 Bioactive gel-glasses with distinctly different compositions: bioactivity, viability of stem cells and antibiofilm effect against *Streptococcus mutans* *Mater. Sci. Eng. C* **76** 233–41
- [20] Mehdikhani M and Ghaziof S 2018 Electrically conductive poly- ϵ -caprolactone/polyethylene glycol/multi-wall carbon nanotube nanocomposite scaffolds coated with fibrin glue for myocardial tissue engineering *Appl. Phys. A Mater. Sci. Process.* **124** 1–15
- [21] Van Der Schueren L, De Schoenmaker B, Öi K and De Clerck K 2011 An alternative solvent system for the steady state electrospinning of polycaprolactone *Eur. Polym. J.* **47** 1256–63
- [22] Shalumon K T, Anulekha K H, Girish C M, Prasanth R, Nair S V and Jayakumar R 2010 Single step electrospinning of chitosan/poly(caprolactone) nanofibers using formic acid/acetone solvent mixture *Carbohydr. Polym.* **80** 413–9
- [23] Türker E, Üh Y and Arslan Yildiz A 2019 Biomimetic hybrid scaffold consisting of co-electrospun collagen and PLLCL for 3D cell culture *Int. J. Biol. Macromol.* **139** 1054–62
- [24] Mahsa Khatami S, Parivar K, Naderi Sohi A, Soleimani M and Hanaee-Ahvaz H 2020 Acetylated hyaluronic acid effectively enhances chondrogenic differentiation of mesenchymal stem cells seeded on electrospun PCL scaffolds *Tissue Cell* **65** 101363
- [25] Kenar H, Ozdogan C Y, Dumlu C, Doger E, Kose G T and Hasirci V 2019 Microfibrous scaffolds from poly(L-lactide-co- ϵ -caprolactone) blended with xeno-free

- collagen/hyaluronic acid for improvement of vascularization in tissue engineering applications *Mater. Sci. Eng. C* **97** 31–44
- [26] Eskandarinia A, Kefayat A, Gharakhloo M, Agheb M, Khodabakhshi D, Khorshidi M, Sheikhmoradi V, Rafienia M and Salehi H 2020 A propolis enriched polyurethane-hyaluronic acid nanofibrous wound dressing with remarkable antibacterial and wound healing activities *Int. J. Biol. Macromol.* **149** 467–76
- [27] van Oss C J 1990 Surface properties of fibrinogen and fibrin *J. Protein Chem.* **9** 487–91
- [28] Li A D, Sun Z Z, Zhou M, Xu X X, Ma J Y, Zheng W, Zhou H M, Li L and Zheng Y F 2013 Electrospun chitosan-graft-PLGA nanofibres with significantly enhanced hydrophilicity and improved mechanical property *Colloids Surf. B Biointerfaces* **102** 674–81
- [29] Li J *et al* 2017 Prevention of intra-abdominal adhesion using electrospun PEG/PLGA nanofibrous membranes *Mater. Sci. Eng. C* **78** 988–97
- [30] Natarajan D and Kiran M S 2019 Fabrication of juglone functionalized silver nanoparticle stabilized collagen scaffolds for pro-wound healing activities *Int. J. Biol. Macromol.* **124** 1002–15
- [31] Braghirolli D I, Zamboni F, Acasigua G A X and Pranke P 2015 Association of electrospinning with electrospaying: a strategy to produce 3D scaffolds with incorporated stem cells for use in tissue engineering *Int. J. Nanomed.* **10** 5159–70
- [32] Reis K P *et al* 2018 Application of PLGA/FGF-2 coaxial microfibers in spinal cord tissue engineering: an *in vitro* and *in vivo* investigation *Regen. Med.* **13** 785–801
- [33] Anitua E, Nurden P, Prado R, Nurden A T and Padilla S 2019 Autologous fibrin scaffolds: when platelet- and plasma-derived biomolecules meet fibrin *Biomaterials* **192** 440–60
- [34] Wolbank S *et al* 2015 Non-invasive *in vivo* tracking of fibrin degradation by fluorescence imaging *J. Tissue Eng. Regen. Med.* **9** 973–6
- [35] Breidenbach A P, Dymant N A, Lu Y, Rao M, Shearn J T, Rowe D W, Kadler K E and Butler D L 2014 Fibrin gels exhibit improved biological, structural, and mechanical properties compared with collagen gels in cell-based tendon tissue-engineered constructs *Tissue Eng. A* **21** 438–50
- [36] Anitua E, Zalduendo M M, Prado R, Alkhraisat M H and Orive G 2015 Morphogen and proinflammatory cytokine release kinetics from PRGF-Endoret fibrin scaffolds: evaluation of the effect of leukocyte inclusion *J. Biomed. Mater. Res. A* **103** 1011–20
- [37] Neuss S, Schneider R K M, Tietze L, Knüchel R and Jähnen-Dechent W 2010 Secretion of fibrinolytic enzymes facilitates human mesenchymal stem cell invasion into fibrin clots *Cells Tissues Organs* **191** 36–46
- [38] Vázquez N *et al* 2019 Influence of the PLGA/gelatin ratio on the physical, chemical and biological properties of electrospun scaffolds for wound dressings *Biomed. Mater.* **14** 045006
- [39] Eren Boncu T, Uskudar Guclu A, Catma M F, Savaser A, Gokce A and Ozdemir N 2020 *In vitro* and *in vivo* evaluation of linezolid loaded electrospun PLGA and PLGA/PCL fiber mats for prophylaxis and treatment of MRSA induced prosthetic infections *Int. J. Pharm.* **573** 118758
- [40] Luo H, Zhang Y, Gan D, Yang Z, Ao H, Zhang Q, Yao F and Wan Y 2019 Incorporation of hydroxyapatite into nanofibrous PLGA scaffold towards improved breast cancer cell behavior *Mater. Chem. Phys.* **226** 177–83
- [41] Deepthi S, Abdul Gafoor A A, Sivashanmugam A, Nair S V and Jayakumar R 2016 Nanostrotrium ranelate incorporated injectable hydrogel enhanced matrix production supporting chondrogenesis: *in vitro* *J. Mater. Chem. B* **4** 4092–103
- [42] Litvinov R I, Faizullin D A, Zuev Y F and Weisel J W 2012 The α -helix to β -sheet transition in stretched and compressed hydrated fibrin clots *Biophys. J.* **103** 1020–7
- [43] Sadeghi-Avalshahr A, Nokhasteh S, Molavi A M, Khorsand-Ghayeni M and Mahdavi-Shahri M 2017 Synthesis and characterization of collagen/PLGA biodegradable skin scaffold fibers *Regen. Biomater.* **4** 309–14
- [44] Law J X, Musa F, Ruszymah B H I, El Haj A J and Yang Y 2016 A comparative study of skin cell activities in collagen and fibrin constructs *Med. Eng. Phys.* **38** 854–61
- [45] Baker S *et al* 2012 The mechanical properties of dry, electrospun fibrinogen fibers *Mater. Sci. Eng. C* **32** 215–21
- [46] Li S, Su L, Li X, Yang L, Yang M, Zong H, Zong Q, Tang J and He H 2020 Reconstruction of abdominal wall with scaffolds of electrospun poly (L-lactide-co caprolactone) and porcine fibrinogen: an experimental study in the canine *Mater. Sci. Eng. C* **110** 110644
- [47] Malikhhammadov E, Tanir T E, Kiziltay A and Hasirci N 2019 Preparation and characterization of poly(ϵ -caprolactone) scaffolds modified with cell-loaded fibrin gel *Int. J. Biol. Macromol.* **125** 683–9
- [48] Setayeshmehr M, Esfandiari E, Hashemibeni B, Tavakoli A H, Rafienia M, Samadikuchaksaraei A, Moroni L and Joghataei M T 2019 Chondrogenesis of human adipose-derived mesenchymal stromal cells on the [devitalized costal cartilage matrix/poly(vinyl alcohol)/fibrin] hybrid scaffolds *Eur. Polym. J.* **118** 528–41
- [49] Blackwood K A *et al* 2008 Development of biodegradable electrospun scaffolds for dermal replacement *Biomaterials* **29** 3091–104
- [50] Ma C, Huang D L, Chen H C, Chen D L and Xiong Z C 2012 Preparation and characterization of electrospun poly (lactide-co-glycolide) membrane with different L-lactide and D-lactide ratios *J. Polym. Res.* **19** 1–6
- [51] Kubo M *et al* 2001 Fibrinogen and fibrin are anti-adhesive for keratinocytes: a mechanism for fibrin eschar slough during wound repair *J. Invest. Dermatol.* **117** 1369–81
- [52] Sese N, Cole M and Tawil B 2011 Proliferation of human keratinocytes and cocultured human keratinocytes and fibroblasts in three-dimensional fibrin constructs *Tissue Eng. A* **17** 429–37
- [53] Talens S, Leebeek F W G, Demmers J A A and Rijken D C 2012 Identification of fibrin clot-bound plasma proteins *PLoS ONE* **7** e41966
- [54] Kim J P, Zhang K, Chen J D, Wynn K C, Kramer R H and Woodley D T 1992 Mechanism of human keratinocyte migration on fibronectin: unique roles of RGD site and integrins *J. Cell. Physiol.* **151** 443–50
- [55] Yamamoto M, Yanaga H, Nishina H, Watabe S and Mamba K 2005 Fibrin stimulates the proliferation of human keratinocytes through the autocrine mechanism of transforming growth factor- α and epidermal growth factor receptor *Tohoku J. Exp. Med.* **207** 33–40

5. Capítulo 2

Bilayer scaffold from PLGA/fibrin electrospun membrane and fibrin hydrogel layer supports wound healing *in vivo*

Artigo submetido ao periódico *Biomedical Materials*. Fator de impacto 4.103 (2021)

6. Capítulo 3

Secretome of stem cells from human exfoliated deciduous teeth (SHED) improves keratinocytes migration, viability and attenuation of H₂O₂ induced cytotoxicity

Artigo a ser submetido

7. Discussão

O objetivo do presente estudo foi desenvolver estratégias para a regeneração cutânea com base em um biomaterial nanofibroso de PLGA/fibrina e secretoma de células-tronco. A fim de atingir esse objetivo, foi necessário desenvolver um *scaffold* fibroso pela técnica de *electrospinning* a partir de uma solução polimérica homogênea contendo o polímero sintético PLGA e o polímero natural fibrina. O polímero natural foi isolado a partir do plasma sanguíneo de ratos, após induzir a polimerização do fibrinogênio. Todos os parâmetros da eletrofiação precisaram ser otimizados, incluindo os solventes, concentração dos polímeros, velocidade, voltagem e distância da agulha à placa coletora. Foi necessário o uso de ácido fórmico para dissolver a fibrina e de hexafluoro 2-propanol (HFIP) e polietilenoglicol (PEG) para estabilizar o processo.

A matriz extracelular compreende uma rede heterogênea de fibras dentre as quais se encontram as fibras de colágeno tipo I com um diâmetro de 1-20 μm , as fibras reticulares (colágeno tipo III) com diâmetro de cerca de 30nm, e fibrilas de elastina com cerca de 0,1-0,2 μm de diâmetro (USHIKI, 2002). Portanto, um *scaffold* apropriado deveria mimetizar o tamanho da rede de fibras da MEC intersticial, sendo indispensável para promover a regeneração tecidual (FRANTZ; STEWART; WEAVER, 2010). Considerando o precedente, os *scaffolds* de PLGA/fibrina apresentaram fibras com diâmetro heterogêneo entre 200 nm e 1.300 nm, com média de $639,8 \pm 241,8$ nm. Dessa forma, o material produzido conseguiu mimetizar o tamanho da rede de fibras da MEC intersticial.

Por outro lado, quando incorporada a fibrina aos *scaffolds* de PLGA, os testes físicos demonstraram uma melhora nas propriedades mecânicas do biomaterial ao aumentar a tensão e diminuir a deformação do material, propriedades interessantes para o melhor manuseio do material durante o procedimento cirúrgico e que garantem a integridade estrutural, a longo prazo. A avaliação por FTIR confirmou a presença da fibrina no material e a análise de estabilidade térmica mostrou que a incorporação de fibrina facilitou a degradação do *scaffold*. Além disso, os *scaffolds* demonstraram compatibilidade sanguínea e a incorporação de fibrina melhorou a adesão e a viabilidade celular de queratinócitos e células-tronco. Portanto, esses testes sugerem que os biomateriais produzidos foram capazes de fornecer suporte estrutural para a fixação das células e subsequente desenvolvimento do tecido.

Uma importante vantagem desses *scaffolds* consiste na utilização de fibrina derivada do plasma sanguíneo, pois é um material com boa disponibilidade e cujo processamento é relativamente fácil. Além disso, existe a possibilidade da utilização de plasma alogênico, com baixo potencial para provocar reação imune significativa, já que é desprovido de células.

Alguns estudos têm comprovado a segurança e eficácia de trabalhar com derivados plasmáticos alogênicos no tratamento de feridas cutâneas ao não apresentar reações imunes adversas (SEMENIČ *et al.*, 2018; BARRIONUEVO *et al.*, 2015; LIAO *et al.*, 2020). Todavia, mais estudos deverão ser realizados para caracterizar melhor a resposta imune local.

Posteriormente, a fim de testar o *scaffold* desenvolvido *in vivo*, utilizou-se um modelo de lesão cutânea de espessura completa em ratos Wistar Kyoto machos, por serem animais isogênicos e permitirem simular um transplante de células autólogo. Para essas análises, foi criado um biomaterial em bicamada, usando a membrana de *electrospinning* anteriormente avaliada *in vitro*, com adição de uma camada de hidrogel de fibrina, usando ácido tranexâmico para retardar a fibrinólise. Assim, a hipótese foi de que a membrana de *electrospinning* poderia suportar a migração e proliferação de queratinócitos (como visto no estudo *in vitro*), enquanto a camada de hidrogel de fibrina poderia suportar a proliferação, migração e deposição de colágeno de fibroblastos, para dessa forma obter um substituto dermo-epidérmico. No momento da cirurgia os *scaffolds* demonstraram fácil manuseio e puderam ser fixados por pontos de sutura.

Esse substituto dermo-epidérmico produzido foi então avaliado com a incorporação ou não de células em um modelo de lesão de espessura total. Os tecidos foram analisados no dia 14 e 21. Os *scaffolds* em bicamada contribuíram com a formação do tecido de granulação e a deposição precoce de colágeno. Resultados similares foram obtidos por CHUNG e colaboradores (CHUNG *et al.*, 2016), em que os *scaffolds* híbridos de PEG/fibrina contribuíram com a formação do tecido de granulação. Entretanto, a utilização desses *scaffolds* híbridos de PEG/fibrina não induziu diferenças significativas na deposição de colágeno entre os grupos no dia 21. Ainda, os resultados obtidos neste trabalho de doutorado não demonstraram diferenças entre os grupos com a incorporação ou não de células quando analisada a espessura epitelial, a espessura do tecido de granulação e da derme e o índice de colágeno. Assim, os testes indicaram que a incorporação de células não influenciou no processo de cicatrização.

Os testes com os marcadores de cicatrização de feridas no dia 14 mostraram o aumento da expressão de proteínas anti-inflamatórias e EGF, quando os *scaffolds* foram implantados. Esses resultados estão de acordo com o estágio de cicatrização da ferida (fase proliferativa), sendo que a expressão elevada de TGF- β 1 e IL-10 contribuíram com a deposição de MEC e supressão da inflamação (KRZYSZCZYK *et al.*, 2018; LIARTE; BERNABÉ-GARCÍA; NICOLÁS, 2020). O EGF é conhecido por ter um papel importante durante o processo de cicatrização de feridas, não apenas na proliferação e migração de queratinócitos, mas também na de fibroblastos (CHEN *et al.*, 1993; LAATO *et al.*, 1987). Em contrapartida, não houve

diferença na expressão de VEGF entre os grupos, o que sugere que os *scaffolds* não interferiram na angiogênese do tecido.

As atividades de GPx e SOD foram diminuídas em relação ao controle positivo e negativo. A baixa atividade de GPx e SOD sugere que o *scaffold* conseguiu reduzir diretamente os níveis de espécies reativas de oxigênio (EROs) e indiretamente causar uma diminuição na expressão desses antioxidantes enzimáticos. No entanto, uma amostra baixa (n=4) foi um aspecto limitante deste experimento, sendo necessária a realização de mais estudos para confirmar a redução dos níveis de EROs.

A segunda estratégia proposta para promover a regeneração cutânea baseou-se na utilização do secretoma de SHED para melhorar a viabilidade, migração e atenuação de danos induzidos durante as agressões cutâneas. Os resultados do presente estudo mostraram que tanto o MC em uma concentração de 50%, quanto as VE de SHED em uma concentração de 0,4 µg/ml conseguiram aumentar significativamente a viabilidade celular e atenuar os efeitos de H₂O₂ em um modelo *in vitro* de lesão cutânea. Além disso, o tratamento com MC e VE aumentou de forma significativa a expressão de VEGF nos queratinócitos, o que significa que um dos mecanismos usados para promover as funções dos queratinócitos tratados com o secretoma estariam relacionados com a sinalização parácrina através de VEGF. A escolha para avaliar especialmente esse mecanismo baseou-se principalmente no aspecto de que apesar do VEGF ser amplamente reconhecido como promotor de angiogênese, esse fator de crescimento também estimula a proliferação de queratinócitos. Além disso, em estudos anteriores foi demonstrado que os queratinócitos normais podem expressar os três receptores de VEGF (VEGFR-1, VEGFR-2, e VEGFR-3) (MAN *et al.*, 2006; WILGUS *et al.*, 2005) e que o meio condicionado de SHED é rico em VEGF (DE CARA *et al.*, 2019; BHANDI *et al.*, 2021).

Devido à relevância da implantação de *scaffolds* e às propriedades do secretoma de células-tronco no reparo tecidual, nos últimos anos alguns pesquisadores têm proposto adicionar VEs aos biomateriais. Dessa forma, é possível obter duplo benefício, de sustentação celular e de liberação controlada de VEs. Adicionalmente, a liberação controlada de VEs garante um efeito terapêutico sustentado, diferente da administração sistêmica de VEs, que resulta em uma alta taxa de depuração pela circulação sanguínea, ou a administração local direta com uma rápida renovação de fluidos (RIAU *et al.*, 2019). Portanto, as perspectivas futuras com o trabalho desenvolvido nesta tese consistem na incorporação das VEs de SHED na camada de hidrogel de fibrina a fim de potencializar o efeito terapêutico do *scaffold*. Também seria interessante estudar o perfil proteômico do MC e das VEs, assim como realizar uma

análise de sequenciamento dos miRNA presentes nas VEs para aprofundar o estudo dos mecanismos envolvidos.

Por outro lado, uma outra perspectiva deste trabalho seria procurar alternativas que consigam ativar as CTs para obter um melhor rendimento de VEs, pois a principal limitação que a literatura relata com relação ao uso de VEs na medicina regenerativa consiste na baixa taxa de liberação dessas nanopartículas pelas CT. Assim, alguns pesquisadores têm proposto estratégias como a extrusão de células vivas através de microfiltros, ou o pré-condicionamento dessas células, como mostrado no artigo de revisão. No entanto, é necessário otimizar esses processos para a sua produção em larga escala.

Com o presente estudo, foi demonstrado que a incorporação do polímero natural fibrina ao polímero sintético PLGA melhorou as propriedades biológicas do biomaterial através de um método de processamento simples, que mimetizou a MEC intersticial e permitiu um processo de reparo tecidual acelerado. Adicionalmente, demonstrou-se que o secretoma de SHED é uma fonte interessante de moléculas bioativas capazes de melhorar a viabilidade e migração de queratinócitos, além de atenuar os efeitos citotóxicos induzidos por H₂O₂. Essas duas estratégias abrem a oportunidade de novas abordagens de tratamento, utilizando fontes facilmente acessíveis como o fibrinogênio do plasma sanguíneo e CT de dentes decíduos que geralmente são descartados.

8. Conclusões

Na presente investigação, foram produzidos *scaffolds* híbridos nanofibrosos através da técnica de *electrospinning* usando o polímero sintético PLGA e o polímero natural fibrina. Foi demonstrado que a incorporação de 1% de fibrina permitiu a produção de um material com propriedades mecânicas aprimoradas, boa compatibilidade sanguínea, que garantiu a viabilidade das células cultivadas. Além disso, o método de isolamento da fibrina mostrou-se um método simples e eficiente para a obtenção dessa proteína, que melhorou as propriedades biológicas do *scaffold*. Por outro lado, as análises *in vivo* do substituto dermo-epidérmico mostraram que os *scaffolds* contribuíram para a formação do tecido de granulação, deposição precoce de colágeno e reepitelização, aumentando a expressão de TGFβ1 e EGF. No entanto, a incorporação de células não influenciou nas características histológicas do tecido de granulação e epitélio, nem no índice de colágeno.

Os resultados do subprojeto 2 demonstraram que o secretoma de SHED efetivamente promoveu as funções (viabilidade, migração e atenuação da citotoxicidade induzida por H₂O₂) dos queratinócitos de forma parácrina através da sinalização por meio do VEGF. Assim, as SHED são uma fonte interessante de MC e VEs para aplicações clínicas devido à sua fácil acessibilidade, excelente proliferação e nenhuma morbidade associada. Tanto o SHED-MC quanto SHED-VEs podem ser ferramentas terapêuticas promissoras para acelerar a re-epitelização na cicatrização de feridas.

Finalmente, o presente estudo demonstrou que as estratégias propostas para contribuir com a regeneração cutânea foram eficazes. Desenvolveu-se um *scaffold* de fácil processamento, que suportou efetivamente a formação de novo tecido. Adicionalmente, o secretoma de SHED constitui uma alternativa inovadora, livre de células, que poderia atuar como molécula bioativa na tríade da Engenharia tecidual para contribuir positivamente na re-epitelização de feridas. Assim, a implementação de ambos os métodos, tem potencial para a obtenção de resultados promissores no tratamento de lesões cutâneas.

9. Referências

ADDOR, F. A. S. A.; AOKI, V. Barreira cutânea na dermatite atópica. **Anais Brasileiros de Dermatologia**, [s. l.], v. 85, n. 2, p. 184–194, 2010. Disponível em: <http://www.scielo.br/j/abd/a/hfXznRXzgzY8YRkyqT8kLZM/?lang=pt>. Acesso em: 12 jul. 2022.

AL KAYAL, T. *et al.* A New Method for Fibrin-Based Electrospun/Sprayed Scaffold Fabrication. **Scientific reports**, [s. l.], v. 10, n. 1, 2020. Disponível em: <https://pubmed.ncbi.nlm.nih.gov/32198419/>. Acesso em: 19 jul. 2022.

BARBIERI, J. S.; WANAT, K.; SEYKORA, J. Skin: Basic Structure and Function. **Pathobiology of Human Disease: A Dynamic Encyclopedia of Disease Mechanisms**, [s. l.], p. 1134–1144, 2014.

BARRIONUEVO, D. V. *et al.* Comparison of experimentally-induced wounds in rabbits treated with different sources of platelet-rich plasma. **Laboratory animals**, [s. l.], v. 49, n. 3, p. 209–214, 2015. Disponível em: <https://pubmed.ncbi.nlm.nih.gov/25586936/>. Acesso em: 26 jul. 2022.

BHANDI, S. *et al.* Comparative analysis of cytokines and growth factors in the conditioned media of stem cells from the pulp of deciduous, young, and old permanent tooth. **Saudi Journal of Biological Sciences**, [s. l.], v. 28, n. 6, p. 3559–3565, 2021.

BIKLE, D. D. Vitamin D: Newer Concepts of Its Metabolism and Function at the Basic and Clinical Level. **Journal of the Endocrine Society**, [s. l.], v. 4, n. 2, 2020. Disponível em: <https://academic.oup.com/jes/article/4/2/bvz038/5731496>. Acesso em: 17 jul. 2022.

BIKLE, D. D. Vitamin D Metabolism and Function in the Skin. **Molecular and cellular endocrinology**, [s. l.], v. 347, n. 1–2, p. 80, 2011. Disponível em: [/pmc/articles/PMC3188673/](https://pubmed.ncbi.nlm.nih.gov/21111111/). Acesso em: 17 jul. 2022.

BOUWSTRA, J. A.; HELDER, R. W. J.; EL GHALBZOURI, A. Human skin equivalents: Impaired barrier function in relation to the lipid and protein properties of the stratum corneum. **Advanced drug delivery reviews**, [s. l.], v. 175, 2021. Disponível em: <https://pubmed.ncbi.nlm.nih.gov/34015420/>. Acesso em: 12 jul. 2022.

CHEN, J. D. *et al.* Epidermal Growth Factor (EGF) Promotes Human Keratinocyte Locomotion on Collagen by Increasing the $\alpha 2$ Integrin Subunit. **Experimental Cell Research**, [s. l.], v. 209, n. 2, p. 216–223, 1993.

CHUNG, E. *et al.* Fibrin-based stem cell containing scaffold improves the dynamics of burn wound healing. **Wound Repair and Regeneration**, [s. l.], v. 24, n. 5, p. 810–819, 2016. Disponível em: <https://onlinelibrary.wiley.com/doi/full/10.1111/wrr.12459>. Acesso em: 31 jul. 2022.

COATES, M. *et al.* The Skin and Intestinal Microbiota and Their Specific Innate Immune Systems. **Frontiers in Immunology**, [s. l.], v. 10, p. 2950, 2019.

CORUH, A.; YONTAR, Y. Application of Split-Thickness Dermal Grafts in Deep Partial- and Full-Thickness Burns A New Source of Auto-Skin Grafting. **Journal of Burn Care & Research**, [s. l.], v. 33, n. 3, p. e95–e101, 2012. Disponível em: <https://academic.oup.com/jbcr/article/33/3/e95/4588695>. Acesso em: 18 jul. 2022.

DE CARA, S. P. H. M. *et al.* Angiogenic properties of dental pulp stem cells conditioned medium on endothelial cells in vitro and in rodent orthotopic dental pulp regeneration. **Heliyon**, [s. l.], v. 5, n. 4, p. e01560, 2019.

DOMINICI, M. *et al.* Minimal criteria for defining multipotent mesenchymal stromal cells. The International Society for Cellular Therapy position statement. **Cytotherapy**, [s. l.], v. 8, n. 4, p. 315–317, 2006. Disponível em: <https://pubmed.ncbi.nlm.nih.gov/16923606/>. Acesso em: 23 jul. 2022.

EL-CHAMI, C. *et al.* Role of organic osmolytes in water homeostasis in skin. **Experimental dermatology**, [s. l.], v. 23, n. 8, p. 534–537, 2014. Disponível em: <https://pubmed.ncbi.nlm.nih.gov/24942488/>. Acesso em: 11 jul. 2022.

EYERICH, S. *et al.* Cutaneous Barriers and Skin Immunity: Differentiating A Connected Network. **Trends in immunology**, [s. l.], v. 39, n. 4, p. 315–327, 2018. Disponível em: <https://pubmed.ncbi.nlm.nih.gov/29551468/>. Acesso em: 11 jul. 2022.

FITZSIMMONS, R. E. B. *et al.* Mesenchymal stromal/stem cells in regenerative medicine and tissue engineering. **Stem Cells International**, [s. l.], v. 2018, 2018.

FRANTZ, C.; STEWART, K. M.; WEAVER, V. M. The extracellular matrix at a glance. **Journal of Cell Science**, [s. l.], v. 123, n. 24, p. 4195, 2010. Disponível em: </pmc/articles/PMC2995612/>. Acesso em: 25 jul. 2022.

FRIEDENSTEIN, A. J. Precursor Cells of Mechanocytes. **International Review of Cytology**, [s. l.], v. 47, n. C, p. 327–359, 1976.

FRIEDENSTEIN, A. J.; CHAILAKHYAN, R. K.; GERASIMOV, U. V. Bone marrow osteogenic stem cells: in vitro cultivation and transplantation in diffusion chambers. **Cell Proliferation**, [s. l.], v. 20, n. 3, p. 263–272, 1987. Disponível em: <https://onlinelibrary.wiley.com/doi/full/10.1111/j.1365-2184.1987.tb01309.x>. Acesso em: 9 ago. 2022.

GUNNARSSON, M. *et al.* Extraction of natural moisturizing factor from the stratum corneum and its implication on skin molecular mobility. **Journal of Colloid and Interface Science**, [s. l.], v. 604, p. 480–491, 2021.

HARRIS-TRYON, T. A.; GRICE, E. A. Microbiota and maintenance of skin barrier function. **Science (New York, N.Y.)**, [s. l.], v. 376, n. 6596, p. 940–945, 2022. Disponível em: <https://pubmed.ncbi.nlm.nih.gov/35617415/>. Acesso em: 13 jul. 2022.

HEHER, P. *et al.* Fibrin-based delivery strategies for acute and chronic wound healing. **Advanced Drug Delivery Reviews**, [s. l.], v. 129, p. 134–147, 2018.

HUANG, J. *et al.* Dermal extracellular matrix molecules in skin development, homeostasis,

wound regeneration and diseases. **Seminars in cell & developmental biology**, [s. l.], v. 128, p. 137–144, 2022. Disponível em: <https://pubmed.ncbi.nlm.nih.gov/35339360/>. Acesso em: 13 jul. 2022.

J GORDON. 5.1 Layers of the Skin - Anatomy and Physiology | OpenStax. In: ANATOMY AND PHYSIOLOGY. Houston, Texas: OpenStax, 2013. *E-book*. Disponível em: <https://openstax.org/books/anatomy-and-physiology/pages/5-1-layers-of-the-skin>. Acesso em: 12 jul. 2022.

KALRA, H.; DRUMMEN, G. P. C.; MATHIVANAN, S. Focus on Extracellular Vesicles: Introducing the Next Small Big Thing. **International journal of molecular sciences**, [s. l.], v. 17, n. 2, 2016. Disponível em: <https://pubmed.ncbi.nlm.nih.gov/26861301/>. Acesso em: 2 out. 2022.

KO, C.-S.; CHEN, J.-H.; SU, W.-T. Stem Cells from Human Exfoliated Deciduous Teeth: A Concise Review. **Current stem cell research & therapy**, [s. l.], v. 15, n. 1, p. 61–76, 2020. Disponível em: <https://pubmed.ncbi.nlm.nih.gov/31648649/>. Acesso em: 23 jul. 2022.

KOBAYASHI, N. *et al.* Supranuclear Melanin Caps Reduce Ultraviolet Induced DNA Photoproducts in Human Epidermis. **Journal of Investigative Dermatology**, [s. l.], v. 110, n. 5, p. 806–810, 1998.

KRZYSZCZYK, P. *et al.* The role of macrophages in acute and chronic wound healing and interventions to promote pro-wound healing phenotypes. **Frontiers in Physiology**, [s. l.], v. 9, n. MAY, p. 419, 2018.

LAATO, M. *et al.* Epidermal growth factor increases collagen production in granulation tissue by stimulation of fibroblast proliferation and not by activation of procollagen genes. **Biochemical Journal**, [s. l.], v. 247, n. 2, p. 385, 1987. Disponível em: </pmc/articles/PMC1148420/?report=abstract>. Acesso em: 7 maio 2022.

LAI-CHEONG, J. E.; MCGRATH, J. A. Structure and function of skin, hair and nails. **Medicine**, [s. l.], v. 45, n. 6, p. 347–351, 2017.

LÄSSER, C.; JANG, S. C.; LÖTVALL, J. Subpopulations of extracellular vesicles and their therapeutic potential. **Molecular aspects of medicine**, [s. l.], v. 60, p. 1–14, 2018. Disponível em: <https://pubmed.ncbi.nlm.nih.gov/29432782/>. Acesso em: 3 out. 2022.

LAURENS, N.; KOOLWIJK, P.; DE MAAT, M. P. Fibrin structure and wound healing. **Journal of Thrombosis and Haemostasis**, [s. l.], v. 4, n. 5, p. 932–939, 2006. Disponível em: <https://onlinelibrary.wiley.com/doi/full/10.1111/j.1538-7836.2006.01861.x>. Acesso em: 20 jul. 2022.

LIAO, X. *et al.* Allogeneic Platelet-Rich Plasma Therapy as an Effective and Safe Adjuvant Method for Chronic Wounds. **Journal of Surgical Research**, [s. l.], v. 246, p. 284–291, 2020.

LIARTE, S.; BERNABÉ-GARCÍA, Á.; NICOLÁS, F. J. Role of TGF- β in Skin Chronic Wounds: A Keratinocyte Perspective. **Cells**, [s. l.], v. 9, n. 2, 2020. Disponível em: <https://pubmed.ncbi.nlm.nih.gov/32012802/>. Acesso em: 4 maio 2022.

MAN, X. Y. *et al.* Immunolocalization and expression of vascular endothelial growth factor receptors (VEGFRs) and neuropilins (NRPs) on keratinocytes in human epidermis. **Molecular Medicine**, [s. l.], v. 12, n. 7–8, p. 127–136, 2006. Disponível em: <https://molmed.biomedcentral.com/articles/10.2119/2006-00024.Man>. Acesso em: 28 jun. 2022.

MARKIEWICZ, A. *et al.* Burn Wound Healing: Clinical Complications, Medical Care, Treatment, and Dressing Types: The Current State of Knowledge for Clinical Practice. **International Journal of Environmental Research and Public Health**, [s. l.], v. 19, n. 3, p. 1338, 2022. Disponível em: </pmc/articles/PMC8834952/>. Acesso em: 18 jul. 2022.

MAURMANN, N.; SPERLING, L. E.; PRANKE, P. Electrospun and Electrospayed Scaffolds for Tissue Engineering. **Advances in Experimental Medicine and Biology**, [s. l.], v. 1078, p. 79–100, 2018. Disponível em: https://link.springer.com/chapter/10.1007/978-981-13-0950-2_5. Acesso em: 22 jul. 2022.

MAYNARD, R. L.; DOWNES, N. The Skin or the Integument. **Anatomy and Histology of the Laboratory Rat in Toxicology and Biomedical Research**, [s. l.], p. 303–315, 2019.

MCKNIGHT, G.; SHAH, J.; HARGEST, R. Physiology of the skin. **Surgery (Oxford)**, [s. l.], v. 40, n. 1, p. 8–12, 2022.

MEKALA, N. K. *et al.* Physical and degradation properties of PLGA scaffolds fabricated by salt fusion technique. **Journal of Biomedical Research**, [s. l.], v. 27, n. 4, p. 318, 2013. Disponível em: </pmc/articles/PMC3721041/>. Acesso em: 21 jul. 2022.

MICHAEL H. ROSS, W. P. **Histology: A Text and Atlas : with Correlated Cell and Molecular Biology**. 7. ed. [S. l.: s. n.], 2016.

MIURA, M. *et al.* SHED: Stem cells from human exfoliated deciduous teeth. **Proceedings of the National Academy of Sciences of the United States of America**, [s. l.], v. 100, n. 10, p. 5807, 2003. Disponível em: </pmc/articles/PMC156282/>. Acesso em: 22 jun. 2022.

MOHAMED, S. A.; HARGEST, R. Surgical anatomy of the skin. **Surgery (Oxford)**, [s. l.], v. 40, n. 1, p. 1–7, 2022.

MÚZES, G.; SIPOS, F. Mesenchymal Stem Cell-Derived Secretome: A Potential Therapeutic Option for Autoimmune and Immune-Mediated Inflammatory Diseases. **Cells** 2022, Vol. 11, Page 2300, [s. l.], v. 11, n. 15, p. 2300, 2022. Disponível em: <https://www.mdpi.com/2073-4409/11/15/2300/htm>. Acesso em: 2 out. 2022.

OKUTAN, N.; TERZI, P.; ALTAY, F. Affecting parameters on electrospinning process and characterization of electrospun gelatin nanofibers. **Food Hydrocolloids**, [s. l.], v. 39, p. 19–26, 2014.

OLSSON, M. *et al.* The humanistic and economic burden of chronic wounds: A systematic review. **Wound repair and regeneration : official publication of the Wound Healing Society [and] the European Tissue Repair Society**, [s. l.], v. 27, n. 1, p. 114–125, 2019. Disponível em: <https://pubmed.ncbi.nlm.nih.gov/30362646/>. Acesso em: 18 jul. 2022.

OUALLA-BACHIRI, W. *et al.* From Grafts to Human Bioengineered Vascularized Skin Substitutes. **International Journal of Molecular Sciences** 2020, Vol. 21, Page 8197, [s. l.], v. 21, n. 21, p. 8197, 2020. Disponível em: <https://www.mdpi.com/1422-0067/21/21/8197/htm>. Acesso em: 19 jul. 2022.

OVALLE, W. K.; NAHIRNEY, P. C. Netter Bases da Histologia. *In*: [S. l.]: Elsevier, 2008. p. 252. *E-book*. Disponível em: [https://books.google.com.br/books?id=fbwGWHIO6s0C&pg=PA156&dq=pele+órgão+sensorial&hl=es&sa=X&ved=2ahUKEwiYgI6X5YD5AhWYu5UCHZxdAJAQ6AF6BAgIEAI#v=onepage&q=pele órgão sensorial&f=false](https://books.google.com.br/books?id=fbwGWHIO6s0C&pg=PA156&dq=pele+órgão+sensorial&hl=es&sa=X&ved=2ahUKEwiYgI6X5YD5AhWYu5UCHZxdAJAQ6AF6BAgIEAI#v=onepage&q=pele%20órgão%20sensorial&f=false). Acesso em: 17 jul. 2022.

RAMAKRISHNA, S. *et al.* An introduction to electrospinning and nanofibers. **An Introduction to Electrospinning and Nanofibers**, [s. l.], p. 90–154, 2005.

RIAU, A. K. *et al.* Sustained delivery system for stem cell-derived exosomes. **Frontiers in Pharmacology**, [s. l.], v. 10, p. 1368, 2019.

ROBSON, S. C.; SHEPHARD, E. G.; KIRSCH, R. E. Fibrin degradation product D-dimer induces the synthesis and release of biologically active IL-1 β , IL-6 and plasminogen activator inhibitors from monocytes in vitro. **British Journal of Haematology**, [s. l.], v. 86, n. 2, p. 322–326, 1994. Disponível em: <http://doi.wiley.com/10.1111/j.1365-2141.1994.tb04733.x>. Acesso em: 19 fev. 2020.

SEMENIČ, D. *et al.* REGENERATION OF CHRONIC WOUNDS WITH ALLOGENEIC PLATELET GEL VERSUS HYDROGEL TREATMENT: A PROSPECTIVE STUDY. **Acta Clinica Croatica**, [s. l.], v. 57, n. 3, p. 434, 2018. Disponível em: </pmc/articles/PMC6536287/>. Acesso em: 26 jul. 2022.

SPROUL, E.; NANDI, S.; BROWN, A. Fibrin biomaterials for tissue regeneration and repair. *In*: PEPTIDES AND PROTEINS AS BIOMATERIALS FOR TISSUE REGENERATION AND REPAIR. [S. l.]: Elsevier Inc., 2017. p. 127–150.

USHIKI, T. Collagen fibers, reticular fibers and elastic fibers. A comprehensive understanding from a morphological viewpoint. **Archives of histology and cytology**, [s. l.], v. 65, n. 2, p. 109–126, 2002. Disponível em: <https://pubmed.ncbi.nlm.nih.gov/12164335/>. Acesso em: 25 jul. 2022.

WILGUS, T. A. *et al.* Novel Function for Vascular Endothelial Growth Factor Receptor-1 on Epidermal Keratinocytes. **The American Journal of Pathology**, [s. l.], v. 167, n. 5, p. 1257–1266, 2005.

WOO, W. M. Skin Structure and Biology. *In*: IMAGING TECHNOLOGIES AND TRANSDERMAL DELIVERY IN SKIN DISORDERS. [S. l.]: John Wiley & Sons, Ltd, 2019. p. 1–14. *E-book*. Disponível em: <https://onlinelibrary.wiley.com/doi/full/10.1002/9783527814633.ch1>. Acesso em: 18 jul. 2022.

XUE, J. *et al.* Electrospinning and Electrospun Nanofibers: Methods, Materials, and Applications. **Chemical reviews**, [s. l.], v. 119, n. 8, p. 5298, 2019. Disponível em: </pmc/articles/PMC6589095/>. Acesso em: 22 jul. 2022.

ZAKRZEWSKI, W. *et al.* Stem cells: past, present, and future. **Stem Cell Research & Therapy**, [s. l.], v. 10, n. 1, 2019. Disponível em: [/pmc/articles/PMC6390367/](https://pubmed.ncbi.nlm.nih.gov/35312367/). Acesso em: 23 jul. 2022.

ZHAO, W. *et al.* Fabrication of functional PLGA-based electrospun scaffolds and their applications in biomedical engineering. **Materials Science and Engineering: C**, [s. l.], v. 59, p. 1181–1194, 2016.

ZHENG, Y. Fabrication on bioinspired surfaces. **Bioinspired Design of Materials Surfaces**, [s. l.], p. 99–146, 2019.

10. Anexos

10.1. Parecer da Comissão de Ética no Uso de Animais



U F R G S
UNIVERSIDADE FEDERAL
DO RIO GRANDE DO SUL

PRÓ-REITORIA DE PESQUISA

Comissão De Ética No Uso De Animais



CARTA DE APROVAÇÃO

Comissão De Ética No Uso De Animais analisou o projeto:

Número: 36484

Título: Desenvolvimento de um substituto cutâneo com técnicas da engenharia tecidual, por meio de scaffolds nanoestruturados, células-tronco, queratinócitos e fibroblastos

Vigência: 08/01/2019 à 31/03/2022

Pesquisadores:

Equipe UFRGS:

PATRICIA HELENA LUCAS PRANKE - coordenador desde 08/01/2019

NATASHA MAURMANN - pesquisador desde 08/01/2019

Juliana Giròn Bastidas - Aluno de Doutorado desde 08/01/2019

Comissão De Ética No Uso De Animais aprovou o mesmo , em reunião realizada em 13/05/2019 - Sala 223 do Prédio do Instituto de ciências Básicas da Saúde - ICBS - Campus Centro UFRGS- Bairro Farroupilha - Porto Alegre, em seus aspectos éticos e metodológicos, para a utilização de 78 ratos machos Wistar Kyoto isogênicos, de 8 a 12 semanas de vida, obtidos do Biotério Setorial do Departamento de Bioquímica-UFRGS, de acordo com os preceitos das Diretrizes e Normas Nacionais e Internacionais, especialmente a Lei 11.794 de 08 de novembro de 2008, o Decreto 6899 de 15 de julho de 2009, e as normas editadas pelo Conselho Nacional de Controle da Experimentação Animal (CONCEA), que disciplinam a produção, manutenção e/ou utilização de animais do filo Chordata, subfilo Vertebrata (exceto o homem) em atividade de ensino ou pesquisa.

Porto Alegre, Sexta-Feira, 24 de Maio de 2019

ALEXANDRE TAVARES DUARTE DE OLIVEIRA
Coordenador da comissão de ética

10.2. Parecer da Plataforma Brasil



PARECER CONSUBSTANCIADO DO CEP

DADOS DO PROJETO DE PESQUISA

Título da Pesquisa: Avaliação do efeito do meio condicionado de células-tronco da polpa dental na proliferação celular

Pesquisador: Patricia Helena Lucas Pranke

Área Temática:

Versão: 2

CAAE: 12892419.0.0000.5347

Instituição Proponente: Universidade Federal do Rio Grande do Sul

Patrocinador Principal: Conselho Nacional de Desenvolvimento Científico e Tecnológico
FUND COORD DE APERFEICOAMENTO DE PESSOAL DE NIVEL SUP
MINISTERIO DA CIENCIA, TECNOLOGIA, INOVACOES E COMUNICACOES

DADOS DO PARECER

Número do Parecer: 3.335.805

Apresentação do Projeto:

Trata-se de projeto coordenado por Patricia Helena Lucas Pranke (Faculdade de Farmácia) com a participação de Juliana Girón Bastidas e Natasha Maurmann (Faculdade de Farmácia). As células-tronco mesenquimais provenientes da polpa de dentes decíduos esfoliados (SHED – Stem Cells from Human Exfoliated Deciduous Teeth) são uma fonte atrativa para utilização em pesquisas na área de engenharia tecidual com mínimo dano invasivo ao doador. Atualmente tem se estudado a capacidade de secreção de diferentes fatores de crescimento e citocinas (VEGF, IGFBP-3, BMP2, TGF-1, FGF-2) pelas células-tronco. No cultivo in vitro, esses fatores são secretados no meio de cultura, chamado de meio condicionado. O meio permite a conversão de um ambiente pró- inflamatório em um ambiente anti-inflamatório. Os experimentos consistirão no cultivo de SHED a fim de obter um meio condicionado para avaliar o efeito na proliferação de diferentes tipos de células. Essa abordagem representa uma estratégia promissora de avaliação preliminar do efeito do meio condicionado de SHED para futuros testes e usos em medicina regenerativa.

Objetivo da Pesquisa:

Objetivo Geral

Realizar avaliações in vitro do efeito do meio condicionado de SHEDs na proliferação de diferentes tipos de células.

Endereço: Av. Paulo Gama, 110 - Sala 317 do Prédio Anexo 1 da Reitoria - Campus Centro

Bairro: Farroupilha

CEP: 90.040-060

UF: RS

Município: PORTO ALEGRE

Telefone: (51)3308-3738

Fax: (51)3308-4085

E-mail: etica@propesq.ufrgs.br



Continuação do Parecer: 3.335.805

Objetivos específicos

- Isolar, cultivar, caracterizar e coletar o meio de cultura de células-tronco mesenquimais obtidas da polpa de dentes decíduos esfoliados (SHED).
- Avaliar o efeito do meio condicionado de SHED na viabilidade de diferentes tipos celulares (células envolvidas no reparo tecidual como linhagens de fibroblastos e linhagens de queratinócitos bem como o efeito desse meio em linhagens de células tumorais).
- Avaliar a viabilidade celular em matrizes de nanofibras produzidas por electrospinning coaxial com incorporação de meio condicionado no polímero usual utilizado (PLGA).

Avaliação dos Riscos e Benefícios:

Riscos:

Os riscos foram reescritos.

O dente removido é um material que seria descartado no lixo. Portanto o risco existente em participar do projeto seria o de desistir após ter realizado a doação. Porém, neste caso entre em contato com o pesquisador responsável para que o descarte do material doado seja feito.

Benefícios:

O único benefício em participar desse projeto é que, ao doar o dente para pesquisa, ajuda-se a melhor conhecer a biologia das células-tronco em testes para medicina regenerativa. O paciente com indicação de exodontia terá essa necessidade de tratamento suprida e o dente será extraído com a técnica habitualmente utilizada na clínica. Os resultados desta pesquisa poderão beneficiar a utilização das células-tronco em pacientes.

Comentários e Considerações sobre a Pesquisa:

Trata-se de um estudo laboratorial experimental in vitro. Para obtenção das células tronco serão selecionados 6 dentes em processo de esfoliação de pacientes com necessidade de exodontia encaminhado para a Clínica Infante-Juvenil da Faculdade de Odontologia da Universidade Federal do Rio Grande do Sul (FO-UFRGS).

Critério de Inclusão

1. Dentes decíduos hígidos removidos por meio da técnica de exodontia simples.
2. Ausência de anquilose, verificada através do exame clínico e radiográfico (encaminhado pelo

Endereço: Av. Paulo Gama, 110 - Sala 317 do Prédio Anexo 1 da Reitoria - Campus Centro

Bairro: Farroupilha

CEP: 90.040-060

UF: RS

Município: PORTO ALEGRE

Telefone: (51)3308-3738

Fax: (51)3308-4085

E-mail: etica@propesq.ufrgs.br



Continuação do Parecer: 3.335.805

dentista que indicou a exodontia)

3. Ausência de história de trauma alvéolo-dental.
4. Sem sinais clínicos e radiográficos de comprometimento pulpar
5. Apresentando pelo menos 1/3 de absorção radicular.

Pacientes de seis a doze anos, independentemente de sexo, cor, classe ou grupos sociais, apresentando bom estado de saúde geral, sem doenças sistêmicas, sem utilização crônica de medicamentos poderão doar seus dentes. Cada paciente poderá contribuir com um ou mais dentes, dependendo da necessidade clínica de cada caso. Fica a critério do responsável, bem como da criança, contribuir com um ou mais dentes para a pesquisa.

Trata-se de um estudo laboratorial experimental in vitro. Para obtenção das células tronco serão selecionados 6 dentes em processo de esfoliação de pacientes com necessidade de exodontia encaminhado para a Clínica Infante-Juvenil da Faculdade de Odontologia da Universidade Federal do Rio Grande do Sul (FO-UFRGS).

Critério de Inclusão

1. Dentes decíduos hígidos removidos por meio da técnica de exodontia simples.
2. Ausência de anquilose, verificada através do exame clínico e radiográfico (encaminhado pelo dentista que indicou a exodontia)
3. Ausência de história de trauma alvéolo-dental.
4. Sem sinais clínicos e radiográficos de comprometimento pulpar
5. Apresentando pelo menos 1/3 de absorção radicular.

Pacientes de seis a doze anos, independentemente de sexo, cor, classe ou grupos sociais, apresentando bom estado de saúde geral, sem doenças sistêmicas, sem utilização crônica de medicamentos poderão doar seus dentes. Cada paciente poderá contribuir com um ou mais dentes, dependendo da necessidade clínica de cada caso. Fica a critério do responsável, bem como da criança, contribuir com um ou mais dentes para a pesquisa.

A coleta da amostra (dentes decíduos) ocorrerá na Clínica Infante-Juvenil da Faculdade de Odontologia da Universidade Federal do Rio Grande do Sul (FO-UFRGS), por dentistas capacitados que darão aviso aos pesquisadores quando tiverem programado uma exodontia. O dia do procedimento a aluna Juliana Girón estará presente para falar diretamente com o participante e o responsável a fim de explicar detalhadamente os objetivos da pesquisa, riscos, e benefícios, assim como para tirar dúvidas que possam ter na hora de assinar o Termo de Assentimento.

Endereço: Av. Paulo Gama, 110 - Sala 317 do Prédio Anexo 1 da Reitoria - Campus Centro

Bairro: Farroupilha

CEP: 90.040-060

UF: RS

Município: PORTO ALEGRE

Telefone: (51)3308-3738

Fax: (51)3308-4085

E-mail: etica@propesq.ufrgs.br



Continuação do Parecer: 3.335.805

Considerações sobre os Termos de apresentação obrigatória:

Apresenta

TCLE

TALE

Termo de doação de material biológico

Termo de Concordância da Clínica Infanto-juvenil da Faculdade de Odontologia da UFRGS

Conclusões ou Pendências e Lista de Inadequações:

Resposta ao recomendações feitas

1. Não está descrito quando quem e como será o contato com o participante e com o responsável.

No projeto foi detalhado que o contato com o participante e com o responsável será feito no dia programado para a exodontia, quem terá direito contato será a aluna de doutorado Juliana Girón que será responsável por explicar os objetivos da pesquisa e obter a assinatura do assentimento. O parágrafo adicionado no projeto foi o seguinte:

“A coleta da amostra (dentes decíduos) ocorrerá na Clínica Infanto-Juvenil da Faculdade de Odontologia da Universidade Federal do Rio Grande do Sul (FO-UFRGS), por dentistas capacitados que darão aviso aos pesquisadores quando tiverem programado uma exodontia. O dia do procedimento a aluna Juliana Girón estará presente para falar diretamente com o participante e o responsável a fim de explicar detalhadamente os objetivos da pesquisa, riscos, e benefícios, assim como para tirar dúvidas que possam ter na hora de assinar o Termo de Assentimento.” (Pendência atendida)

2. Não está descrito a idade dos participantes na pesquisa.

Foi esclarecido na página 8 do projeto que os participantes deveram ter uma idade entre 6 e 12 anos(Pendência atendida)

3. O TALE deve apresentar linguagem adequada para crianças e/ou jovens.

A linguagem foi adaptada a fim de que as crianças e/ou jovens tivessem uma melhor compreensão. (Pendência atendida)

Endereço: Av. Paulo Gama, 110 - Sala 317 do Prédio Anexo 1 da Reitoria - Campus Centro

Bairro: Farroupilha

CEP: 90.040-060

UF: RS

Município: PORTO ALEGRE

Telefone: (51)3308-3738

Fax: (51)3308-4085

E-mail: etica@propesq.ufrgs.br



Continuação do Parecer: 3.335.805

4. Rever riscos adequando aos participantes

Os riscos foram reescritos.

"O dente removido é um material que seria descartado no lixo. Portanto o risco existente em participar do projeto seria o de desistir após ter realizado a doação. Porém, neste caso entre em contato com o pesquisador responsável para que o descarte do material doado seja feito." (Pendência atendida)

Esses questionamentos foram incorporados no Projeto de Pesquisa em realce bem como modificados na Plataforma Brasil.

Considerações Finais a critério do CEP:

Aprovado.

Este parecer foi elaborado baseado nos documentos abaixo relacionados:

Tipo Documento	Arquivo	Postagem	Autor	Situação
Informações Básicas do Projeto	PB_INFORMAÇÕES_BÁSICAS_DO_PROJETO_1286935.pdf	10/05/2019 12:11:47		Aceito
Recurso Anexado pelo Pesquisador	respostasPB.docx	10/05/2019 12:05:05	JULIANA GIRON BASTIDAS	Aceito
TCLE / Termos de Assentimento / Justificativa de Ausência	ANEXO3termoassentimento.docx	10/05/2019 11:58:45	JULIANA GIRON BASTIDAS	Aceito
Projeto Detalhado / Brochura Investigador	projetocondicionado.docx	10/05/2019 11:57:33	JULIANA GIRON BASTIDAS	Aceito
Declaração de Instituição e Infraestrutura	AprovacaoPesquisaComissaoPesquisaFacFarmaciaCondicionado.pdf	30/04/2019 15:58:53	Natasha Maurmann	Aceito
TCLE / Termos de Assentimento / Justificativa de Ausência	termoassentimento.docx	30/04/2019 14:56:42	JULIANA GIRON BASTIDAS	Aceito
Projeto Detalhado / Brochura Investigador	projetocondicionado.pdf	30/04/2019 14:43:42	JULIANA GIRON BASTIDAS	Aceito

Endereço: Av. Paulo Gama, 110 - Sala 317 do Prédio Anexo 1 da Reitoria - Campus Centro

Bairro: Farroupilha

CEP: 90.040-060

UF: RS

Município: PORTO ALEGRE

Telefone: (51)3308-3738

Fax: (51)3308-4085

E-mail: etica@propesq.ufrgs.br



UFRGS - PRÓ-REITORIA DE
PESQUISA DA UNIVERSIDADE
FEDERAL DO RIO GRANDE DO



Continuação do Parecer: 3.335.805

Folha de Rosto	folhaderostomeiocond.pdf	30/04/2019 14:38:29	JULIANA GIRON BASTIDAS	Aceito
----------------	--------------------------	------------------------	---------------------------	--------

Situação do Parecer:

Aprovado

Necessita Apreciação da CONEP:

Não

PORTO ALEGRE, 20 de Maio de 2019

Assinado por:
MARIA DA GRAÇA CORSO DA MOTTA
(Coordenador(a))

Endereço: Av. Paulo Gama, 110 - Sala 317 do Prédio Anexo 1 da Reitoria - Campus Centro

Bairro: Farroupilha

CEP: 90.040-060

UF: RS

Município: PORTO ALEGRE

Telefone: (51)3308-3738

Fax: (51)3308-4085

E-mail: etica@propesq.ufrgs.br

10.3. Produção acadêmica durante o doutorado

GIRÓN, J.; MAURMANN, N.; OLIVEIRA L.; ALCANTARA, B.; PINHEIRO, C.; LEIPNITZ, G.; MEYER F.; OLIVEIRA M.; RIGON, P.; PRANKE, P. Bilayer scaffold from PLGA/fibrin electrospun membrane and fibrin hydrogel layer supports wound healing in vivo. (Artigo submetido ao periódico *Biomedical Materials*).

GIRÓN, J., MAURMANN N., SCHOLL, J.N., FIGUEIRÓ F., MARCON B., PRANKE, P. *In vitro* evaluation of SHED extracellular vesicles on keratinocytes proliferation, migration, and H2O2 attenuation. (Artigo a ser submetido).

BALDIN, E. K., SANTOS, P. B., DE CASTRO, V. V., AGUZZOLI, C., MAURMANN, N., GIRÓN, J., PRANKE, P. & MALFATTI, C. de F. (2022). Plasma Electrolytic Oxidation (PEO) Coated CP-Ti: Wear Performance on Reciprocating Mode and Chondrogenic–Osteogenic Differentiation. *Journal of Bio- and Tribo-Corrosion*, 8(1), 1–16. <https://doi.org/https://doi.org/10.1007/s40735-021-00627-z>

GIRÓN, J., BALDIN, E., MEDEIROS, T., OLIVEIRA, L., MACHADO, G. M., MALFATTI, C. F. & PRANKE, P. (2021). Biomaterials for bone regeneration: an orthopedic and dentistry overview. *Brazilian Journal of Medical and Biological Research = Revista Brasileira de Pesquisas Medicas e Biologicas*, 54(9). <https://doi.org/10.1590/1414-431X2021E11055>

GIRÓN, J., MAURMANN, N., & PRANKE, P. (2021). The role of stem cell-derived exosomes in the repair of cutaneous and bone tissue. *Journal of Cellular Biochemistry*. <https://doi.org/10.1002/JCB.30144>

GIRÓN, J., MAURMANN, N., DA SILVEIRA, M. R., FERREIRA, C. A. & PRANKE, P. (2020). Development of fibrous PLGA/fibrin scaffolds as a potential skin substitute. *Biomedical Materials*, 15(5), 055014. <https://doi.org/10.1088/1748-605X/ABA086>

MAURMANN, N., GIRÓN, J., BORSTMANN, B., LEAL, J. & PRANKE, P. (2019). 3D electrospinning used in medical materials. *International Journal of Advances in Medical Biotechnology - IJAMB*, 2(1), 27–32. <https://doi.org/10.25061/2595-3931/IJAMB/2019.v2i1.26>

10.4. Resumos publicados em anais de congressos

GIRÓN, J.; MAURMANN, N.; OLIVEIRA L.; MEYER F.; ALCANTARA B.; OLIVEIRA M., RIGON, P.; PRANKE, P. *In Vivo* Evaluation of a Bilayer Scaffold from PLGA/Fibrin Spun Membrane and Fibrin Hydrogel Layer for Skin Regeneration. Congresso Internacional Digital em Biofabricação e Bioimpressão 3D. 23-25 de março de 2022. https://editorarealize.com.br/editora/ebooks/3dbb/2022/62acad28722b1_17062022133448.pdf

GIRÓN, J.; MAURMANN, N.; OLIVEIRA, L.; MEYER, F.; ALCANTARA, B.; OLIVEIRA, M.; RIGON, P.; PRANKE, P. *In vivo* evaluation of a bilayer scaffold from PLGA/Fibrin and Fibrin hydrogel used as a skin substitute. TERMIS 6th world congress. Maastricht. 15-16 novembro 2021.

MACHADO, G. M.; KASPER, R. H.; MAURMANN, N.; GIRÓN, J.; PRANKE, P.; BREW, M. C. Desenvolvimento um novo bioestimulador de células-tronco, baseado em um polímero com propriedades bactericidas/bacteriostáticas para aplicação em harmonização orofacial. In: II Congresso Brasileiro de Harmonização Orofacial (II CONGREHOF), Gramado, 2021

MACHADO, G. M.; OLIVEIRA, L.; MAURMANN, N.; GIRÓN, J.; BORGES, M. F.; PRANKE, P. Testes *in vitro* por bioimpressão: uma nova alternativa para avaliação de novas tecnologias. In: . II Congresso Brasileiro de Harmonização Orofacial (II CONGREHOF), Gramado, 2021.

MACHADO, G. M.; KASPER, R. H.; GIRÓN, JULIANA; OLIVEIRA, L.; MAURMANN, N.; PRANKE, P.; BAVARESCO, C. S.; BREW, M. C. Desenvolvimento de biomateriais para regeneração óssea guiada: novas perspectivas para a engenharia tecidual. In: 38^a Reunião Anual da Sociedade Brasileira de Pesquisa Odontológica (SBPqO), 2021, Virtual. 38^a Reunião Anual da Sociedade Brasileira de Pesquisa Odontológica (SBPqO), 2021.

OLIVEIRA, L.; MAURMANN, N.; GIRON, J.; BORGES, M. F.; PRANKE, P. Study of bioink formulation and influence of bioprinting in cell viability. In: 1st International Digital Congress on 3D Biofabrication and Bioprinting (3DBB), 2020, Araraquara, remotamente. International Journal of Advances in Medical Biotechnology (IJAMB), 2020

GIRÓN, J.; MAURMANN, N.; SCHOLL, J.N.; FIGUEIRO, F.; PRANKE, P. Paracrine Effects of secretome from Stem Cells in the cultivation of Keratinocytes. In: 6^a Edição do Workshop de Biomateriais, Engenharia de Tecidos e Órgãos Artificiais (6^o OBI). 29 a 31 de outubro de 2019, SP - Brasil.

GIRÓN, J.; MAURMANN, N.; MARTINS, M.C.S.; PRANKE, P. Production of PLGA/fibrin scaffolds and *in vitro* test. In: 6^a Edição do Workshop de Biomateriais, Engenharia de Tecidos e Órgãos Artificiais (6^o OBI). 29 a 31 de outubro de 2019, SP - Brasil.

OLIVEIRA, L.; MAURMANN, N.; BORGES, M.F.; GIRON, J.; PRANKE, P. Use of a Bioprinter with Alginate as the Bioink. In: 6^a Edição do Workshop de Biomateriais, Engenharia de Tecidos e Órgãos Artificiais (6^o OBI). 29 a 31 de outubro de 2019, SP - Brasil.

MACHADO, G. M.; KASPER, R. H.; MAURMANN, N.; GIRÓN, J.; COUTO, M; BREW, M. C.; PRANKE, P.; BAVARESCO, C. S. Cytoprotective effect of a bioactive molecule on different cells treated with zolendronate: application in tissue engineering. In: 36^a Reunião Anual da SBPqO (Sociedade Brasileira de Pesquisa Odontológica), 2019, Campinas. 36^a Reunião Anual da SBPqO (Sociedade Brasileira de Pesquisa Odontológica), 2019.

GIRON, J.; MAURMANN, N; PRANKE, P. In Vitro Paracrine Effects of Stem Cells From Human Exfoliated Deciduous Teeth On Epithelial Cell. In: 2019 TERMIS-AM Annual Conference, 2019, Orlando. 2019 TERMIS-AM Annual Conference, 2019.

VIDAL, T.R.; GIRON, J.; MAURMANN, N.; PRANKE, P. Modulação da viabilidade celular de queratinócitos e células leucêmicas, a partir de meio condicionado de células estromais mesenquimais. III Encontro do Programa de Pós-Graduação em Biociências e Encontro de Pesquisa em Biologia Celular da UFCSPA. Porto Alegre, 13 e 14 de novembro de 2018.

10.5. Prêmios

Menção honrosa na modalidade de comunicação oral pelo trabalho: *In Vivo* Evaluation of a Bilayer Scaffold from PLGA/Fibrin Spun Membrane and Fibrin Hydrogel Layer for Skin Regeneration. GIRON, J.; MAURMANN, N.; OLIVEIRA, L.; MEYER, F.; ALCANTARA, B.; OLIVEIRA, M.; RIGON, P.; PRANKE, P. Congresso Internacional Digital em Biofabricação e Bioimpressão 3D. 23-25 de março de 2022.

Menção Honrosa com o trabalho: Testes *in vitro* por bioimpressão: uma nova alternativa para avaliação de novas tecnologias. MACHADO, G. M.; OLIVEIRA, L.; MAURMANN, N.; GIRÓN, J.; BORGES, M. F.; PRANKE, P. In: II Congresso Brasileiro de Harmonização Orofacial (II CONGREHOF), 2021, Gramado